

Nitrogen transformation pathways, rates, and isotopic signatures in Lake Lugano

Inauguraldissertation

zur

Erlangung der Würde eines Doktors der Philosophie
vorgelegt der
Philosophisch-Naturwissenschaftlichen Fakultät
der Universität Basel

von

Christine B. Wenk
aus Basel, Basel-Stadt

Basel, 2014

Genehmigt von der Philosophisch-Naturwissenschaftlichen Fakultät
auf Antrag von:

Prof. Dr. Moritz F. Lehmann

Prof. Dr. Bernhard Wehrli

Basel, den 18. Juni 2013

Prof. Dr. Jörg Schibler
Dekan

Contents

Abstract	v
1 Introduction	1
1.1 Nitrogen cycle - a transgressed planetary boundary	2
1.2 Pathways and players in the microbial nitrogen cycle	3
1.3 Tracing N transformations by measuring natural abundance stable N and O isotope ratios	5
1.4 Objectives and outline of the thesis	8
1 - References	11
2 Anammox bacteria and sulfide-dependent denitrifiers coexist in the water column of a meromictic south-alpine lake	17
Abstract	18
2.1 Introduction	19
2.2 Methods	21
2.2.1 Study site and sampling	21
2.2.2 Water column profiling and hydrochemical analyses	22
2.2.3 Flux calculations	22
2.2.4 Phylogenetic analysis	23
2.2.5 Quantitative polymerase chain reaction (qPCR)	24
2.2.6 ¹⁵ N incubation experiments	24
2.3 Results	25
2.3.1 Water column hydrochemistry	25
2.3.2 Molecular analyses	26
2.3.3 ¹⁵ N incubation experiments	28
2.4 Discussion	29
2.4.1 Hydrochemical evidence for fixed N elimination in the RTZ . .	29
2.4.2 Anammox bacteria in the RTZ: Diversity, abundance, and activity	31
2.4.3 Sulfide-dependent denitrification is the dominant fixed N elim- ination process in the RTZ	32

2.4.4	Anammox bacteria coexist with sulfide-dependent denitrifiers .	37
2 -	References	39
3	Community N and O isotope fractionation by sulfide-dependent denitrification and anammox in a stratified lacustrine water column	45
	Abstract	46
3.1	Introduction	47
3.2	Methods	50
3.2.1	Study site and sampling	50
3.2.2	Concentration and isotope analyses	50
3.3	Results	51
3.4	Discussion	53
3.4.1	Low community isotope enrichment factor for NO_3^- reduction in the water column	54
3.4.2	Oxygen vs. nitrogen isotope enrichment during NO_3^- reduction in the RTZ	62
3.4.3	Low community isotope enrichment for NH_4^+ consumption in the RTZ	64
3.5	Summary and implications for N isotope budgets	66
3 -	References	69
4	Partitioning between benthic and pelagic nitrate reduction in the Lake Lugano south basin	75
	Abstract	76
4.1	Introduction	77
4.2	Methods	79
4.2.1	Study site and sampling	79
4.2.2	Continuous-flow sediment core incubations	80
4.2.3	Hydrochemical analyses	80
4.2.4	Stable isotope analyses	81
4.2.5	Benthic flux calculations and N transformation rates	82
4.3	Results	83
4.3.1	Dissolved concentrations and natural abundance stable N and O isotope profiles in the water column	83
4.3.2	Benthic N transformation rates and fluxes at the sediment-water interface	87
4.4	Discussion	87
4.4.1	N_2 production during hypolimnetic anoxia	88
4.4.2	Isotopic constraints on denitrification in the sediment and the anoxic water column	92

4.4.3	Ammonium consumption at the oxic-anoxic interface as elucidated by NO_3^- isotope ratios	94
4 -	References	99
5	Nitrous oxide cycling in a mono- and a meromictic lake basin inferred from stable isotope and isotopomer distributions	105
	Abstract	106
5.1	Introduction	107
5.2	Methods	109
5.2.1	Study site and sampling	109
5.2.2	N_2O and nutrient concentrations	109
5.2.3	N_2O isotope and isotopomer analyses	110
5.3	Results	111
5.3.1	N_2O concentration and isotope composition in the Lake Lugano south basin	111
5.3.2	N_2O concentration and isotope composition in the Lake Lugano north basin	114
5.4	Discussion	114
5.4.1	N_2O production and accumulation in the south basin	114
5.4.2	Isotopic constraints on N_2O formation mechanisms in the south basin	117
5.4.3	The isotopic signature of N_2O consumption in the Lake Lugano north basin	119
5.4.4	Summary and concluding remarks	121
5 -	References	123
6	Conclusions and Outlook	129
6.1	Conclusions and implications	130
6.2	Outlook	131
6 -	References	133
	Acknowledgments	136

Abstract

The consequences of detrimental alterations caused to the natural nitrogen (N) cycle are manifold. To tackle problems, such as eutrophication of coastal marine and lacustrine environments, or increasing emissions of greenhouse gas nitrous oxide (N_2O), requires a clear understanding of the microbial N cycle. A promising tool to study N transformations is the measurement of the stable isotope composition of N compounds. The overall goal of this project was to improve the understanding of N transformation pathways and associated isotope effects, using the meromictic northern and the monomictic southern basins of Lake Lugano as natural model systems. Toward this goal, we collected samples from the water column of both basins for dissolved inorganic nitrogen (DIN) analyses (including $\text{N}_2:\text{Ar}$, N_2O), molecular microbiological phylogenetic analyses, ^{15}N -labeling experiments (water column and sediments), and stable N and O isotope (and N_2O isotopomer) measurements.

First, we identified the main processes responsible for fixed N elimination in the Lake Lugano north basin. The stable redox transition zone (RTZ) in the mid-water column provides environmental conditions that are favorable for both, anaerobic ammonium oxidation (anammox), as well as sulfur-driven denitrification. Previous marine studies suggested that sulfide (H_2S) inhibits the anammox reaction. In contrast to this we demonstrated that anammox bacteria coexist with sulfide-dependent denitrifiers in the water column of the Lake Lugano north basin. The maximum potential rates of both processes were comparatively low, but consistent with nutrient fluxes calculated from concentration gradients. Furthermore, we showed that organotrophic denitrification is a negligible nitrate-reducing pathway in the Lake Lugano north basin.

Based on these findings, we next interpreted the N and O isotope signatures in the Lake Lugano north basin. Anammox and sulfide-dependent denitrification left clear N (in NO_3^- and NH_4^+) and O (in NO_3^-) isotope patterns in the water column. However, the associated isotope effects were low compared to previous reports on isotope fractionation by organotrophic denitrification and aerobic ammonium oxidation. We attribute this apparent under-expression to two possible explanations: 1) The biogeochemical conditions (i.e., substrate limitation, low cell specific N transformation

rates) that are particularly conducive in the Lake Lugano RTZ to an N isotope effect under-expression at the cellular-level, or 2) a low process-specific isotope fractionation at the enzyme-level. Moreover, an ^{18}O to ^{15}N enrichment ratio of ~ 0.89 associated with NO_3^- reduction suggested that the periplasmic dissimilatory nitrate reductase Nap was more important than the membrane-bound dissimilatory Nar.

While in the meromictic north basin, most fixed N elimination took place within the water column RTZ, seasonal mixing and re-oxygenation of the water column in the south basin suggests N_2 production within the sediments. We showed that denitrification was the major benthic NO_3^- reduction pathway in the southern basin. Benthic anammox and dissimilatory nitrate reduction to ammonium (DNRA) rates remained close to the detection limit. A comparison between benthic N_2 production rates and water column N_2 fluxes revealed that during anoxic bottom water conditions, $\sim 40\%$ of total N_2 production was associated with benthic and $\sim 60\%$ with pelagic processes. This quantitative partitioning was confirmed by N isotope analysis of water column NO_3^- . The N isotope enrichment factor associated with total NO_3^- reduction was $\sim 14\text{‰}$. This translates into a sedimentary N_2 contribution of 36-51%, if canonical assumptions for N isotope fractionation associated with water column ($^{15}\epsilon_{\text{water}} = 20\text{-}25\text{‰}$) and sedimentary ($^{15}\epsilon_{\text{sed}} = 1.5\text{-}3\text{‰}$) denitrification are made.

Finally, we compared the N_2O production and consumption pathways in the northern and southern basin and found contrasting N_2O dynamics. Maximum N_2O concentrations in the south basin ($>900 \text{ nmol L}^{-1}$) greatly exceeded maximum concentrations in the north basin ($<13 \text{ nmol L}^{-1}$). ^{15}N site preference (SP) values $>32\text{‰}$ in the south basin indicated nitrification via hydroxylamine (NH_2OH) oxidation as the prime N_2O source, whereas in the north basin N_2O production was attributed to nitrifier denitrification. In the north basin, N_2O was completely reduced within the RTZ. This chemolithotrophic N_2O reduction occurred with an ^{18}O to ^{15}N enrichment ratio of ~ 2.5 , which is consistent with previous reports for organotrophic N_2O reduction.

In conclusion, our study highlights the importance of chemolithotrophic processes in aquatic ecosystems. Moreover, the expression of N isotope fractionation can be variable in nature and depends on various factors such as the pathways of NO_3^- dissimilation (organotrophic vs. chemolithotrophic), the main catalyzing enzymes, the pathways of NH_4^+ oxidation (nitrification vs. anammox), and the controlling environmental conditions (e.g., substrate limitation, cell specific N transformation rates). Hence, this study suggests to refrain from universal, canonical assumptions of N isotope fractionation in N budget calculations. Additional stable isotope measurements such as O isotopes in NO_3^- , or the ^{15}N site preference in N_2O are powerful tools to identify and quantify microbial N transformation pathways occurring simultaneously or in close vicinity. For a successful interpretation of such data, however, a mechanistic understanding of the processes leading to certain characteristic isotopic signatures in the environment is needed.

CHAPTER 1

Introduction

1.1 Nitrogen cycle - a transgressed planetary boundary

Nitrogen (N) is one of the most abundant elements on earth and an important nutrient for organisms. Most of it is present as atmospheric dinitrogen gas (N_2). In order to sustain life, N_2 needs to be fixed, i.e., transformed into compounds that can be incorporated into biomass. In nature, this process can only be conducted by few specialized organisms.

Since the middle of the 20th century, human intervention in the natural N cycle has rapidly increased. For instance, with the development of the Haber process ($N_2 + 3 H_2 \rightarrow 2 NH_3$) and its extensive application as agricultural N-fertilizer, huge amounts of anthropogenically fixed N have been added to the environment. This has resulted in increased N levels in coastal marine and lacustrine ecosystems throughout the world and caused excessive algal growth and enhanced organic matter decomposition. The direct consequences are a decrease in, or even absence of, dissolved oxygen, leading to strong redox gradients and a severe decline in water quality. Eutrophication of coastal marine and lacustrine environments, however, is by far not the only impact of human alteration of the N cycle. The consequences are many and include increased emissions of the greenhouse gas nitrous oxide (N_2O), stratospheric ozone loss, global acidification, and alteration of other elemental cycles, such as carbon (C), phosphorous (P), or sulfur (S) (Gruber and Galloway, 2008; Galloway et al., 2003).

A new approach for defining preconditions for human development has recently been proposed (Rockström et al., 2009) and promoted by international policy advisory boards on global change. In this approach, nine earth systems have been defined, which are thought to control the current global climate state. Based on a synthesis of current research, biophysical thresholds (such as rate of biodiversity loss or global freshwater use) were identified that the international community should not overstep. The N cycle is one of three earth systems that has already transgressed its planetary boundary. The authors estimate that anthropogenic N_2 -fixation has to be reduced to 25% of its current value to avoid the risk of disastrous consequences for humanity. In order to reach this target but also to better constrain the proposed threshold, they call for more research on a better understanding of the global N cycle and its interactions with other elemental cycles. In particular, there is an urgent need to estimate global N budgets, to assess N transformation pathways and rates, and to understand where and under what conditions N cycle reactions take place. In this thesis, I directly take on this challenge, and provide new constraints on microbial N-cycle pathways, especially in regions of strong redox gradients.

In the following two sections I will first briefly review our current understanding of the microbial N cycle pathways, in particular the processes taking place in redox transition zones (RTZs). Second, I will introduce the measurement of natural abundance stable N and O isotope ratios as a tool to study N transformation processes.

1.2 Pathways and players in the microbial nitrogen cycle

Before reaching the ocean, part of the anthropogenically fixed N loadings can be mitigated by microbially mediated processes in RTZs in lakes (Seitzinger et al., 2006). Nitrification, i.e., the aerobic oxidation of ammonium (NH_4^+) to nitrite (NO_2^-) and nitrate (NO_3^-), and subsequent denitrification, i.e., the stepwise reduction of NO_3^- to NO_2^- , nitric oxide (NO), nitrous oxide (N_2O) and N_2 , have long been viewed as the only drivers for fixed N elimination from aquatic systems (Fig. 1.1). However, in recent years, not only new players but also new pathways have been discovered, which fundamentally altered the canonical view of the microbial N cycle (reviewed in Hulth et al., 2005; Burgin and Hamilton, 2007). The following paragraphs highlight some of these more recent discoveries concerning NO_3^- reduction and NH_4^+ oxidation, respectively (Fig. 1.1).

Nitrification has for long been thought to be mediated by two lithotrophic groups of bacteria: Ammonia-oxidizing bacteria (AOB) gaining energy from aerobically oxidizing ammonia to NO_2^- , and nitrite-oxidizing bacteria (NOB) gaining energy from the oxidation of NO_2^- to NO_3^- . AOB and NOB belong to the β - or γ -subclasses and α - or γ -subclasses of *Proteobacteria*, respectively (reviewed in Bock and Wagner, 2006). The twin discoveries of ammonia-oxidizing archaea, as well as the ability of methane oxidizing bacteria to oxidize ammonia within their methane-oxidizing enzymatic machinery, added two new players to the picture of the microbial N cycle (reviewed in Francis et al., 2007; Bedard and Knowles, 1989).

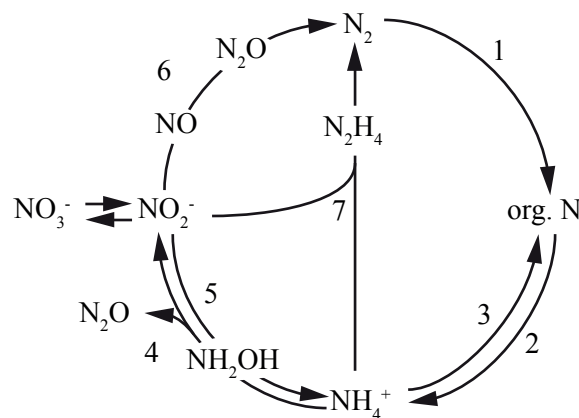


Figure 1.1: Simplified scheme of the microbial nitrogen cycle. The illustrated pathways are 1) N_2 -fixation, 2) mineralization, 3) assimilation, 4) nitrification, 5) dissimilatory nitrate reduction to ammonium (DNRA), 6) denitrification, and 7) anaerobic ammonium oxidation (anammox).

Similarly, organotrophic **denitrification**, i.e., the oxidation of organic matter with oxidized N compounds as electron acceptors, is the dominant pathway for fixed N elimination in many marine and lacustrine environments (Zumft, 1997). However, chemolithotrophic denitrifiers, i.e., denitrifiers that gain energy from oxidizing inorganic substrates such as reduced sulfur compounds, iron (Fe), manganese (Mn), or even methane (CH₄) have become increasingly recognized in many natural habitats (Burgin and Hamilton, 2007).

Anaerobic ammonium oxidation (**anammox**) is an alternative pathway for fixed N elimination, which was first discovered in a wastewater treatment plant (Mulder et al., 1995; Van de Graaf et al., 1995) and later in natural environments (Thamdrup and Dalsgaard, 2002; Kuypers et al., 2003; Schubert et al., 2006; Humbert et al., 2010). Anammox bacteria belong to the order *Planctomycetales* and to date, five *Candidatus* genera have been described: *Candidatus* Brocadia, *Candidatus* Kuenenia, *Candidatus* Scalindua, *Candidatus* Anammoxoglobus, and *Candidatus* Jettenia (reviewed in Van Niftrik and Jetten, 2012). Anammox bacteria have a peculiar cell structure with an internal region called the anammoxosome (Lindsay et al., 2001). This compartment is surrounded by a dense membrane of ladderane lipids, and is the proposed site for metabolic processes (review in Van Niftrik and Jetten, 2012). The chemoautotrophic anammox bacteria oxidize NH₄⁺ and reduce NO₂⁻ to form N₂ with hydrazine (N₂H₄) as an intermediate (Fig. 1.1). Since the discovery of this pathway, anammox has been shown to be an important driver for fixed N elimination in many marine (Kuypers et al., 2003, 2005; Thamdrup et al., 2006; Jensen et al., 2008; Dalsgaard et al., 2003), as well as in some lacustrine environments (Hamersley et al., 2009; Schubert et al., 2006).

The pathways described above eventually lead to fixed N elimination from the aquatic environment. In contrast, dissimilatory nitrate reduction to ammonium (**DNRA**) recycles bioavailable nitrogen. Microbes performing DNRA are found in different bacterial phyla, such as *Firmicutes*, or δ - and γ - *Proteobacteria* (reviewed in Burgin and Hamilton, 2007). They reduce NO₃⁻ by coupling it to the oxidation of organic matter or reduced sulfur compounds, and are important players in many marine as well as lacustrine settings (An and Gardner, 2002; McCarthy et al., 2007; Otte et al., 1999; Zopfi et al., 2008).

Finally, during most of the described processes, N₂O can be produced, with the potential to accumulate in the water column and eventually be transferred to the atmosphere (Fig. 1.1). Incomplete denitrification (Baumann et al., 1997), decomposition of the nitrification intermediate hydroxylamine (NH₂OH) (Hooper and Terry, 1979), and even reduction of NO₂⁻ by nitrifiers (nitrifier denitrification; Poth and Focht, 1985) have been identified as potential N₂O sources. To date, the only known pathway for microbial N₂O consumption is its dissimilatory reduction to N₂.

There is a variety of approaches to assess microbial N transformation pathways

in aquatic environments, including molecular microbiological techniques, in situ as well as ex situ tracer experiments, and the analysis of controlling environmental conditions. However, an elegant method is to measure natural abundance stable isotope ratios of N and O. Such measurements are non-invasive and have the potential to constrain several processes occurring simultaneously, in close vicinity, and - if studied in geological records - to constrain past environmental conditions. Yet, the interpretation of stable N (and O) isotope signatures requires a solid understanding of the various N transformation specific isotope effects. In the next section I will briefly introduce the principles of microbial N and O isotope fractionation and their expression in aquatic environments.

1.3 Tracing N transformations by measuring natural abundance stable N and O isotope ratios

There are two stable isotopes of N: ^{14}N and ^{15}N , and three of O: ^{16}O , ^{17}O , and ^{18}O . ^{17}O is the least abundant of these isotopes and will not be further investigated in this thesis. Isotope ratios are usually expressed in permil relative to a standard:

$$\delta_{\text{sample}} = \left(\frac{R_{\text{sample}}}{R_{\text{standard}}} - 1 \right) 1000 \quad (1.1)$$

where $R = ^{15}\text{N}/^{14}\text{N}$ or $^{18}\text{O}/^{16}\text{O}$, respectively. The standards for N and O are atmospheric N_2 with an ^{15}N abundance of 0.003677 (Junk and Swec, 1958), and Vienna Standard Mean Ocean water (VSMOW) with an ^{18}O abundance of 0.0020052 (Baertschi, 1976).

Biological isotope fractionation is based on the fact that organisms typically transform compounds containing lighter isotopes (e.g., ^{14}N) at a slightly higher rate compared to the heavier isotopologues, e.g., ^{15}N . This leads to a measurable enrichment of the heavier isotopes in the substrate pool. The N isotope enrichment factor, $^{15}\epsilon$, associated with this kinetic fractionation is defined as:

$$^{15}\epsilon = \left(\frac{{}^{14}k}{{}^{15}k} - 1 \right) 1000 \quad (1.2)$$

where ${}^{14}k$ and ${}^{15}k$ refer to the reaction rates of ^{14}N and ^{15}N bearing isotopologues, respectively (Mariotti et al., 1981). The consumption of a substrate together with its isotopic fractionation can therefore provide information about transformation processes and fluxes. For a correct interpretation of isotopic imprints in environmental

systems, however, detailed knowledge about single reactions and fractionations is required. A series of studies have investigated the N and O isotope effects of N cycling processes. It has, for example, been reported that reactive N added to an ecosystem via N_2 -fixation has a $\delta^{15}N$ close to atmospheric N_2 (i.e., $^{15}\epsilon = 0$ to 2‰) (Carpenter et al., 1997; Montoya et al., 2002). In contrast, N isotope enrichment factors associated with nitrification range between 12‰ and 38‰ (Casciotti et al., 2003; Horrigan et al., 1990; Mariotti et al., 1981). While this pathway leads to the formation of NO_3^- with a relatively low $\delta^{15}N$, denitrification leaves the residual NO_3^- pool enriched in the heavier isotope ^{15}N . Some culture based experimental data as well as most studies from the open ocean report $^{15}\epsilon$ values of 20‰ to 30‰ for organotrophic denitrification (Brandes et al., 1998; Voss et al., 2001; Barford et al., 1999; Granger et al., 2008; Mariotti et al., 1981; Wellman et al., 1968). While these values provide a basis for the interpretation of isotopic signatures in a specific environment, it has to be taken into account that the expression of isotope fractionation on the ecosystem level can be variable. In this regard, it is important to understand what drives isotope fractionation and which are the crucial steps that lead to the expression (or under-expression) of this signature in the environment.

The step that is usually responsible for isotope fractionation in kinetic (unidirectional) biological reactions is enzymatic bond breakage. It is thus crucial to identify the active enzymes in a natural system. For example, NO_3^- reduction can be catalyzed by four different enzymatic complexes: The bacterial membrane-bound dissimilatory Nar, the bacterial periplasmic dissimilatory Nap, the bacterial cytoplasmic assimilatory Nas, and the eukaryotic assimilatory eukNR. Aerobic ammonium oxidation is either catalyzed by the ammonia monooxygenase (AMO) in the case of nitrification or by the methane monooxygenase (MMO) in the case of methanotrophic nitrification, whereas the enzyme catalyzing anaerobic ammonium oxidation is hydrazine synthase (Hzs) (reviewed in Simon and Klotz, 2012).

The degree of enzymatic isotope fractionation depends on various factors. For nitrification, for example, it has been shown that variations in the amino acid sequence of the α -subunit of the AMO between different groups of organisms causes different N isotope fractionation (Casciotti et al., 2003). For denitrification, the degree to which the enzymatic isotope fractionation (ϵ_{Nar}) is expressed outside the cell can vary with changing environmental conditions. In a set of culture experiments with denitrifying strains, Kritee et al. (2012) showed that the cellular-level isotope effect (ϵ_{cell}) can be significantly reduced relative to ϵ_{Nar} . This occurs at low cell specific nitrate reduction (CSNR) rates, at low ambient NO_3^- concentrations, when the carbon source is thermodynamically less favorable, when O_2 is present, under unstirred conditions, and with bacterial cultures in their early stationary growth phase. These observations have been interpreted by variations of the NO_3^- efflux to uptake ratio by a denitrifying cell. If the ratio is high, ϵ_{Nar} would be nearly fully expressed outside the cell (i.e., $\epsilon_{cell} \approx \epsilon_{Nar}$). If the ratio is low, ϵ_{cell} can be significantly reduced (i.e.,

$\epsilon_{\text{cell}} < \epsilon_{\text{Nar}}$ (Shearer et al., 1991; Granger et al., 2008; Kritee et al., 2012).

The interpretation of N isotope signatures in nature becomes even more complex by taking into account that the ecosystem-level isotope effect (ϵ_{app}) can be reduced relative to ϵ_{cell} . This has, for example, been shown for sedimentary denitrification when it is limited by the rate of NO_3^- supply to the denitrifying zone (Brandes and Devol, 1997; Lehmann et al., 2003). In the extreme, the observed isotope effect of sedimentary denitrification in the overlying water column can be as low as 0 to 4‰ (Alkhatib et al., 2012; Lehmann et al., 2007).

Independent of the degree of N isotope fractionation at the ecosystem level, an increase in $\delta^{15}\text{N-NO}_3^-$ during NO_3^- reduction is distinctively coupled to an increase in $\delta^{18}\text{O-NO}_3^-$ (Granger et al., 2008; Lehmann et al., 2004; Sigman et al., 2005). In marine environments and in most culture experiments the ^{18}O to ^{15}N isotope enrichment ratio (i.e., $^{18}\epsilon : ^{15}\epsilon$) during NO_3^- reduction is ~ 1 (Casciotti et al., 2002; Granger et al., 2008; Sigman et al., 2005), whereas it appears to be lower (i.e., $^{18}\epsilon : ^{15}\epsilon = 0.5 - 0.7$) for freshwater denitrification (Böttcher et al., 1990; Lehmann et al., 2003; Mengis et al., 1999). The conundrum of the apparent difference between freshwater and marine environments remains unresolved, but potential explanations include differences in the mode of denitrification (i.e., source of electron donor), differences in the involved NO_3^- reducing enzymes, or differences in the importance of NO_3^- regenerating processes. Nitrification, for example, yields NO_3^- with $\delta^{15}\text{N}$ and $\delta^{18}\text{O}$ values that are affected differently. In natural environments, an observed decoupling of $\delta^{15}\text{N}$ and $\delta^{18}\text{O}$ values (i.e., a deviation from a parallel $\delta^{15}\text{N}$ and $\delta^{18}\text{O}$ evolution in the NO_3^- -pool) has been used to diagnose NO_3^- consumption and regeneration processes occurring simultaneously (e.g., Bourbonnais et al., 2012; Casciotti and McIlvin, 2007; Lehmann et al., 2003; Sigman et al., 2009; Wankel et al., 2009).

Major gaps remain in understanding microbial N (and O) isotope fractionation. For example, nearly all culture and field studies investigating the isotope dynamics of NO_3^- reduction focus on organotrophic denitrification. Despite the increasingly acknowledged importance of alternative fixed N elimination pathways, such as sulfur-driven denitrification or anammox, reports on the expression of their isotope effects on the ecosystem level do not exist.

There are several approaches to gain knowledge about N (and O) isotope fractionation. Laboratory culture experiments are of crucial importance to gain mechanistic understanding of single N transformation pathways and their associated isotope effects. There is, however, some uncertainty as to how scale up the outcomes and new insights of such experiments to a natural ecosystem. On the other hand, using an environment as a natural laboratory involves dealing with a complex network of simultaneous processes and players. In this thesis we chose the latter approach, using Lake Lugano as a natural model system.

1.4 Objectives and outline of the thesis

The main objectives of this work were to investigate the microbial processes that are responsible for fixed N elimination in Lake Lugano, to quantify the reaction rates, to link the community structures and biogeochemical activities, and to constrain the N and O isotope signatures in the water column to specific N cycling reactions. We chose Lake Lugano as a model system of an anthropogenically affected lake. Increased nutrient loadings, originating mainly from household sources, in the last century, has led to the eutrophication of the lake. Lake Lugano is located on the southern slopes of the Alps, at the Swiss-Italian border. A natural dam separates the lake into two narrow, elongated main basins. The northern basin is 288 m deep, with a major portion of the water body remaining anoxic throughout most of the past 40 years. The southern basin has a maximum depth of 95 m and is characterized by a monomictic mixing regime, with bottom water anoxia during summer and fall and re-oxygenation of the water column in winter.

This thesis focuses on processes taking place in the RTZ. In Lake Lugano this is the hypolimnetic zone (and the sediment) where dissolved O₂ concentrations drop below 1 μmol L⁻¹ and organisms start to use alternative electron acceptors. We use hydrochemical parameters (including N₂:Ar and dissolved N₂O concentrations), molecular microbiological phylogenetic analyses, results from water and sediment incubation experiments with ¹⁵N-labeled N-substrates, as well as natural abundance stable N and O isotope ratios of dissolved inorganic nitrogen (DIN) compounds (NO₃⁻, NH₄⁺, N₂O), and the isotopomeric composition of water column N₂O, to answer the following specific questions:

- Where does anammox take place (i) in the water column and (ii) within sediments, and (where) do we find anammox 16S rRNA gene sequences that indicate the presence of microorganisms that mediate anammox?
- Which organisms are responsible for anammox and denitrification? What is their relative abundance and how do they vary temporally and spatially?
- What are the respective rates of the different modes of N₂ production within the water column and in the sediments? What is the magnitude of the benthic DIN, N₂O, and N₂ fluxes and how variable are they?
- Are variations in the absolute denitrification rates a function of bottom water oxygenation?
- What exactly happens to the large amounts of NH₄⁺ that accumulate below the RTZ in the south basin water column? What are the modes of NH₄⁺ oxidation?

- What are the combined N-isotope effects of benthic N-cycle reactions on the N isotope composition of water column NO_3^- ?

This thesis is divided into four main parts, each of which is an individual manuscript. In the first part (chapter 2) we aimed at identifying the main processes responsible for fixed N elimination in the RTZ of the Lake Lugano north basin. Surprisingly, organotrophic denitrification seemed to be negligible. Instead, we identified a stable (both in terms of identity and abundance) anammox bacteria community in the water column, operating at low metabolic activity. We further discovered that these anammox bacteria coexist with sulfide-dependent denitrifiers, and that the latter catalyzed the dominant fixed N elimination pathway in the Lake Lugano north basin. The second part of this thesis (chapter 3) is directly based on the findings from the previous chapter. Here we examine the community N and O isotope effects associated with fixed N elimination in the Lake Lugano north basin. We found very low isotope enrichment factors (ϵ_{app}) and discuss in detail the possible levels and mechanisms of this apparent under-expression. We further confirmed the co-linearity between N and O isotope enrichment during NO_3^- reduction in an environment that is dominated by chemolithotrophic fixed N elimination pathways and speculate about the main enzyme catalyzing NO_3^- reduction in the Lake Lugano north basin.

In the third part (chapter 4) we focus on benthic N transformation rates in the southern basin of Lake Lugano, and the isotopic imprint in the overlying water column. We show that denitrification was the main benthic N_2 production pathway and that anammox and DNRA contributed only minor proportions of the total NO_3^- reduction. We further aimed at quantifying the partitioning between water column and sedimentary denitrification using two independent methods, i.e., a comparison between benthic N_2 production rate measurements and water column N_2 fluxes as well as the interpretation of water column stable isotope signatures using an end-member isotope approach. Both methods yielded consistent results.

In the fourth part (chapter 5) we examine and compare the N_2O biogeochemistry in the northern and southern basins. We use the findings of the previous chapters about general N transformation pathways and rates and gain additional information by invoking an even more complex parameter, i.e., the intramolecular ^{15}N distribution within the asymmetric N_2O molecule.

1 - References

- M. Alkhatib, M. F. Lehmann, and P. A. del Giorgio. The nitrogen isotope effect of benthic remineralization-nitrification-denitrification coupling in an estuarine environment. *Biogeosciences*, 9:1633–1646, 2012.
- S. M. An and W. S. Gardner. Dissimilatory nitrate reduction to ammonium (DNRA) as a nitrogen link, versus denitrification as a sink in a shallow estuary (Laguna Madre/Baffin Bay, Texas). *Marine Ecology Progress Series*, 237:41–50, 2002.
- P. Baertschi. Absolute ^{18}O content of standard mean ocean water. *Earth and Planetary Science Letters*, 31:341–344, 1976.
- C. C. Barford, J. P. Montoya, M. A. Altabet, and R. Mitchell. Steady-state nitrogen isotope effects of N_2 and N_2O production in *Paracoccus denitrificans*. *Applied and Environmental Microbiology*, 65:989–994, 1999.
- B. Baumann, M. Snozzi, J. R. van der Meer, and A. J. B. Zehnder. Development of stable denitrifying cultures during repeated aerobic-anaerobic transient periods. *Water Research*, 31:1947–1954, 1997.
- C. Bedard and R. Knowles. Physiology, biochemistry, and specific inhibitors of CH_4 , NH_4^+ , and CO oxidation by methanotrophs and nitrifiers. *Microbiological Reviews*, 53:68–84, 1989.
- E. Bock and M. Wagner. Oxidation of inorganic nitrogen compounds as an energy source. *Prokaryotes*, 2:457–495, 2006.
- J. Böttcher, O. Strebel, S. Voerkelius, and H.-L. Schmidt. Using isotope fractionation of nitrate-nitrogen and nitrate-oxygen for evaluation of microbial denitrification in a sandy aquifer. *Journal of Hydrology*, 114:413–424, 1990.
- A. Bourbonnais, M. F. Lehmann, D. A. Butterfield, and S. K. Juniper. Subseafloor nitrogen transformations in diffuse hydrothermal vent fluids of the Juan de Fuca Ridge evidenced by the isotopic composition of nitrate and ammonium. *Geochemistry Geophysics Geosystems*, 13, 2012.

- J. A. Brandes and A. H. Devol. Isotopic fractionation of oxygen and nitrogen in coastal marine sediments. *Geochimica et Cosmochimica Acta*, 61:1793–1801, 1997.
- J. A. Brandes, A. H. Devol, T. Yoshinari, D. A. Jayakumar, and S. W. A. Naqvi. Isotopic composition of nitrate in the central Arabian Sea and Eastern Tropical North Pacific: A tracer for mixing and nitrogen cycles. *Limnology and Oceanography*, 43:1680–1689, 1998.
- A. J. Burgin and S. K. Hamilton. Have we overemphasized the role of denitrification in aquatic ecosystems? A review of nitrate removal pathways. *Frontiers in Ecology*, 5:89–96, 2007.
- E. J. Carpenter, H. R. Harvey, B. Fry, and D. G. Capone. Biogeochemical tracers of the marine cyanobacterium *Trichodesmium*. *Deep-Sea Research*, 44:27–38, 1997.
- K. L. Casciotti and M. R. McIlvin. Isotopic analyses of nitrate and nitrite from reference mixtures and application to Eastern Tropical North Pacific waters. *Marine Chemistry*, 107:184–201, 2007.
- K. L. Casciotti, D. M. Sigman, M. Galanter Hastings, J. K. Böhlke, and A. Hilkert. Measurement of the oxygen isotopic composition of nitrate in seawater and freshwater using the denitrifier method. *Analytical Chemistry*, 74:4905–4912, 2002.
- K. L. Casciotti, D. M. Sigman, and B. B. Ward. Linking diversity and stable isotope fractionation in ammonia-oxidizing bacteria. *Geomicrobiology Journal*, 20:335–353, 2003.
- T. Dalsgaard, D. E. Canfield, J. Petersen, B. Thamdrup, and J. Acuña González. N₂ production by the anammox reaction in the anoxic water column of Golfo Dulce, Costa Rica. *Nature*, 422:606–608, 2003.
- C. A. Francis, J. M. Beman, and M. M. M. Kuypers. New processes and players in the nitrogen cycle - The microbial ecology of anaerobic and archaeal ammonia oxidation. *The ISME Journal*, 1:19–27, 2007.
- J. N. Galloway, J. D. Aber, J. W. Erisman, S. P. Seitzinger, R. W. Howart, E. B. Cowling, and B. J. Cosby. The nitrogen cascade. *BioScience*, 53:341–356, 2003.
- J. Granger, D. M. Sigman, M. F. Lehmann, and P. D. Tortell. Nitrogen and oxygen isotope fractionation during dissimilatory nitrate reduction by denitrifying bacteria. *Limnology and Oceanography*, 53:2533–2545, 2008.
- N. Gruber and J. N. Galloway. An Earth-system perspective of the global nitrogen cycle. *Nature*, 451:293–296, 2008.

- M. R. Hamersley, D. Woebken, B. Boehrer, M. Schultze, G. Lavik, and M. M. M. Kuypers. Water column anammox and denitrification in a temperate permanently stratified lake (Lake Rassnitzer, Germany). *Systematic and Applied Microbiology*, 32:571–582, 2009.
- A. B. Hooper and K. R. Terry. Hydroxylamine oxidoreductase of *Nitrosomonas* production of nitric-oxide from hydroxylamine. *Biochimica Et Biophysica Acta*, 571:12–20, 1979.
- S. G. Horrigan, J. P. Montoya, J. L. Nevins, and J. J. McCarthy. Natural isotopic composition of dissolved inorganic nitrogen in the Chesapeake Bay. *Estuarine, Coastal and Shelf Science*, 30:393–410, 1990.
- S. Hulth, R. C. Aller, D. E. Canfield, T. Dalsgaard, P. Engström, F. Gilbert, K. Sundbäck, and B. Thamdrup. Nitrogen removal in marine environments: Recent findings and future research challenges. *Marine Chemistry*, 94:125–145, 2005.
- S. Humbert, S. Tarnawski, N. Fromin, M.-P. Mallet, M. Aragno, and J. Zopfi. Molecular detection of anammox bacteria in terrestrial ecosystems: Distribution and diversity. *The ISME Journal*, 4:450–454, 2010.
- M. M. Jensen, M. M. M. Kuypers, G. Lavik, and B. Thamdrup. Rates and regulation of anaerobic ammonium oxidation and denitrification in the Black Sea. *Limnology and Oceanography*, 53:23–36, 2008.
- G. Junk and H. J. Swec. The absolute abundance of the nitrogen isotopes in the atmosphere and compressed gas from various sources. *Geochimica et Cosmochimica Acta*, 14:234–243, 1958.
- K. Kritee, D. M. Sigman, J. Granger, B. B. Ward, A. Jayakumar, and C. Deutsch. Reduced isotope fractionation by denitrification under conditions relevant to the ocean. *Geochimica et Cosmochimica Acta*, 92:243–259, 2012.
- M. M. M. Kuypers, A. O. Sliemers, G. Lavik, M. Schmid, B. B. Jørgensen, J. G. Kuenen, J. S. S. Damsté, M. Strous, and M. S. M. Jetten. Anaerobic ammonium oxidation by anammox bacteria in the Black Sea. *Nature*, 422:608–611, 2003.
- M. M. M. Kuypers, G. Lavik, D. Woebken, M. Schmid, B. M. Fuchs, R. Amann, B. B. Jørgensen, and M. S. M. Jetten. Massive nitrogen loss from the Benguela upwelling system through anaerobic ammonium oxidation. *Proceedings of the National Academy of Sciences of the United States of America (PNAS)*, 102:6478–6483, 2005.
- M. F. Lehmann, P. Reichert, S. M. Bernasconi, A. Barbieri, and J. A. McKenzie. Modelling nitrogen and oxygen isotope fractionation during denitrification in a

- lacustrine redox-transition zone. *Geochimica Et Cosmochimica Acta*, 67:2529–2542, 2003.
- M. F. Lehmann, D. M. Sigman, and W. M. Berelson. Coupling the $^{15}\text{N}/^{14}\text{N}$ and $^{18}\text{O}/^{16}\text{O}$ of nitrate as a constraint on benthic nitrogen cycling. *Marine Chemistry*, 88:1–20, 2004.
- M. F. Lehmann, D. M. Sigman, D. C. McCorkle, J. Granger, S. Hoffmann, G. Cane, and B. G. Brunelle. The distribution of nitrate $^{15}\text{N}/^{14}\text{N}$ in marine sediments and the impact of benthic nitrogen loss on the isotopic composition of oceanic nitrate. *Geochimica et Cosmochimica Acta*, 71:5384–5404, 2007.
- M. R. Lindsay, R. I. Webb, M. Strous, M. S. M. Jetten, M. K. Butler, R. J. Forde, and J. A. Fuerst. Cell compartmentalisation in planctomycetes: Novel types of structural organisation for the bacterial cell. *Archives of Microbiology*, 175:413–429, 2001.
- A. Mariotti, J. C. Germon, P. Hubert, P. Kaiser, R. Letolle, A. Tardieux, and P. Tardieux. Experimental determination of nitrogen kinetic isotope fractionation: Some principles; Illustration for the denitrification and nitrification processes. *Plant and Soil*, 62:413–430, 1981.
- M. J. McCarthy, P. J. Lavrentyev, L. Yang, L. Zhang, Y. Chen, B. Qin, and W. S. Gardner. Nitrogen dynamics and microbial food web structure during a summer cyanobacterial bloom in a subtropical, shallow, well-mixed, eutrophic lake (Lake Taihu, China). *Hydrobiologia*, 581:195–207, 2007.
- M. Mengis, S. L. Schiff, M. Harris, M. C. English, R. Aravena, R. J. Elgood, and A. MacLean. Multiple geochemical and isotopic approaches for assessing ground water NO_3^- elimination in a riparian zone. *Ground Water*, 37:448–457, 1999.
- J. P. Montoya, E. J. Carpenter, and D. G. Capone. Nitrogen fixation and nitrogen isotope abundances in zooplankton of the oligotrophic North Atlantic. *Limnology and Oceanography*, 47:1617–1628, 2002.
- A. Mulder, A. A. van de Graaf, L. A. Robertson, and J. G. Kuenen. Anaerobic ammonium oxidation discovered in a denitrifying fluidized bed reactor. *FEMS Microbiology Ecology*, 16:177–183, 1995.
- S. Otte, J. G. Kuenen, L. P. Nielsen, H. W. Paerl, J. Zopfi, H. N. Schulz, A. Teske, B. Strotmann, V. A. Gallardo, and B. B. Jørgensen. Nitrogen, carbon, and sulfur metabolism in natural *Thioploca* samples. *Applied and Environmental Microbiology*, 65:3148–3157, 1999.

- M. Poth and D. D. Focht. ^{15}N kinetic analysis of N_2O production by *Nitrosomonas europaea*: An examination of nitrifier denitrification. *Applied and Environmental Microbiology*, 49:1134–1141, 1985.
- J. Rockström, W. Steffen, K. Noone, A. Persson, F. S. Chapin, E. F. Lambin, T. M. Lenton, M. Scheffer, C. Folke, H. J. Schellnhuber, B. Nykvist, C. A. de Wit, T. Hughes, S. van der Leeuw, H. Rodhe, S. Sorlin, P. K. Snyder, R. Costanza, U. Svedin, M. Falkenmark, L. Karlberg, R. W. Corell, V. J. Fabry, J. Hansen, B. Walker, D. Liverman, K. Richardson, P. Crutzen, and J. A. Foley. A safe operating space for humanity. *Nature*, 461:472–475, 2009.
- C. J. Schubert, E. Durisch-Kaiser, B. Wehrli, B. Thamdrup, P. Lam, and M. M. M. Kuypers. Anaerobic ammonium oxidation in a tropical freshwater system (Lake Tanganyika). *Environmental Microbiology*, 8:1857–1863, 2006.
- S. Seitzinger, J. A. Harrison, J. K. Böhlke, A. F. Bouwman, R. Lowrance, B. Peterson, C. Tobias, and G. Van Drecht. Denitrification across landscapes and waterscapes: A synthesis. *Ecological Applications*, 16:2064–2090, 2006.
- G. Shearer, J. D. Schneider, and D. H. Kohl. Separating the efflux and influx components of net nitrate uptake by *Synechococcus* R2 under steady-state conditions. *Journal of General Microbiology*, 137:1179–1184, 1991.
- D. M. Sigman, J. Granger, P. J. DiFiore, M. F. Lehmann, R. Ho, G. Cane, and A. van Geen. Coupled nitrogen and oxygen isotope measurements of nitrate along the eastern North Pacific margin. *Global Biogeochemical Cycles*, 19, 2005.
- D. M. Sigman, P. J. DiFiore, M. P. Hain, C. Deutsch, Y. Wang, D. M. Karl, A. N. Knapp, M. F. Lehmann, and S. Pantoja. The dual isotopes of deep nitrate as a constraint on the cycle and budget of oceanic fixed nitrogen. *Deep-Sea Research*, 56:1419–1439, 2009.
- J. Simon and M. G. Klotz. Diversity and evolution of bioenergetic systems involved in microbial nitrogen compound transformations. *Biochimica et Biophysica Acta*, 1827:114–135, 2012.
- B. Thamdrup and T. Dalsgaard. Production of N_2 through anaerobic ammonium oxidation coupled to nitrate reduction in marine sediments. *Applied and Environmental Microbiology*, 68:1312–1318, 2002.
- B. Thamdrup, T. Dalsgaard, M. M. Jensen, O. Ulloa, L. Fariás, and R. Escobedo. Anaerobic ammonium oxidation in the oxygen-deficient waters off northern Chile. *Limnology and Oceanography*, 51:2145–2156, 2006.

- A. A. van de Graaf, A. Mulder, P. de Bruijn, M. S. M. Jetten, L. A. Robertson, and J. G. Kuenen. Anaerobic oxidation of ammonium is a biologically mediated process. *Applied and Environmental Microbiology*, 61:1246–1251, 1995.
- L. van Niftrik and M. S. M. Jetten. Anaerobic ammonium-oxidizing bacteria: Unique microorganisms with exceptional properties. *Microbiology and Molecular Biology Reviews*, 76:585–596, 2012.
- M. Voss, J. W. Dippner, and J. P. Montoya. Nitrogen isotope patterns in the oxygen-deficient waters of the Eastern Tropical North Pacific Ocean. *Deep-Sea Research*, 48:1905–1921, 2001.
- S. D. Wankel, C. Kendall, and A. Paytan. Using nitrate dual isotopic composition ($\delta^{15}\text{N}$ and $\delta^{18}\text{O}$) as a tool for exploring sources and cycling of nitrate in an estuarine system: Elkhorn Slough, California. *Journal of Geophysical Research*, 114, 2009.
- R. P. Wellman, F. D. Cook, and H. R. Krouse. Nitrogen-15: Microbiological alteration of abundance. *Science*, 161:269–270, 1968.
- J. Zopfi, M. E. Böttcher, and B. B. Jørgensen. Biogeochemistry of sulfur and iron in *Thioploca*-colonized surface sediments in the upwelling area off central Chile. *Geochimica et Cosmochimica Acta*, 72:827–843, 2008.
- W. G. Zumft. Cell biology and molecular basis of denitrification. *Microbiology and Molecular Biology Reviews*, 61:533–616, 1997.

CHAPTER 2

Anammox bacteria and sulfide-dependent denitrifiers coexist in the water column of a meromictic south-alpine lake

C. B. Wenk, J. Brees, J. Zopfi, M. Veronesi, A. Bourbonnais, C. J. Schubert, H. Niemann, and M. F. Lehmann

Limnology and Oceanography 2013, 58(1): 1-12
(doi:10.4319/lo.2013.58.1.0001)

Abstract

In addition to organotrophic denitrification, alternative pathways, such as anaerobic ammonium oxidation (anammox) or sulfide-dependent denitrification may be important modes for the removal of fixed nitrogen (N) from lakes. We used Lake Lugano as a model system to assess possible controls on the concurrence of multiple suboxic N₂ production pathways in a lacustrine water column. In the northern basin of Lake Lugano, concentration gradients of dissolved inorganic N (DIN) toward the hypolimnetic redox transition zone (RTZ) indicate ammonium oxidation and nitrate reduction occurring in close vicinity. Ammonium reaches undetectable levels 15 m below the depth of oxygen disappearance, indicating its anaerobic consumption. The presence of anammox bacteria was confirmed by 16S rRNA gene sequencing. Quantitative polymerase chain reaction (qPCR) revealed a maximum in anammox bacterial abundance at the same water depth where ammonium becomes exhausted. ¹⁵N-labeling experiments indicate that anammox activity within the Lake Lugano RTZ can contribute up to ~30% of total N₂ production. Incubation experiments with various potential electron donors - glucose, acetate, Mn(II), Fe(II), and H₂S - revealed that N₂ formation was sulfide-dependent and that organotrophic denitrification is only of minor importance for the elimination of fixed N from the Lake Lugano north basin. Maximum potential rates of anammox and chemolithotrophic denitrification were comparatively low but consistent with nutrient fluxes calculated from concentration gradients. This study provides evidence for the coexistence of anammox bacteria and sulfide-dependent denitrifiers in the stratified water column of a lacustrine environment.

2.1 Introduction

Increased nitrogen (N) loadings in lacustrine and coastal marine ecosystems from anthropogenic sources have resulted in excessive algal growth and increased rates of organic matter decomposition, which in turn can lead to oxygen (O₂) deficiency, or even anoxic water column conditions. N loading is partially mitigated by microbial processes that take place in redox transition zones (RTZs), both in the water column and within sediments. Organotrophic denitrification, i.e., the oxidation of organic carbon coupled to the reduction of nitrate (NO₃⁻) to dinitrogen gas (N₂), has for a long time been viewed as the only pathway for fixed N removal. However, recent observations (reviewed in Hulth et al., 2005) indicate that the canonical concepts of suboxic N₂ production are incomplete. Alternative pathways, such as anaerobic ammonium oxidation (anammox) or sulfide-dependent chemolithotrophic denitrification, were identified as important modes of fixed N elimination in aquatic ecosystems. The discovery of these pathways implies that we may have underestimated important N sinks within the global N cycle.

Bacteria performing anammox were first identified in a wastewater treatment system (Mulder et al., 1995) and later in natural environments (Thamdrup and Dalsgaard, 2002; Kuypers et al., 2003; Humbert et al., 2010). All anammox bacteria found to date belong to the order *Planctomycetales* and have been classified into five *Candidatus* genera: *Candidatus* Brocadia, *Candidatus* Kuenenia, *Candidatus* Scalindua, *Candidatus* Anammoxoglobus, and *Candidatus* Jettenia (e.g., review in Van Niftrik and Jetten, 2012). Recently, Kartal et al. (2011) resolved the complex enzymatic machinery of the N₂ forming anammox reaction $\text{NH}_4^+ + \text{NO}_2^- \rightarrow \text{N}_2 + 2 \text{H}_2\text{O}$ originally postulated by Van de Graaf et al. (1995). They showed that *Candidatus* Kuenenia stuttgartiensis first reduces nitrite (NO₂⁻) to nitric oxide (NO), which then reacts in a one-to-one stoichiometry with ammonium (NH₄⁺) to form hydrazine (N₂H₄), and finally N₂ (Kartal et al., 2011). Since its discovery, anammox has been shown to be an important driver for fixed N elimination in many marine ecosystems, such as the Black Sea (Kuypers et al., 2003; Jensen et al., 2008), the Golfo Dulce (Dalsgaard et al., 2003), or the upwelling regions off the coasts of Namibia (Kuypers et al., 2005) and Chile (Thamdrup et al., 2006)

Another alternative pathway for fixed N elimination is chemolithotrophic denitrification with sulfide as the electron donor. All nitrate-dependent sulfide oxidizers discovered so far in the environment belong to the classes of α -, β -, γ -, and ϵ -*Proteobacteria* (review in Shao et al., 2010). They can use reduced sulfur compounds such as sulfide (H₂S), elemental sulfur (S⁰), or thiosulfate (S₂O₃²⁻) as electron donors for the reduction of NO₃⁻ to NO₂⁻ and eventually to N₂. Chemolithotrophic denitrification coupled to H₂S oxidation has been shown to be operative in the water column of various marine settings, including the Gotland Deep in the Baltic Sea (Brettar

and Rheinheimer, 1991), the Mariager Fjord (Jensen et al., 2009), and the upwelling systems off the coasts of Namibia (Lavik et al., 2009) and Chile (Canfield et al., 2010). While the exact role of H_2S in controlling the relative importance of anammox vs. denitrification remains unknown, putative evidence indicates that H_2S inhibits the anammox reaction. Dalsgaard et al. (2003), for example, observed a decline in anammox activity toward the sulfidic bottom waters in the anoxic basin of Golfo Dulce (Costa Rica), and interpreted this as direct (or competitive) inhibition of anammox by H_2S . Similarly, Hannig et al. (2007) observed a shift from sulfide-dependent denitrification to anammox in the Gotland Deep (Central Baltic Sea) after lateral intrusions of oxygen-rich water and subsequent restabilization of the water column. They argued that this inflow event caused the oxidation of dissolved Mn(II) to particulate MnO_x , which subsequently settled to anoxic bottom waters and reacted with H_2S . This resulted in the spatial separation of NO_3^- and H_2S , favoring anammox over sulfide-dependent denitrification. In agreement with these interpretations, Jensen et al. (2008) showed in ^{15}N -labeling experiments that H_2S had a direct inhibiting effect on anammox activity in the Black Sea. In contrast to these findings, Kalyuzhnyi et al. (2006) showed in laboratory tests of a new wastewater treatment system that at least some anammox bacteria can tolerate H_2S .

So far, most studies on the global importance of anammox and sulfide-dependent denitrification have focused on marine ecosystems, while the role of lakes as a terrestrial sink of fixed N is still poorly constrained. Furthermore, modes of N_2 production other than organotrophic denitrification have barely been investigated in freshwater. To date, few studies have investigated sulfide-dependent denitrification (Burgin et al., 2012) or the importance of anammox bacteria in the water column of a lacustrine environment (Schubert et al., 2006; Hamersley et al., 2009), and none have addressed the influence of H_2S on anammox activity.

Lake Lugano is an excellent example of an anthropogenically affected lake and a hot-spot for redox-driven N transformations. Previous studies (Lehmann et al., 2004) revealed that this lake is an important sink for fixed N, mainly originating from household sources. Yet, pathways, rates, and microorganisms involved in suboxic N_2 production remain to be ascertained.

Here, we used the deep, meromictic northern basin of Lake Lugano as a model system to study possible interactions between various fixed N elimination pathways in the water column of a lacustrine water body. We predicted that the stable RTZ within the deep hypolimnion of the lake provides environmental conditions that are favorable for anammox bacterial activity. Furthermore, the close proximity of sulfidic bottom water to the RTZ likely makes this environment particularly suitable for sulfide-dependent denitrifiers. We used a combined geochemical and microbiological approach (1) to identify the dominant fixed N elimination pathways in the RTZ of the permanently stratified Lake Lugano north basin (denitrification vs. anammox), (2) to assess the effect of sulfide-dependent denitrification on anammox, and (3) to understand possible

environmental controls on the relative importance of the various fixed N elimination pathways. Our combined field and laboratory incubation data provide evidence that anammox bacteria and sulfide-dependent denitrifiers can coexist in the same water layer.

2.2 Methods

2.2.1 Study site and sampling

Lake Lugano is located in southern Switzerland on the Italian border at an altitude of 271 m above sea level (Fig. 2.1). The lake is separated into a permanently stratified northern basin and a monomictic southern basin by a natural dam. The northern basin has a maximum depth of 288 m and is surrounded by steep mountains that shield the lake from wind stress. Water samples were collected from the northern basin at a site (46.01°N , 9.02°E) south of the village of Gandria, close to the point of maximum water depth (Fig. 2.1). Samples were collected by hydrocast, using 5 liter or 10 liter Niskin bottles during sampling campaigns in 2009 (March, August, September, October, November, December), 2010 (January, March, August), and 2011 (July, September, October, November). For each sampling campaign, water was collected from up to 24 different depths.

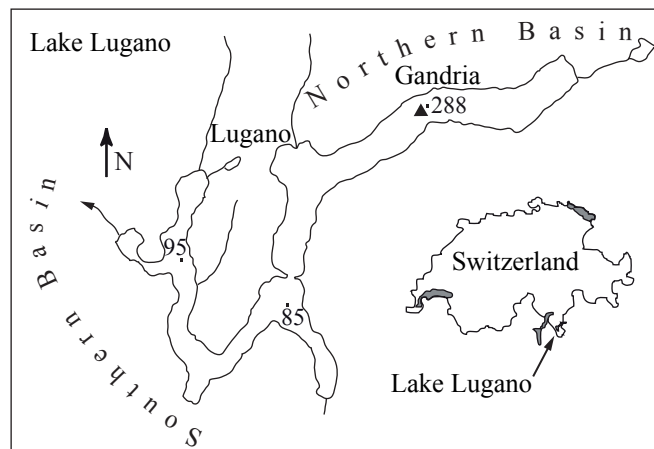


Figure 2.1: Map of Lake Lugano, showing the sampling station (black triangle) close to the point of maximum water depth (adapted from Barbieri and Polli, 1992).

2.2.2 Water column profiling and hydrochemical analyses

Profiles of temperature and dissolved O₂ concentrations were obtained with a conductivity, temperature, depth (CTD) device (Ocean Seven 316Plus, Idronaut), and O₂ concentrations were calibrated against Winkler titration measurements. The detection limit for dissolved [O₂] was 1 μmol L⁻¹.

Water from Niskin bottles was filtered through 0.45 μm syringe filters and separate aliquots were frozen for subsequent NO₂⁻, NO₃⁻, and NH₄⁺ analyses. NO₂⁻ and NO_x (i.e., NO₂⁻ + NO₃⁻) were quantified on a NO_x-Analyzer (Antek Model 745) by reduction to nitric oxide (NO) in a sodium iodide or acidic V₃⁺ solution, respectively, followed by chemiluminescence detection of NO (Garside, 1982; Braman and Hendrix, 1989). [NO₃⁻] was calculated from the difference of [NO_x] and [NO₂⁻]. NH₄⁺ concentrations were determined photometrically using the indophenol method.

For H₂S concentration measurements, 8 mL of fresh water sample were immediately amended with 0.4 mL zinc acetate (20% w:v) in order to fix dissolved H₂S. Sulfide was then quantified photometrically using the ethylene blue reaction according to Rees et al. (1971).

For dissolved N₂:Ar measurements, sample water from Niskin bottles was filled directly into 12 mL exetainers (Labco). Overflow of at least three exetainer volumes was assured to avoid N₂ contamination from air. After addition of 0.1 mL HgCl₂ (5% w:v) (as precipitate in the caps) to stop microbial activity, exetainers were sealed without headspace. Samples were taken in triplicate and stored underwater close to in situ temperatures. Samples were analyzed within 3 days after sampling using a membrane inlet mass spectrometer (MIMS, Pfeiffer Vacuum Prisma™), as described by Kana et al. (1994), in line with a copper furnace at 650°C to remove O₂. N₂ saturation is reported as the N₂:Ar ratio of the sample divided by the N₂:Ar ratio at equilibrium for a given temperature, calculated according to Weiss (1970).

2.2.3 Flux calculations

In 2009 (August, October) and 2010 (January) vertical NH₄⁺ and NO₃⁻ fluxes in the water column were calculated according to the following equation:

$$F_Z = -K_Z \times \frac{dC}{dz} \quad (2.1)$$

where F_Z is the vertical solute flux, K_Z is the vertical eddy diffusivity, and $\frac{dC}{dz}$ is the concentration gradient. The vertical eddy diffusivity is a function of the buoyancy frequency (Brunt-Väisälä frequency) and can be approximated as (Gargett, 1984):

$$K_Z = a_0 \times \left(-\frac{g}{\rho_Z} \frac{d\rho}{dz} \right)^{-0.5} \quad (2.2)$$

where g is the gravitational constant, ρ_Z is the density at a given depth z , and $\frac{d\rho}{dz}$ is the density gradient at this depth. The factor a_0 was estimated as described by Zopfi et al. (2001). Briefly, we combined Eqs. 2.1 and 2.2 (substituting K_Z) and solved for a_0 . a_0 is a system-specific constant. Thus, we can use the flux of any given solute at any given depth (F_Z), together with the density (ρ_Z), and the density gradient at this depth ($\frac{d\rho}{dz}$) to determine a_0 . In this study we approximated a_0 based on core-incubation experiment-derived nutrient fluxes (F_Z) at the sediment-water interface in the Lake Lugano south basin during stratification. The average estimates for a_0 ranged from 0.00028 cm² s⁻² (beginning of stratification) to 0.00014 cm² s⁻² (maximum stratification). The lower value (0.00014 cm² s⁻²), which is consistent with a_0 values reported for a restricted basin (Gargett, 1984), was applied to the permanently stratified Lake Lugano north basin. Vertical eddy diffusivities (K_Z) were then calculated for a depth interval above and below the RTZ and resulted in average values of 1.48 and 2.07 m² d⁻¹, respectively. These values for K_Z are well within the range of previously reported vertical diffusivities for the Lake Lugano north basin (Wüest et al., 1992).

2.2.4 Phylogenetic analysis

In 2009 (March, August, October) and 2010 (January, August) suspended particulate organic matter from selected depths was collected on 0.2 μm polycarbonate membrane filters (Cyclopore, Whatman, Art.-No. 7060-4702) by filtration of 500 mL of lake water. The filters were immediately frozen and stored at -70°C until deoxyribonucleic acid (DNA) extraction (FastDNA[®] SPIN Kit for Soil, MP Biomedicals). Anammox bacteria were detected by a nested polymerase chain reaction (PCR) approach: The extracted DNA was first subjected to a PCR using the primer pair Pla46f (Neef et al., 1998) and Univ1390r (Zheng et al., 1996). The obtained PCR product was then subjected to a second PCR with primers Amx368f (Schmid et al., 2003) and Amx820r (Schmid et al., 2000) targeting anammox bacterial 16S ribosomal ribonucleic acid (rRNA) genes. For selected samples, fresh PCR products from this second step were cloned in *Escherichia coli* using a TOPO[®] TA cloning[®] kit (Invitrogen), and 100 clones per sample were examined. Plasmid amplifications were purified (Invitex) and subsequently digested with Msp1 (Promega). Based on the restriction fragment length pattern, a total of 24 different inserts were selected for sequencing (Eurofins MWG Operon). Sequences have been deposited in EMBL-Bank under accession numbers HE775113 - HE775126. Sequence alignment and phylogenetic analyses were done in

Molecular Evolutionary Genetics Analysis (MEGA) software version 4.0 (Tamura et al., 2007).

2.2.5 Quantitative polymerase chain reaction (qPCR)

Anammox bacterial 16S rRNA gene copy numbers were determined by SYBR Green qPCR with anammox-specific primers A438f (5'GTCRGGAGTTADGAAATG3') and A684r (5'ACCAGAAGTTCCACTCTC3') (Humbert et al., 2012). The reaction mixture consisted of 0.5x SensiMixPlus SYBR[®] qPCR master mix (Quantace), 1200 nmol L⁻¹ of A438f, 300 nmol L⁻¹ of A684r, and 10% v:v of template DNA. Amplification was done on a Rotor-gene[™] 3000 (Corbett Research) in 10 μ L volumes using the following conditions: Initial activation at 95°C for 15 min, followed by 40 cycles of denaturation at 95°C for 30 s, annealing at 55.5°C for 15 s and elongation at 72°C for 30 s. Samples and standards were analyzed in triplicate, and control reactions without template were included in every run. Standard curves were prepared from serial dilution of a plasmid preparation of a *Brocadia*-related clone (Humbert et al., 2012) or an anammox clone from Lake Lugano (HE775126). The amplification efficiency was 0.95 and single-peak melting curve derivatives were obtained after 40 cycles. The amplicon length was additionally verified by agarose gel electrophoresis.

For the quantification of *nirS* genes, diluted DNA samples were amplified with the primer pair 2F and 3R (Braker et al., 1998), following the protocol in Chon et al. (2011) and adapted by A. Bourbonnais (unpubl.). The reaction mixture consisted of 0.5x SsoFast[™] EvaGreen[®] Supermix, 500 nmol L⁻¹ of 2F, 500 nmol L⁻¹ of 3R, and 10% v:v of template DNA. Amplification was done on a Bio-Rad's CFX96 system in 20 μ L using the following conditions: Initial activation at 98°C for 2 min, followed by 45 cycles of denaturation at 98°C for 1 s and annealing/elongation at 67°C for 5 s. Standard curves were prepared by serial dilution of a plasmid preparation of a *nirS* clone from hydrothermal vent fluids from the Juan de Fuca Ridge, as described in A. Bourbonnais (unpubl.). All samples and standards were analyzed in triplicate. The amplification efficiency ranged between 0.95 and 1.05, and single-peak melting curves were obtained after 45 cycles. The amplicon length was additionally verified by agarose gel electrophoresis.

2.2.6 ¹⁵N incubation experiments

¹⁵N incubations were conducted in 2011 (July, September, October, November), following the protocol previously described by Dalsgaard et al. (2003) with some modifications. Briefly, 160 mL serum bottles (Wheaton, Art.-No. 216-3012) were filled directly from Niskin bottles, allowing two to three volumes of overflow before sealing them bubble-free with halo-butyl rubber stoppers that had been kept under helium-atmosphere after cleaning and anoxification in boiling water for 8 hours. In

order to minimize the risk of O₂ contamination during sampling, only two thirds of the water from a 10 L Niskin bottle were used for the incubations. The serum bottles were stored in the dark and submerged in water at in situ temperature prior to ¹⁵N-label addition. A 10 mL helium (He) headspace was introduced to all samples, within 6 hours after sampling, and ¹⁵N-labeled substrates and various electron donors were added from freshly prepared anoxic stock solutions. In October 2011, potential denitrification rates were measured upon addition of a) 1.7 μmol L⁻¹ ¹⁵NO₃⁻ (> 99% ¹⁵N-KNO₃, Spectra Stable Isotopes) and b) 1.7 μmol L⁻¹ ¹⁵NO₃⁻ plus 10 μmol L⁻¹ H₂S. In November 2011, the incubations were amended with a) 10 μmol L⁻¹ ¹⁵NH₄⁺ (> 99% ¹⁵N-NH₄Cl, Spectra Stable Isotopes) and b) 10 μmol L⁻¹ ¹⁵NH₄⁺ plus 5 μmol L⁻¹ NO₂⁻. For the July and September 2011 experiments, ¹⁵N-label and other compounds were added as shown in Table 2.1. Fe(II) and Mn(II) were added as FeSO₄ and MnCl₂, respectively. Each treatment was run in replicates, and several blank controls without any label addition were included. All samples were submerged in water and incubated in the dark at 7°C, close to the in situ temperature. After equilibration overnight, the headspace was analyzed daily for ¹⁵N-N₂ production (29:28 and 30:28 mass ratios) using an isotope ratio mass spectrometer (Delta V Advantage, Thermo Scientific). Denitrification and anammox rates were calculated according to the isotope pairing equations of Nielsen (1992) and Thamdrup et al. (2006). The detection limit for the rate measurements was estimated from incubations that were run as blanks (i.e., no label addition, but not killed). All blank incubations were treated the same way as the incubations with ¹⁵N-label addition, and potential anammox and denitrification rates were calculated accordingly. The detection limit was defined as the average rate calculated from the slopes of the linear regression lines of the blank incubations plus one standard deviation. This approach includes all uncertainties such as sample treatment variability, analytical precision, and instrument drift. Accordingly, detection limits for anammox and denitrification rates were 2.4 nmol N₂ L⁻¹ d⁻¹ and 7.1 nmol N₂ L⁻¹ d⁻¹, respectively.

2.3 Results

2.3.1 Water column hydrochemistry

Photosynthetic activity from April onwards led to an O₂ maximum at ~10 m depth and to nitrate-limiting conditions in the surface water during summer and fall (Figs. 2.2, 2.3). Thermal stratification during summer months caused a density gradient at ~15 m depth, limiting the supply of O₂ to deeper water depths (Fig. 2.2). A pronounced local O₂ concentration minimum, concomitantly with a NO₂⁻ and NH₄⁺ concentration peak at this depth, indicated enhanced microbial respiration and increased nutrient turnover. For all sampling campaigns, hypolimnetic O₂ concentra-

tions systematically decreased with depth and reached values $< 1 \mu\text{mol L}^{-1}$ between 125 and 135 m (Fig. 2.3). The anoxic hypolimnion below 150 m depth was sulfidic with H_2S concentrations of up to $12 \mu\text{mol L}^{-1}$ (Fig. 2.3). Nitrate concentrations decreased from approximately $30 \mu\text{mol L}^{-1}$ at 15 m depth to undetectable levels within the RTZ. Highest NH_4^+ concentrations ($\sim 40 \mu\text{mol L}^{-1}$) were measured in near-bottom waters. The decline in NH_4^+ concentrations from the bottom of the lake basin toward the RTZ indicated ammonium oxidation below the depth of O_2 disappearance (i.e., $< 1 \mu\text{mol L}^{-1}$) (Figs. 2.3, 2.4). Nitrite did not accumulate in the anoxic water column. Concentrations were $< 0.02 \mu\text{mol L}^{-1}$ below 50 m depth (Fig. 2.3).

Measured $\text{N}_2:\text{Ar}$ profiles (Fig. 2.3) revealed that the deep hypolimnion was oversaturated (relative to equilibrium saturation with the atmosphere) with respect to N_2 . Maximum N_2 oversaturation reached 6% in the deep hypolimnion, which is markedly higher than observed in other natural aquatic systems (Fuchsman et al., 2008).

2.3.2 Molecular analyses

We could detect anammox bacterial 16S rRNA genes in all samples from below the RTZ by nested PCR (data not shown). Furthermore, we established clone libraries for selected samples in 2009 (March, August, October) and 2010 (January, August). All retrieved sequences were highly similar ($> 99\%$), suggesting that there was no significant seasonal variability with regard to the phylogenetic composition of the anammox guild (Fig. 2.5). Similarly, we did not find any depth-dependent genetic variability. All sequenced Lake Lugano clones branched within the anammox group

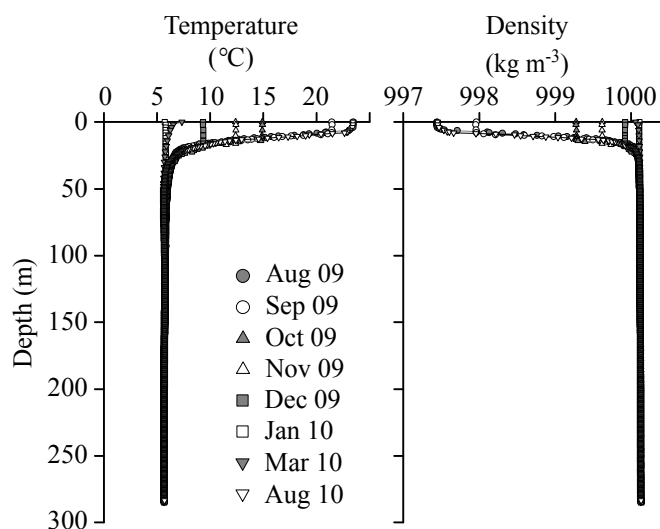


Figure 2.2: Temperature and density profiles for the Lake Lugano north basin.

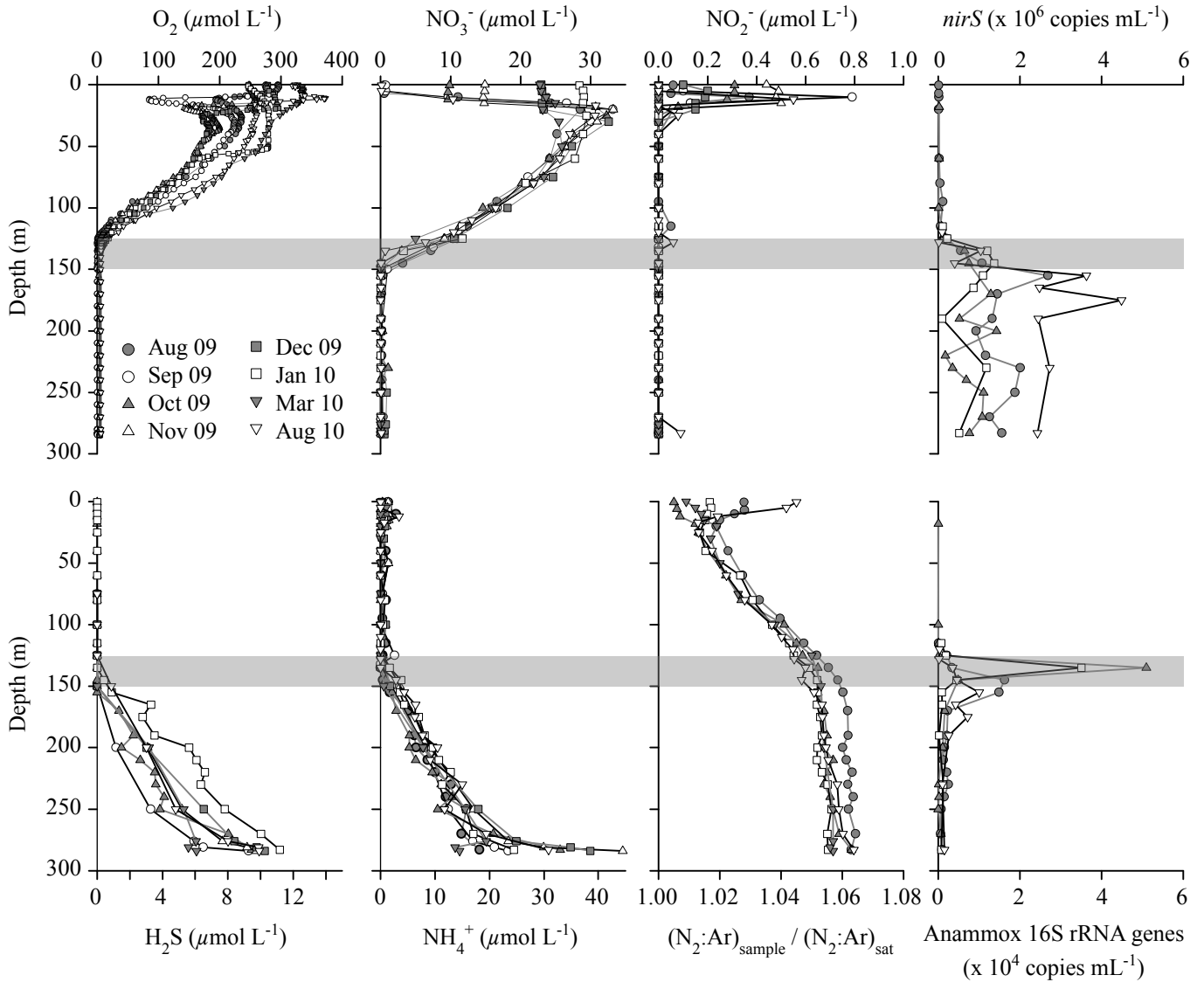


Figure 2.3: Water column profiles of dissolved oxygen, nitrate, nitrite, ammonium, and sulfide concentrations, as well as N₂:Ar ratios, and *nirS* and anammox bacteria 16S rRNA gene copy numbers in the northern basin of Lake Lugano. The suboxic and non-sulfidic water layer is indicated by a grey bar.

and formed a separate cluster together with anammox bacteria 16S rRNA gene sequences from other freshwater environments (Fig. 2.5).

Quantification of anammox bacterial 16S rRNA gene copies in the water column was done by qPCR at four occasions. In October 2009 and January 2010 we observed an anammox bacteria maximum at 135 m depth with 5.1×10^4 and 3.5×10^4 copies mL^{-1} , respectively (Fig. 2.3). In August 2009 and 2010, anammox bacteria peaked at 145 m (1.6×10^4 copies mL^{-1}) and at 155 m depth (1.0×10^4 copies mL^{-1}), respectively (Fig. 2.3). Accordingly, the depth segment of maximum anammox bacterial abundance was always 10 to 15 m below the depth of O_2 disappearance and corresponded to the depth where the concentration gradients indicate active NO_3^- and NH_4^+ consumption (Figs. 2.3, 2.4).

To estimate the relative importance of anammox and denitrification, we used a similar approach as in Ward et al. (2009). We compared the anammox bacteria 16S rRNA gene abundance to the copy numbers of *nirS*, the functional gene encoding the enzyme that catalyzes the reduction of NO_2^- to NO gas. Our results showed that *nirS* genes were at least two orders of magnitude more abundant than the anammox 16S rRNA genes (Fig. 2.3), suggesting that anammox bacteria play a much less important role in the water column compared to denitrifying bacteria. Furthermore, we found high copy numbers of *nirS* genes (maximum of 4.5×10^6 copies mL^{-1} in August 2010 at 175 m depth) throughout the anoxic part of the water column, whereas anammox bacteria were mainly found in the lower part of the chemocline.

2.3.3 ^{15}N incubation experiments

During the first ^{15}N incubation experiments in 2011 (July, September) with different combinations of $^{15}\text{NO}_3^-$, $^{15}\text{NH}_4^+$, and NO_2^- amendments (Table 2.1), the production of $^{29}\text{N}_2$ and $^{30}\text{N}_2$ (and thus anammox and denitrification rates) remained below the detection limit. In order to test for potential substrate limitation, we performed a series of additional ^{15}N incubation experiments, by adding various possible electron donors for the reduction of NO_3^- (Table 2.1). The addition of glucose, acetate, Fe(II), and Mn(II) did not significantly enhance potential denitrification. Upon the addition of $10 \mu\text{mol L}^{-1}$ H_2S , however, potential denitrification increased (Table 2.1). Additional experiments with sulfite (SO_3^{2-}), a reduced sulfur species less commonly used by microorganisms, and with thiosulfate ($\text{S}_2\text{O}_3^{2-}$), an intermediate in the microbial sulfur cycle were carried out. In the incubations where $^{15}\text{NO}_3^-$ and SO_3^{2-} were added, no production of ^{15}N -labeled N_2 was observed, whereas the addition of $\text{S}_2\text{O}_3^{2-}$ clearly stimulated N_2 production (Table 2.1).

In October 2011, we measured potential denitrification rates under sulfide-replete conditions (addition of $10 \mu\text{mol L}^{-1}$ H_2S) throughout the water column (Fig. 2.6). Denitrification rates were undetectable above 130 m depth and then increased to $91.5 \pm 32 \text{ nmol N}_2 \text{ L}^{-1} \text{ d}^{-1}$ at 160 m depth (Fig. 2.6). Excess ^{15}N - N_2 generally increased

linearly over time in the incubations with added H_2S , and remained close to the detection limit in the control experiments without H_2S (Fig. 2.7). Potential anammox rates were estimated from the same set of experiments (i.e., with $^{15}\text{NO}_3^-$ and H_2S additions), according to Thamdrup et al. (2006). Anammox bacteria were only active in a well-confined zone between 135 and 145 m depth. There, maximum potential anammox rates were $14.5 \pm 3.0 \text{ nmol N}_2 \text{ L}^{-1} \text{ d}^{-1}$. Hence, potential denitrification rates always exceeded anammox rates by at least a factor of two (Fig. 2.6). In November 2011, when we determined anammox in $^{15}\text{NH}_4^+$ incubation experiments without H_2S addition, anammox rates remained below the detection limit throughout the RTZ between 125 and 150 m depth (data not shown). The inactivity of anammox bacteria under sulfide-limited conditions in November, together with the fact that anammox was detected after H_2S addition during the previous sampling campaign, suggests a direct or indirect H_2S dependence of anammox in Lake Lugano (see Discussion).

2.4 Discussion

2.4.1 Hydrochemical evidence for fixed N elimination in the RTZ

Anoxia in the deep hypolimnion of the Lake Lugano north basin has prevailed throughout most of the last 40 years, with the exception of two exceptionally cold winters between 2004 and 2006, when a complete mixing of the water column occurred (CIP AIS, 2005, 2006; Holzner et al., 2009). During the following years, temperature gradients re-developed and since 2009 quasi-steady-state conditions seem to have re-established (Fig. 2.3; M. F. Lehmann unpubl.). The stratification of the water column in combination with aerobic degradation of sinking organic matter, led again to a stable oxycline between 125 and 135 m depth and an essentially permanent RTZ (Figs. 2.2, 2.3). The NO_3^- concentration gradients toward the RTZ suggest that NO_3^- is used as an alternative electron acceptor in the suboxic or anoxic part of the RTZ. The observed N_2 oversaturation in the anaerobic part of the water column is consistent with microbial fixed N reduction to N_2 . The linear gradients of normalized $\text{N}_2:\text{Ar}$ ratios indicate N_2 production at and below the RTZ (where we find maximum excess N_2 concentrations), with a flux of N_2 toward the epilimnion. Ammonium is released from organic matter decomposition mainly in the sediments. The decline of NH_4^+ concentrations toward the RTZ to levels below the detection limit, indicate NH_4^+ consumption in the same water mass where NO_3^- is being consumed. Thus, while the hydrochemical profiles clearly document that fixed N is turned over into N_2 , they are ambiguous with regard to the possible processes that lead to N_2 production: Denitrification, coupled nitrification-denitrification or anammox. The disappearance of NH_4^+ 10 to 15 m below the depth of undetectable O_2 levels (Figs. 2.3, 2.4) suggests an anaerobic mode of ammonium oxidation (i.e., anammox). In the next sections,

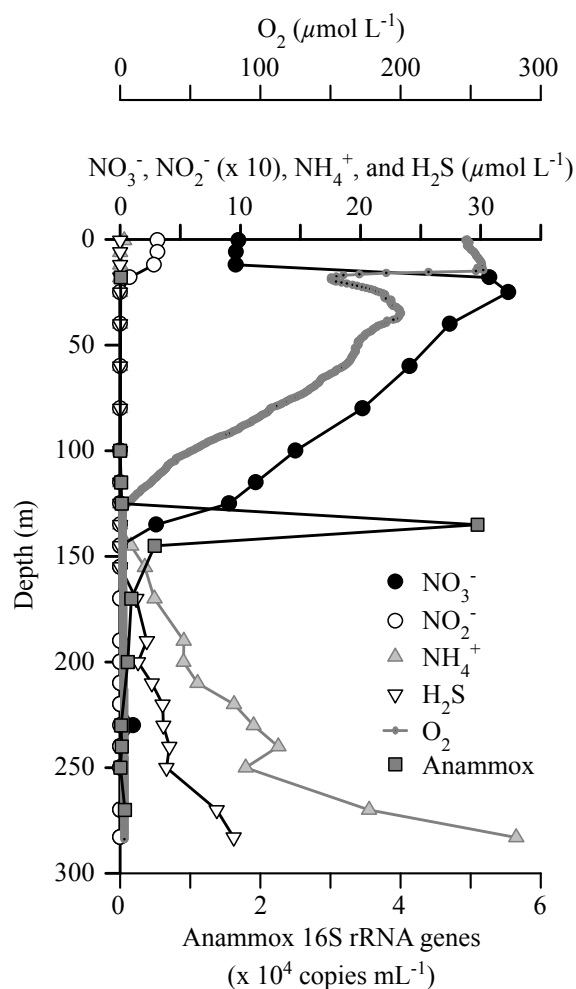


Figure 2.4: Concentrations of dissolved oxygen, nitrogen compounds, and sulfide, as well as anammox 16S rRNA gene copy numbers in October 2009 (Excerpt from Fig. 2.3).

we will discuss the molecular (qualitative) and ¹⁵N-label (quantitative) evidence for both anammox and denitrification as the likely origin for the excess N₂ in the water column, and we will elucidate the possible environmental controls (e.g., electron donor limitation) on these two fixed N elimination pathways in the Lake Lugano north basin.

2.4.2 Anammox bacteria in the RTZ: Diversity, abundance, and activity

Phylogenetic analysis of extracted DNA from the water column, and qPCR results confirm the presence of anammox bacteria right where NH_4^+ and NO_3^- profiles predict anaerobic ammonium oxidation (Figs. 2.4, 2.5). Freshwater systems seem to display a larger diversity of anammox bacteria, compared to marine water columns, where *Candidatus Scalindua* dominates the anammox bacteria community. Hamersley et al. (2009), for example, recovered sequences from Lake Rassnitzer, which are closely related to *Candidatus Scalindua*, *Candidatus Brocadia*, and *Candidatus Kuenenia*. In contrast, the anammox bacterial 16S rRNA gene sequences retrieved from the Lake Lugano north basin are most closely related to *Candidatus Brocadia* but form a separate cluster together with clones previously detected in water columns and sediments of other freshwater systems, such as Lake Kitaura (AB509331-AB509332), Lake Biwa (AB522718), Lake Taihu (GQ148894), Yodo River (AB522729) or the Songhua Delta freshwater wetland (GU084034) (Fig. 2.5). Together with these clones, Lake Lugano anammox bacteria might form a freshwater-specific group. Only little variation in the phylogenetic composition of the Lake Lugano anammox guild was observed between different sampling depths and dates, which may reflect the prevailing stable environmental conditions and the limited niche diversity in the water column.

Anammox bacteria abundance data show that they preferentially grow in a 15 m thick layer, expanding from just below the depth of O_2 disappearance to the beginning of the sulfidic water column (Figs. 2.3, 2.4). The absolute anammox bacteria cell numbers varied not only with depth but also between sampling dates. Maximum abundance of recovered anammox 16S rRNA genes was highest in October 2009 (5.1×10^4 copies mL^{-1}) and lowest in August 2010 (1.0×10^4 copies mL^{-1}). This is within the range of previously reported maximum anammox bacteria cell counts in Lake Rassnitzer ($2.7 - 5.2 \times 10^4 \text{ mL}^{-1}$) (Hamersley et al., 2009) and in marine environments ($1.3 - 2.2 \times 10^4 \text{ mL}^{-1}$) (Kuypers et al., 2003, 2005; Hannig et al., 2007). It should be noted, however, that anammox cell abundance in this study was determined by quantitative PCR (Humbert et al. 2012) and not by direct cell counts. In theory, anammox cell abundances derived from 16S rRNA gene copy numbers may yield erroneous results, because a bacterial cell might have more than one 16S rRNA gene copy. While this may be a problem with fast-growing bacterial strains (Klappenbach et al., 2000), it should not be an issue in the case of anammox bacteria that have a comparably slow doubling time of about 2 weeks in bioreactors under optimal conditions (Strous et al., 1999) and probably an even longer doubling time in the natural environment.

Although maximum anammox bacterial cell abundances determined for the Lake Lugano water column were within the range of those in other aquatic environments, the anammox-driven N turnover was low. For comparison, maximum rates for Lake

Tanganyika were reported to be $240 \text{ nmol N}_2 \text{ L}^{-1} \text{ d}^{-1}$ (Schubert et al., 2006) and in Lake Rassnitzer anammox rates reached up to $540 \text{ nmol N}_2 \text{ L}^{-1} \text{ d}^{-1}$ (Hamersley et al., 2009). Maximum anammox N_2 production rates in marine environments range between 17 and $430 \text{ nmol N}_2 \text{ L}^{-1} \text{ d}^{-1}$ (Dalsgaard et al., 2003; Kuypers et al., 2005; Thamdrup et al., 2006). In Lake Lugano, potential anammox rates were only measurable in October 2011 when we added H_2S to the ^{15}N -label incubations throughout the water column. Potential anammox rates then reached a maximum of $14.5 \pm 3.0 \text{ nmol N}_2 \text{ L}^{-1} \text{ d}^{-1}$, which is still at the lower end of reported values from aquatic environments. From these results we conclude that anammox bacteria, although present in the water column throughout the year, 1) overcome limiting conditions only episodically under favorable conditions, 2) may be active at low rates and on a temporal scale that is barely covered by our sampling scheme, and 3) seem to play only a minor role in the fixed N budget of Lake Lugano.

2.4.3 Sulfide-dependent denitrification is the dominant fixed N elimination process in the RTZ

Similar to anammox rates, denitrification was below detection limit in all incubations under in situ conditions when only $^{15}\text{NO}_3^-$ was added, suggesting that the process was electron-donor limited. Surprisingly, results from ex situ incubations with the addition of carbon substrates (glucose and acetate) indicate that organotrophic denitrification did not play a major role in fixed N removal from the water column (Table 2.1). Only after a lag phase of more than 60 hours, N_2 production was measurable in these C-source amended incubations (data not shown). After the initial lag phase, produced $^{15}\text{N-N}_2$ increased exponentially, indicating growth of an organotrophic denitrifying community in our incubations. From this non-linear N_2 production we conclude that organotrophic denitrifiers are present in the water column, but only at low abundances. To test for chemolithotrophic denitrification, we added Fe(II) , Mn(II) , and H_2S as electron donors to the $^{15}\text{NO}_3^-$ incubations. Yet, only upon the addition of H_2S , N_2 concentrations increased linearly (Table 2.1, Fig. 2.7). Sulfide, however, may not have stimulated denitrification directly (i.e., sulfide-oxidation coupled to denitrification), but could have affected denitrification indirectly as an effective O_2 scavenger that generated sufficiently reduced conditions for organotrophic denitrification. To exclude this possibility, we added $100 \mu\text{mol L}^{-1} \text{ Fe(II)}$ and $20 \mu\text{mol L}^{-1} \text{ SO}_3^{2-}$, respectively, as alternative O_2 buffers. Although $100 \mu\text{mol L}^{-1} \text{ Fe(II)}$ and $20 \mu\text{mol L}^{-1} \text{ SO}_3^{2-}$ have an O_2 buffering capacity equivalent to $10 \mu\text{mol L}^{-1}$ and $5 \mu\text{mol L}^{-1} \text{ H}_2\text{S}$, respectively, denitrification rates remained undetectable in both incubations (Table 2.1). To finally test whether H_2S is the electron donor that primarily drives denitrification in the Lake Lugano north basin, $\text{S}_2\text{O}_3^{2-}$, an intermediate in the microbial sulfur cycle, was added to the $^{15}\text{NO}_3^-$ incubations. The fact that N_2 production rates in those experiments were

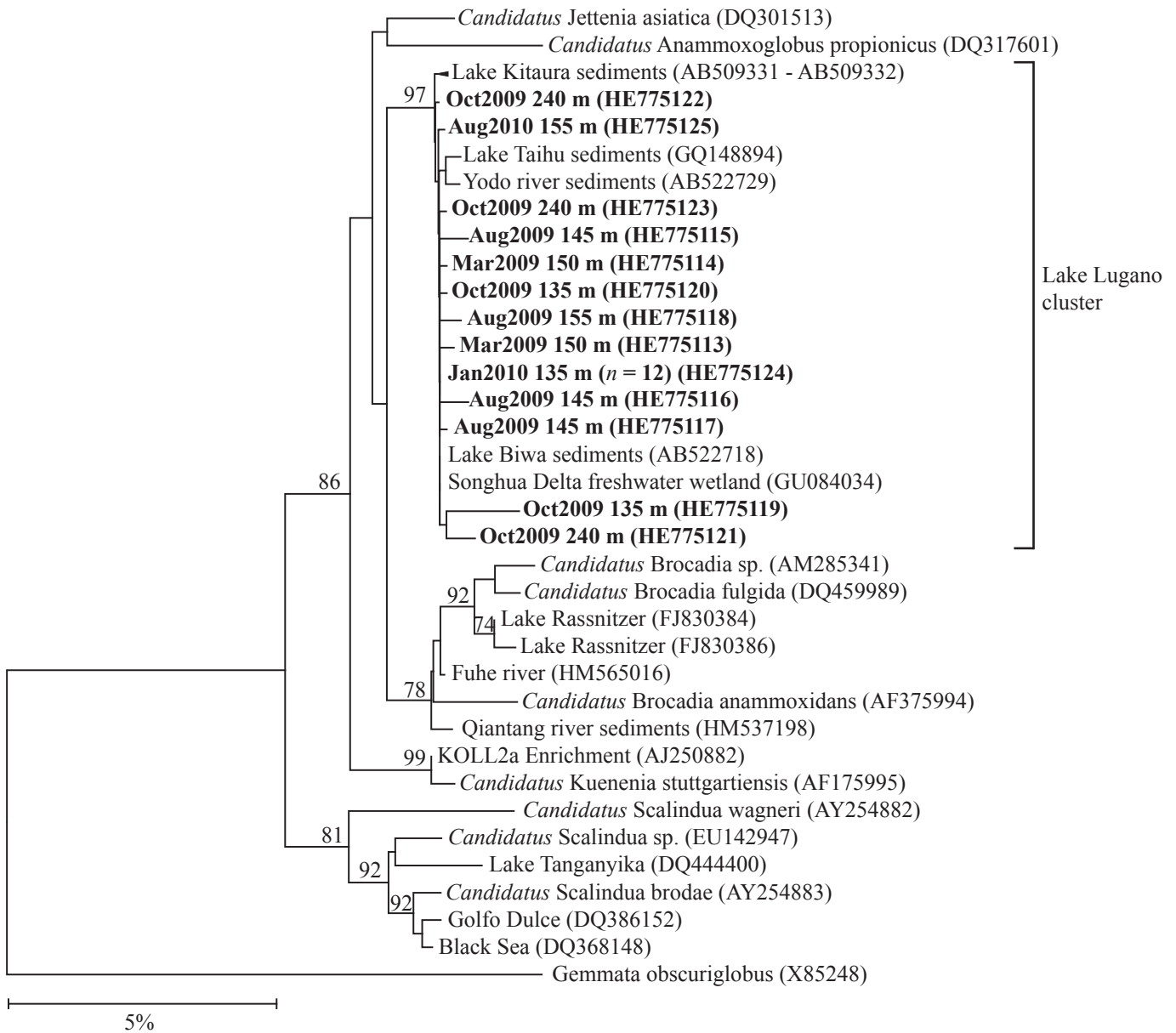


Figure 2.5: Neighbor-Joining phylogenetic tree of anammox bacterial 16S rRNA gene sequences retrieved from Lake Lugano (in bold) and other aquatic environments. The scale bar represents 5% sequence divergence. Bootstrap values > 70 based on 1000 replications are shown at the branching nodes. Sequence names are followed by their EMBL-Bank accession numbers in parentheses. ($n = 12$) indicates that the same sequence (HE775124) was recovered 12 times from different months and depths.

Table 2.1: Potential rates of denitrification and anammox determined using ex situ ^{15}N -label incubation experiments. In July and September 2011, water from the RTZ was incubated with different additions of ^{15}N -labeled and other compounds for 60 hours. Numbers in parentheses represent concentrations in $\mu\text{mol L}^{-1}$. Rates are given in $\text{nmol N}_2 \text{ L}^{-1} \text{ d}^{-1} \pm$ standard error of replicate incubations. nd = not detectable.

Sampling date	Depth (m)	Compounds added	Denitrification rate ($\text{nmol N}_2 \text{ L}^{-1} \text{ d}^{-1}$)	Anammox rate ($\text{nmol N}_2 \text{ L}^{-1} \text{ d}^{-1}$)
12 July 2011	150	$^{15}\text{NO}_3^-$ (20)	nd	nd
		$^{15}\text{NH}_4^+$ (20)	-	nd
		$^{15}\text{NH}_4^+$ (20) + NO_2^- (2)	-	nd
		$^{15}\text{NO}_3^-$ (20) + glucose (20)	nd	nd
		$^{15}\text{NO}_3^-$ (20) + acetate (20)	nd	nd
		$^{15}\text{NO}_3^-$ (20) + Fe(II) (5)	nd	nd
		$^{15}\text{NO}_3^-$ (20) + Mn(II) (2)	nd	nd
		$^{15}\text{NO}_3^-$ (20) + H_2S (10)	46.6 ± 11.7	nd
12 September 2011	152	$^{15}\text{NO}_3^-$ (10)	nd	nd
		$^{15}\text{NH}_4^+$ (10)	-	nd
		$^{15}\text{NH}_4^+$ (10) + NO_2^- (5)	-	3.4 ± 2.1
		$^{15}\text{NO}_3^-$ (10) + glucose (20)	nd	nd
		$^{15}\text{NO}_3^-$ (10) + Fe(II) (20)	nd	nd
		$^{15}\text{NO}_3^-$ (10) + Fe(II) (100)	nd	nd
		$^{15}\text{NO}_3^-$ (10) + Mn(II) (10)	nd	nd
		$^{15}\text{NO}_3^-$ (10) + H_2S (10)	165.8 ± 51.7	nd
		$^{15}\text{NO}_3^-$ (10) + SO_3^{2-} (20)	nd	nd
		$^{15}\text{NO}_3^-$ (10) + $\text{S}_2\text{O}_3^{2-}$ (10)	37.0 ± 16.1	nd

strongly enhanced we take as conclusive evidence for sulfide-dependent denitrification as the dominant N_2 -producing process in the water column.

Interestingly, sulfide-dependent denitrification did not seem to be restricted to a band within the RTZ (Fig. 2.6). Instead, we measured potential denitrification rates well below the depth of NO_3^- disappearance. One reason for this observation could be that facultative denitrification is a widespread feature in natural environments (Zumft, 1997). Under nitrate-replete conditions a variety of organisms can use the energetically more favorable pathway of denitrification. The presence of facultative denitrifiers is consistent with the detection of *nirS* genes throughout the anoxic water column (Figs. 2.3). It may also be possible, that the denitrifiers below 145 m depth are exposed to episodic injections of NO_3^- . Although we never detected NO_3^- below 150 m depth, there has been a weakened density stratification since the mixing events during the winters of 2005 and 2006 (Holzner et al., 2009). Hence,

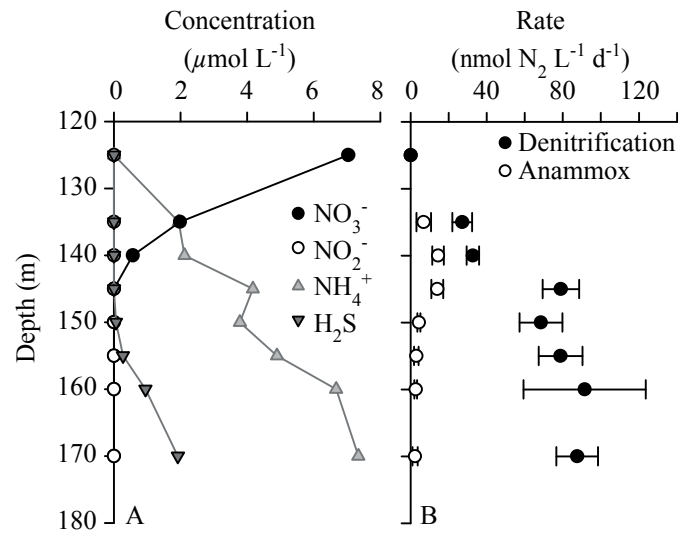


Figure 2.6: (A) Water column profiles of nitrate, nitrite, ammonium, and sulfide concentrations, as well as (B) potential rates of denitrification and anammox in the RTZ in October 2011. Denitrification and anammox rates were measured upon the addition of $1.7 \mu\text{mol L}^{-1} \text{}^{15}\text{NO}_3^-$ plus $10 \mu\text{mol L}^{-1} \text{H}_2\text{S}$. Error bars represent standard errors between triplicate measurements.

nitrate-replete cold-water masses could episodically sink into the anoxic hypolimnion but such events, if they occurred at all, must have remained undetected due to the relatively low sampling frequency and rapid NO_3^- consumption. Ventilation of deep waters in stratified lakes through sinking of cold fluvial water has been reported for other south alpine lakes, leading to measurable O_2 concentrations below the actual RTZ (Ambrosetti et al., 2010).

In October 2011, maximum potential sulfide-dependent denitrification ($91.5 \pm 32 \text{ nmol N}_2 \text{L}^{-1} \text{d}^{-1}$) was still low (Fig. 2.6). Only few studies have addressed sulfide-dependent denitrification thus far, and most of them were conducted in marine environments. Reported maximum rates range between 88 and 18600 $\text{nmol N}_2 \text{L}^{-1} \text{d}^{-1}$ (Brettar and Rheinheimer, 1991; Jensen et al., 2009; Lavik et al., 2009). Thus, our potential rates determined for the Lake Lugano water column are at the lower end of most previous estimates. Similarly low rates were observed in the Gotland Deep in the Central Baltic Sea (Brettar and Rheinheimer, 1991). It is surprising, how such low N turnover rates in the water column can result in stable and comparatively strong dissolved inorganic nitrogen (DIN) concentration gradients as observed in this study (without the contribution, for example, from fixed N elimination processes within sediments on the flanks of the lake basin). To verify independently the low anammox and denitrification rates determined in the incubation experiments, we used the NH_4^+ and

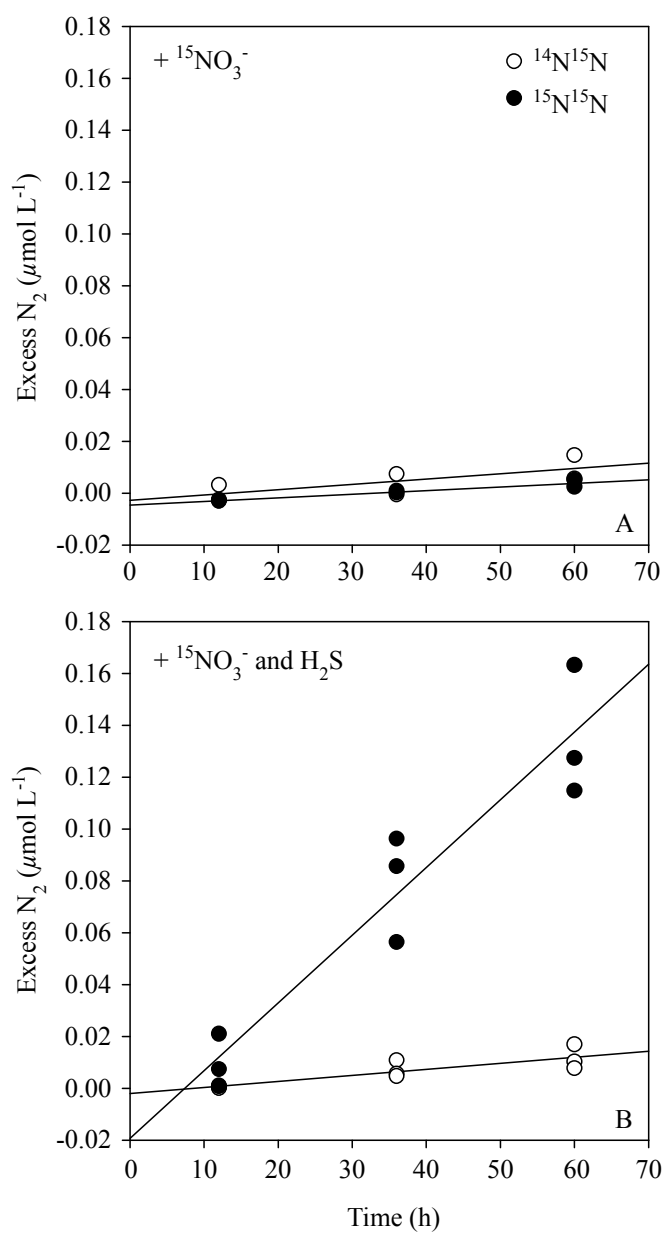


Figure 2.7: Example of ^{15}N -labeled N_2 production during ex situ incubation experiments with water from 150 m depth (October 2011). The incubations were amended with (A) $1.7 \mu\text{mol L}^{-1} \text{}^{15}\text{NO}_3^-$ and (B) $1.7 \mu\text{mol L}^{-1} \text{}^{15}\text{NO}_3^-$ plus $10 \mu\text{mol L}^{-1} \text{H}_2\text{S}$. Excess $^{14}\text{N}^{15}\text{N}$ (open circles) and $^{15}\text{N}^{15}\text{N}$ (black circles) increased linearly over time.

NO_3^- concentration gradients to calculate vertical DIN fluxes in the water column. The turbulent-diffusive fluxes of NH_4^+ and NO_3^- toward the RTZ were on average ~ 11 and $\sim 19 \mu\text{mol h}^{-1} \text{m}^{-2}$, respectively. Assuming a 15 m thick water layer of active N_2 production, NH_4^+ and NO_3^- consumption rates of only 18 and 31 $\text{nmol N L}^{-1} \text{d}^{-1}$ are necessary to explain the observed fluxes. Hence, the direct and flux-based rate measurement results are consistent, confirming that the overall N-turnover activity is comparatively low in the northern basin of Lake Lugano. The agreement between the two approaches also suggests that the observed DIN concentration gradients in the water column are the result of water column processes only, without significant contribution from benthic processes on the steep and barely sedimented flanks of the basin.

2.4.4 Anammox bacteria coexist with sulfide-dependent denitrifiers

Our results demonstrate that anammox bacteria and chemolithotrophic denitrifiers coexist in the RTZ of the Lake Lugano north basin, with sulfide-dependent denitrification being the dominant fixed N elimination pathway. Interestingly, in our incubation experiments (October 2011), the addition of H_2S did not only enhance N_2 production by denitrification, but also stimulated anammox activity. Based on these observations, we may speculate that anammox bacteria in Lake Lugano rely on the NO_2^- released as intermediate during sulfide-dependent NO_3^- reduction.

Fuchsman et al. (2012) recently showed that in the Black Sea, most *Planctomyces* were associated with suspended aggregates, and only members of *Candidatus Scalindua* were found to be free-living. In contrast, Woebken et al. (2007) hypothesized that anammox bacteria in the upwelling region off Namibia grow in the interior of aggregates composed of nitrifying archaea, heterotrophic bacteria, and organic matter. They speculated that in the aggregate interior, anammox bacteria encounter microenvironmental conditions that are more favorable than in the ambient water and benefit from the anoxic conditions and substrate exchange with other microorganisms. In analogy to their model, we suggest that anammox bacteria and sulfide-dependent denitrifying bacteria in the RTZ of Lake Lugano may live in a similar community, where the latter create a sulfide-free microenvironment in an aggregate interior and provide NO_2^- for anammox. Anammox bacteria may thereby elegantly overcome inhibiting or toxic effects of H_2S . While this mechanistic model still needs experimental verification, it could be most appropriate in freshwater ecosystems with low H_2S and relatively high NO_3^- concentrations, as observed in the RTZ of the Lake Lugano north basin.

In this study we showed that anammox bacteria are present in the water column of the Lake Lugano north basin. They preferentially grow in a water layer right below the oxycline where a stable anammox community (both in terms of abundance and

phylogenetic structure) is maintained, yet at comparatively low metabolic activity. At the same depths, we found evidence for sulfide-dependent denitrification as the prime NO_3^- reducing metabolic process. This implies that, in contrast to previous observations in marine environments, anammox bacteria and sulfide-dependent denitrifiers at least coexist in the same water layer of Lake Lugano. Any direct link between anammox and sulfide-dependent denitrification, however, needs further exploration by, for example, studying aggregate-associated processes and nutrient interchange between different groups of organisms. Unexpected for a mesotrophic lake basin, organotrophic denitrification does not seem to play a major role in fixed N elimination from the water column. Instead, our data demonstrate that the observed stable DIN concentration gradients in the water column may be produced principally by chemolithotrophic processes. In agreement with observations from marine environments, this study implies that the role of chemolithotrophic fixed N elimination pathways in aquatic ecosystems may be more important than previously assumed.

2 - References

- W. Ambrosetti, L. Barbanti, and E. A. Carrara. Mechanisms of hypolimnion erosion in a deep lake (Lago Maggiore, N. Italy). *Journal of Limnology*, 69:3–14, 2010.
- A. Barbieri and B. Polli. Description of Lake Lugano. *Aquatic Sciences*, 54:181–183, 1992.
- G. Braker, A. Fesefeldt, and K.-P. Witzel. Development of PCR primer systems for amplification of nitrite reductase genes (*nirK* and *nirS*) to detect denitrifying bacteria in environmental samples. *Applied and Environmental Microbiology*, 64:3769–3775, 1998.
- R. S. Braman and S. A. Hendrix. Nanogram nitrite and nitrate determination in environmental and biological materials by vanadium(III) reduction with chemiluminescence detection. *Analytical Chemistry*, 61:2715–2718, 1989.
- I. Brettar and G. Rheinheimer. Denitrification in the Central Baltic: Evidence for H₂S-oxidation as motor of denitrification at the oxic-anoxic interface. *Marine Ecology Progress Series*, 77:157–169, 1991.
- A. J. Burgin, S. K. Hamilton, S. E. Jones, and J. T. Lennon. Denitrification by sulfur-oxidizing bacteria in a eutrophic lake. *Aquatic Microbial Ecology*, 66:283–293, 2012.
- D. E. Canfield, F. J. Stewart, B. Thamdrup, L. De Brabandere, T. Dalsgaard, E. F. Delong, N. P. Revsbech, and O. Ulloa. A cryptic sulfur cycle in oxygen-minimum-zone waters off the Chilean coast. *Science*, 330:1375–1378, 2010.
- K. Chon, J.-S. Chang, E. Lee, J. Lee, J. Ryu, and J. Cho. Abundance of denitrifying genes coding for nitrate (*narG*), nitrite (*nirS*), and nitrous oxide (*nosZ*) reductases in estuarine versus wastewater effluent-fed constructed wetlands. *Ecological Engineering*, 37:64–69, 2011.
- CIP AIS. Stato limnologico del Lago di Lugano: Circolazione invernale 2004-2005. *Bollettino dei Laghi Maggiore e Lugano*, No. 6, 2005.

- CIPAIS. Stato limnologico del Lago di Lugano: Circolazione invernale 2005-2006. *Bollettino dei Laghi Maggiore e Lugano*, No. 7, 2006.
- T. Dalsgaard, D. E. Canfield, J. Petersen, B. Thamdrup, and J. Acuña González. N₂ production by the anammox reaction in the anoxic water column of Golfo Dulce, Costa Rica. *Nature*, 422:606–608, 2003.
- C. A. Fuchsman, J. W. Murray, and S. K. Kononov. Concentration and natural stable isotope profiles of nitrogen species in the Black Sea. *Marine Chemistry*, 111: 90–105, 2008.
- C. A. Fuchsman, J. T. Staley, B. B. Oakley, J. B. Kirkpatrick, and J. W. Murray. Free-living and aggregate-associated Planctomycetes in the Black Sea. *FEMS Microbiology Ecology*, 80:402–416, 2012.
- A. E. Gargett. Vertical eddy diffusivity in the ocean interior. *Journal of Marine Research*, 42:359–393, 1984.
- C. Garside. A chemiluminescent technique for the determination of nanomolar concentrations of nitrate and nitrite in seawater. *Marine Chemistry*, 11:159–167, 1982.
- M. R. Hamersley, D. Woebken, B. Boehrer, M. Schultze, G. Lavik, and M. M. M. Kuypers. Water column anammox and denitrification in a temperate permanently stratified lake (Lake Rassnitzer, Germany). *Systematic and Applied Microbiology*, 32:571–582, 2009.
- M. Hannig, G. Lavik, M. M. M. Kuypers, D. Woebken, W. Martens-Habbena, and K. Jürgens. Shift from denitrification to anammox after inflow events in the central Baltic Sea. *Limnology and Oceanography*, 52:1336–1345, 2007.
- C. P. Holzner, W. Aeschbach-Hertig, M. Simona, M. Veronesi, D. M. Imboden, and R. Kipfer. Exceptional mixing events in meromictic Lake Lugano (Switzerland/Italy), studied using environmental tracers. *Limnology and Oceanography*, 54: 1113–1124, 2009.
- S. Hulth, R. C. Aller, D. E. Canfield, T. Dalsgaard, P. Engström, F. Gilbert, K. Sundbäck, and B. Thamdrup. Nitrogen removal in marine environments: Recent findings and future research challenges. *Marine Chemistry*, 94:125–145, 2005.
- S. Humbert, S. Tarnawski, N. Fromin, M.-P. Mallet, M. Aragno, and J. Zopfi. Molecular detection of anammox bacteria in terrestrial ecosystems: Distribution and diversity. *The ISME Journal*, 4:450–454, 2010.

- S. Humbert, J. Zopfi, and S.-E. Tarnawski. Abundance of anammox bacteria in different wetland soils. *Environmental Microbiology Reports*, 4:484–490, 2012.
- M. M. Jensen, M. M. M. Kuypers, G. Lavik, and B. Thamdrup. Rates and regulation of anaerobic ammonium oxidation and denitrification in the Black Sea. *Limnology and Oceanography*, 53:23–36, 2008.
- M. M. Jensen, J. Petersen, T. Dalsgaard, and B. Thamdrup. Pathways, rates, and regulation of N_2 production in the chemocline of an anoxic basin, Mariager Fjord, Denmark. *Marine Chemistry*, 113:102–113, 2009.
- S. Kalyuzhnyi, M. Gladchenko, A. Mulder, and B. Versprille. DEAMOX - New biological nitrogen removal process based on anaerobic ammonia oxidation coupled to sulphide-driven conversion of nitrate into nitrite. *Water Research*, 40:3637–3645, 2006.
- T. M. Kana, C. Darkangelo, M. D. Hunt, J. B. Oldham, G. E. Bennett, and J. C. Cornwell. Membrane inlet mass spectrometer for rapid high-precision determination of N_2 , O_2 , and Ar in environmental water samples. *Analytical Chemistry*, 66:4166–4170, 1994.
- B. Kartal, W. J. Maalcke, N. M. de Almeida, I. Cirpus, J. Gloerich, W. Geerts, H. J. M. Op den Camp, H. R. Harhangi, E. M. Janssen-Megens, K.-J. Francoijs, H. G. Stunnenberg, J. T. Keltjens, M. S. M. Jetten, and M. Strous. Molecular mechanism of anaerobic ammonium oxidation. *Nature*, 479:127–130, 2011.
- J. A. Klappenbach, J. M. Dunbar, and T. M. Schmidt. rRNA operon copy number reflects ecological strategies of bacteria. *Applied and Environmental Microbiology*, 66:1328–1333, 2000.
- M. M. M. Kuypers, A. O. Sliemers, G. Lavik, M. Schmid, B. B. Jørgensen, J. G. Kuenen, J. S. S. Damsté, M. Strous, and M. S. M. Jetten. Anaerobic ammonium oxidation by anammox bacteria in the Black Sea. *Nature*, 422:608–611, 2003.
- M. M. M. Kuypers, G. Lavik, D. Woebken, M. Schmid, B. M. Fuchs, R. Amann, B. B. Jørgensen, and M. S. M. Jetten. Massive nitrogen loss from the Benguela upwelling system through anaerobic ammonium oxidation. *Proceedings of the National Academy of Sciences of the United States of America (PNAS)*, 102:6478–6483, 2005.
- G. Lavik, T. Stuhmann, V. Brochert, A. van der Plas, V. Mohrholz, P. Lam, M. Mussmann, B. M. Fuchs, R. Amann, U. Lass, and M. M. M. Kuypers. Detoxification of sulphidic African shelf waters by blooming chemolithotrophs. *Nature*, 457:581–584, 2009.

- M. F. Lehmann, S. M. Bernasconi, A. Barbieri, M. Simona, and J. A. McKenzie. Interannual variation of the isotopic composition of sedimenting organic carbon and nitrogen in Lake Lugano: A long-term sediment trap study. *Limnology and Oceanography*, 49:839–849, 2004.
- A. Mulder, A. A. van de Graaf, L. A. Robertson, and J. G. Kuenen. Anaerobic ammonium oxidation discovered in a denitrifying fluidized bed reactor. *FEMS Microbiology Ecology*, 16:177–183, 1995.
- A. Neef, R. Amann, H. Schlesner, and K.-H. Schleifer. Monitoring a widespread bacterial group: In situ detection of *Planctomycetes* with 16S rRNA-targeted probes. *Microbiology*, 144:3257–3266, 1998.
- L. P. Nielsen. Denitrification in sediment determined from nitrogen isotope pairing. *FEMS Microbiology Ecology*, 86:357–362, 1992.
- T. D. Rees, A. B. Gyllenspetz, and A. C. Docherty. The determination of trace amounts of sulphide in condensed steam with *NN*-diethyl-*p*-phenylenediamine. *Analyst*, 96:201–208, 1971.
- M. Schmid, U. Twachtmann, M. Klein, M. Strous, S. Juretschko, M. Jetten, J. W. Metzger, K. H. Schleifer, and M. Wagner. Molecular evidence for genus level diversity of bacteria capable of catalyzing anaerobic ammonium oxidation. *Systematic and Applied Microbiology*, 23:93–106, 2000.
- M. Schmid, K. Walsh, R. Webb, W. I. C. Rijpstra, K. van de Pas-Schoonen, M. J. Verbruggen, T. Hill, B. Moffett, J. Fuerst, S. Schouten, J. S. S. Damsté, J. Harris, P. Shaw, M. Jetten, and M. Strous. *Candidatus* “*Scalindua brodae*”, sp. nov., *Candidatus* “*Scalindua wagneri*”, sp. nov., two new species of anaerobic ammonium oxidizing bacteria. *Systematic and Applied Microbiology*, 26:529–538, 2003.
- C. J. Schubert, E. Durisch-Kaiser, B. Wehrli, B. Thamdrup, P. Lam, and M. M. M. Kuypers. Anaerobic ammonium oxidation in a tropical freshwater system (Lake Tanganyika). *Environmental Microbiology*, 8:1857–1863, 2006.
- M.-F. Shao, T. Zhang, and H. H.-P. Fang. Sulfur-driven autotrophic denitrification: Diversity, biochemistry, and engineering applications. *Applied Microbiology and Biotechnology*, 88:1027–1042, 2010.
- M. Strous, J. A. Fuerst, E. H. M. Kramer, S. Logemann, G. Muyzer, K. T. van de Pas-Schoonen, R. Webb, J. G. Kuenen, and M. S. M. Jetten. Missing lithotroph identified as new planctomycete. *Nature*, 400:446–449, 1999.

- K. Tamura, J. Dudley, M. Nei, and S. Kumar. MEGA4: Molecular Evolutionary Genetics Analysis (MEGA) software version 4.0. *Molecular Biology and Evolution*, 24:1596–1599, 2007.
- B. Thamdrup and T. Dalsgaard. Production of N_2 through anaerobic ammonium oxidation coupled to nitrate reduction in marine sediments. *Applied and Environmental Microbiology*, 68:1312–1318, 2002.
- B. Thamdrup, T. Dalsgaard, M. M. Jensen, O. Ulloa, L. Fariás, and R. Escribano. Anaerobic ammonium oxidation in the oxygen-deficient waters off northern Chile. *Limnology and Oceanography*, 51:2145–2156, 2006.
- A. A. van de Graaf, A. Mulder, P. de Bruijn, M. S. M. Jetten, L. A. Robertson, and J. G. Kuenen. Anaerobic oxidation of ammonium is a biologically mediated process. *Applied and Environmental Microbiology*, 61:1246–1251, 1995.
- L. van Niftrik and M. S. M. Jetten. Anaerobic ammonium-oxidizing bacteria: Unique microorganisms with exceptional properties. *Microbiology and Molecular Biology Reviews*, 76:585–596, 2012.
- B. B. Ward, A. H. Devol, J. J. Rich, B. X. Chang, S. E. Bulow, H. Naik, A. Pratihary, and A. Jayakumar. Denitrification as the dominant nitrogen loss process in the Arabian Sea. *Nature*, 461:78–81, 2009.
- R. F. Weiss. The solubility of nitrogen, oxygen and argon in water and seawater. *Deep-Sea Research*, 17:721–735, 1970.
- D. Wobken, B. M. Fuchs, M. M. M. Kuypers, and R. Amann. Potential interactions of particle-associated anammox bacteria with bacterial and archaeal partners in the Namibian upwelling system. *Applied and Environmental Microbiology*, 73:4648–4657, 2007.
- A. Wüest, W. Aeschbach-Hertig, H. Baur, M. Hofer, R. Kipfer, and M. Schurter. Density structure and tritium-helium age of deep hypolimnetic water in the northern basin of Lake Lugano. *Aquatic Sciences*, 54:205–218, 1992.
- D. Zheng, E. W. Alm, D. A. Stahl, and L. Raskin. Characterization of universal small-subunit rRNA hybridization probes for quantitative molecular microbial ecology studies. *Applied and Environmental Microbiology*, 62:4504–4513, 1996.
- J. Zopfi, T. G. Ferdelman, B. B. Jørgensen, A. Teske, and B. Thamdrup. Influence of water column dynamics on sulfide oxidation and other major biogeochemical processes in the chemocline of Mariager Fjord (Denmark). *Marine Chemistry*, 74:29–51, 2001.

W. G. Zumft. Cell biology and molecular basis of denitrification. *Microbiology and Molecular Biology Reviews*, 61:533–616, 1997.

CHAPTER 3

Community N and O isotope fractionation by sulfide-dependent denitrification and anammox in a stratified lacustrine water column

C. B. Wenk, J. Zopfi, J. Brees, M. Veronesi, H. Niemann, and M. F. Lehmann

Geochimica et Cosmochimica Acta 2014, 125: 551-563
(doi:10.1016/j.gca.2013.10.034)

Abstract

We investigated the community nitrogen (N) and oxygen (O) isotope effects of fixed N loss in the northern basin of Lake Lugano, where sulfide-dependent denitrification and anammox are the main drivers of suboxic N_2 production. A decrease in nitrate (NO_3^-) concentration toward the redox transition zone (RTZ) at mid-water depth was paralleled by an increase in $\delta^{15}N$ and $\delta^{18}O$ from approximately 5‰ to >20‰ and from 0 to >10‰, respectively. Ammonium (NH_4^+) concentrations were highest in the near-bottom water and decreased toward the RTZ concomitant with an increase in $\delta^{15}N-NH_4^+$ from ~ 7 ‰ to >15‰. A diffusion-reaction model yielded N and O isotope enrichment factors that are significantly smaller than isotope effects reported previously for microbial NO_3^- reduction and NH_4^+ oxidation ($^{15}\epsilon_{NO_3} \approx 10$ ‰, $^{18}\epsilon_{NO_3} \approx 7$ ‰, and $^{15}\epsilon_{NH_4} \approx 10$ -12‰). For the Lake Lugano north basin, we constrain the apparent under-expression of the N isotope effects to: (1) environmental conditions (e.g., substrate limitation, low cell specific N transformation rates), or (2) low process-specific (chemolithotrophic denitrification and anammox) isotope fractionation. Our results have confirmed the robust nature of the co-linearity between N and O isotope enrichment during microbial denitrification beyond its organotrophic mode. However, the ratio of ^{18}O to ^{15}N enrichment ($^{18}\epsilon_{NO_3} : ^{15}\epsilon_{NO_3}$) associated with NO_3^- reduction in the RTZ was ~ 0.89 , which is lower than observed in marine environments and in most culture experiments. We propose that chemolithotrophic NO_3^- reduction in the Lake Lugano north basin was partly catalyzed by the periplasmic dissimilatory nitrate reductase (Nap) (rather than the membrane-bound dissimilatory Nar), which is known to express comparably low $^{18}\epsilon_{NO_3} : ^{15}\epsilon_{NO_3}$ ratios in the ambient NO_3^- pool. However, NO_2^- re-oxidation, e.g., during anammox or microaerobic nitrification, could have contributed to the lowered ^{18}O to ^{15}N enrichment ratios. Although we do not yet understand the exact controls on the observed N (and O) isotope fractionation in the Lake Lugano north basin, our study implies that caution is advised when assuming canonical (i.e., high) N isotope effects for NO_3^- reduction and NH_4^+ oxidation in natural environments. In Lake Lugano, the community N (and O) isotope effects by sulfide-dependent denitrification and anammox in a natural ecosystem appear to be significantly lower than for organotrophic denitrification and aerobic ammonium oxidation.

3.1 Introduction

The isotopic composition of dissolved nitrogen (N) species has been used as an indicator of N transformation pathways in aquatic and terrestrial environments. However, the successful interpretation of N (and O) isotope measurements in environmental systems requires a solid understanding of the various transformation-specific isotope effects. Isotope fractionation is based on the fact that organisms transform compounds containing lighter isotopes (e.g., ^{14}N) at a slightly higher rate than compounds containing heavier isotopes, e.g., ^{15}N . The kinetic N isotope effect, $^{15}\epsilon$, is defined as

$$^{15}\epsilon = \left(\frac{^{14}k}{^{15}k} - 1 \right) 1000 \quad (3.1)$$

where ^{14}k and ^{15}k refer to the reaction rates of ^{14}N and ^{15}N bearing isotopologues, respectively. A series of culture experiments have investigated the N (and O) isotope effects of N cycling processes. For example nitrification, the aerobic oxidation of ammonium (NH_4^+) to nitrite (NO_2^-) and nitrate (NO_3^-), leaves the product depleted in ^{15}N relative to the substrate NH_4^+ . Reported N isotope enrichment factors for nitrification range between 12‰ and 38‰ (Casciotti et al., 2003; Horrigan et al., 1990; Mariotti et al., 1981). While nitrification leads to the formation of NO_3^- with a relatively low $\delta^{15}\text{N}$, denitrification, the stepwise anaerobic NO_3^- reduction to N_2 , leaves the residual NO_3^- pool enriched in the heavier isotope ^{15}N . Although strong variations in N isotope effects are observed for denitrification in many environments (see Lehmann et al. 2003 and references therein; Granger et al. 2008), most studies from the open ocean report $^{15}\epsilon$ values of 20‰ to 30‰ (Brandes et al., 1998; Voss et al., 2001), which is consistent with some culture-based experimental data (Barford et al., 1999; Granger et al., 2008; Mariotti et al., 1981; Wellman et al., 1968). Complexity is added to the interpretation of stable N isotope signatures by the fact that the observed (or apparent) isotope effect (ϵ_{app}) of denitrification at the ecosystem level can be reduced relative to the intrinsic (or cellular level) isotope effect (ϵ_{cell}). For example, in oceanic oxygen minimum zones, NO_3^- is not denitrified from a homogenous pool, but denitrification occurs where the NO_3^- pool has already been pre-enriched in ^{15}N by partial denitrification (Altabet, 2007; Deutsch et al., 2004), reducing the overall N isotope effect at the ecosystem level. Similarly, open-system (dilution) aspects result in production of N_2 with a $\delta^{15}\text{N}$ significantly higher than predicted by a biological N isotope effect of 20‰ to 30‰. Altabet (2007) proposed that, considering these (and other) aspects, the net ecosystem N isotope effect for water column denitrification can be as low as 12‰. If denitrification is limited by the rate of NO_3^- supply to the denitrifying zone and NO_3^- consumption is complete, ϵ_{app} can be further reduced. This can, for example, be the case in poorly ventilated, semi-enclosed ocean basins, such as the Cariaco Basin (Thunell et al., 2004), or in

marine sediments (Brandes and Devol, 1997; Lehmann et al., 2004, 2007). In the extreme, the N isotope effect of sedimentary denitrification can be as low as 0 to 4‰, yet the exact controls on benthic ϵ_{app} values are complex (Alkhatib et al., 2012; Lehmann et al., 2007).

Similarly, yet on a different spatial scale, Kritee et al. (2012) systematically explored changes in the denitrification N isotope effects on the cellular level (ϵ_{cell}) relative to isotope fractionation on the enzyme level (ϵ_{enzyme}) as a function of changing environmental conditions. In a set of culture experiments, it has been shown that ϵ_{cell} can be reduced relative to ϵ_{enzyme} at low cell specific nitrate reduction (CSNR) rates. The interpretation of this result is consistent with the “efflux model” by Shearer et al. (1991), and akin to conceptual models by Granger et al. (2004, 2008). Briefly, the effective N isotope effect as observed in the medium (ϵ_{cell}) is the combined result of N isotope fractionation at all steps associated with uptake and reduction of NO_3^- by a denitrifying cell up to, and including, the first irreversible step. Usually, NO_3^- uptake by the cell, as well as binding to the enzyme is reversible, and the actual NO_3^- reduction to NO_2^- is the first irreversible step. It has been shown that neither NO_3^- uptake nor NO_3^- binding to the enzyme occurs with significant isotope fractionation (Granger et al., 2008, 2004). The observed ambient isotope effect is thus dominated by the isotope fractionation during enzymatic NO_3^- reduction to NO_2^- (ϵ_{enzyme}). Furthermore, the degree to which this isotope signature is expressed outside the cell (and thus in the environment) is a function of the NO_3^- efflux to uptake ratio. If this ratio is high, ϵ_{enzyme} would be nearly fully expressed in the environment (i.e., $\epsilon_{\text{enzyme}} = \epsilon_{\text{cell}}$). If the ratio is low, the effective isotope effect (ϵ_{cell}) would be significantly reduced.

Independent of the environmental constraints on the isotope fractionation, both at the ecosystem and the cellular spatial scales, the increase in $\delta^{15}\text{N}-\text{NO}_3^-$ during NO_3^- reduction is distinctively coupled to an increase in $\delta^{18}\text{O}-\text{NO}_3^-$ (Granger et al., 2008; Lehmann et al., 2004; Sigman et al., 2005). In fact, the commonly observed coupling of $\delta^{15}\text{N}$ and $\delta^{18}\text{O}$ has been used as evidence for the occurrence of denitrification. In contrast, during nitrification, the $\delta^{15}\text{N}$ and $\delta^{18}\text{O}$ values of produced NO_3^- are affected differently. Thus, the decoupling of $\delta^{15}\text{N}$ and $\delta^{18}\text{O}$ values (i.e., the deviation from a parallel $\delta^{15}\text{N}$ and $\delta^{18}\text{O}$ evolution in the NO_3^- pool) has been used to diagnose NO_3^- regeneration processes (e.g., nitrification and NO_2^- oxidation) that occur simultaneously in the environment (Bourbonnais et al., 2012; Casciotti and McIlvin, 2007; Lehmann et al., 2003; Sigman et al., 2009, 2005; Wankel et al., 2009). Both, dissimilatory and assimilatory NO_3^- reduction in the ocean and in most culture experiments, demonstrate an unequivocal O to N isotope enrichment ratio of ~ 1 (Casciotti et al., 2002; Granger et al., 2008, 2004; Karsh et al., 2012; Sigman et al., 2005). These results, however, contrast many studies in freshwater environments, which implicate NO_3^- reduction with a ^{15}N enrichment consistently exceeding that of ^{18}O (i.e., $^{18}\epsilon$ to $^{15}\epsilon$ ratios of 0.5 to 0.7) (Lehmann et al. 2003 and references therein). Until today this conundrum regarding the apparent difference in the $^{18}\epsilon$

to $^{15}\epsilon$ ratio between freshwater and marine settings remains unresolved. While NO_3^- regeneration has been invoked as possible explanation for observed nitrate N-to-O isotope patterns that deviate from a fixed $^{18}\epsilon$ to $^{15}\epsilon$ ratio (Lehmann et al., 2003, 2004; Sigman et al., 2005), it remains unclear as to why NO_3^- regeneration would have a systematically different effect on the coupled nitrate N and O isotope signature in ocean compared to freshwater denitrifying environments. Alternative explanations may comprise differences in the mode of denitrification (i.e., source of electron donor) and differences in the involved nitrate reducing enzymes. An important finding in this context comes from culture experiments by Granger et al. (2008), who observed an O to N isotope enrichment of ~ 0.62 when NO_3^- reduction was catalyzed by the periplasmic dissimilatory nitrate reductase (Nap) instead of the membrane-bound dissimilatory nitrate reductase (Nar). Yet, the relative importance of Nap vs. Nar for nitrate reduction in natural environments is not well constrained.

Finally, essentially all culture and field studies investigating the isotope dynamics of NO_3^- reduction focus on organotrophic denitrification. While this mode of denitrification is still considered the dominant N elimination process in most marine and lacustrine environments, recent studies have highlighted the significance of alternative N_2 production pathways such as anaerobic ammonium oxidation (anammox) (Dalsgaard et al., 2003; Kuypers et al., 2003; Thamdrup et al., 2006), or other chemolithotrophic processes such as sulfide-dependent nitrate reduction (Brettar and Rheinheimer, 1991; Canfield et al., 2010; Lavik et al., 2009; Otte et al., 1999). Although the presence of these alternative N-transformations are likely to cause a different propagation of N and O isotope signatures in the natural environment than canonical denitrification, reports on the expression of their isotope effects on the ecosystem level do not exist.

The water column of the deep, mesotrophic Lake Lugano north basin is permanently stratified with an anoxic, mildly sulfidic deep hypolimnion. In a recent study (Wenk et al., 2013), we have identified sulfide-dependent chemolithotrophic denitrification as the dominant fixed N elimination pathway in the water column redox transition zone (RTZ) of the lake basin, while organotrophic denitrification seemed to be negligible. We also found evidence for the presence and activity of anammox bacteria, contributing up to 30% of total fixed N elimination. Lake Lugano is thus an excellent model system to study the isotope effects of several of the non-traditional water column N transformations.

The goal of this study was to investigate the fractionation of NO_3^- (N and O) and NH_4^+ (N) isotopes associated with N turnover in the water column RTZ of the northern basin of Lake Lugano. We were specifically interested in (1) the N isotope effects of chemolithotrophic N_2 production processes like anammox and sulfide-dependent denitrification, (2) the possible environmental controls on their expression in the environment, and (3) the biogeochemical constraints on the coupled N and O isotopic composition of NO_3^- in the RTZ where both microaerophilic NO_3^- regeneration and

(chemolithotrophic) NO_3^- reduction likely occur simultaneously or in close vicinity.

3.2 Methods

3.2.1 Study site and sampling

Lake Lugano is located at 271 m above sea level on the southern slopes of the Alps at the Swiss/Italian border. A natural dam separates the lake into a meromictic northern basin and a monomictic southern basin. The northern basin, which has a maximum depth of 288 m, is the focus of this study. Here, the water column is divided into an aerobic and an anaerobic hypolimnion. A detailed description of the lake and the stability of the water column can be found in Barbieri and Polli (1992) and Holzner et al. (2009). Water samples were collected at a site (46.01°N, 9.02°E), close to the point of maximum water depth using 5 L Niskin bottles during monthly sampling campaigns in 2009 (August - December), and 2010 (January). Water samples were filtered through 0.45 μm syringe filters and separate aliquots were frozen for subsequent NO_x (i.e., $\text{NO}_2^- + \text{NO}_3^-$) and NH_4^+ concentration and isotope analyses.

3.2.2 Concentration and isotope analyses

Concentration data have been published in Wenk et al. (2013). Oxygen (O_2) concentrations were obtained with a conductivity temperature depth (CTD) device with a detection limit of 1 $\mu\text{mol L}^{-1}$ for dissolved $[\text{O}_2]$. $[\text{NH}_4^+]$ was measured photometrically with a detection limit of 0.5 $\mu\text{mol L}^{-1}$ (Koroleff, 1976), and $[\text{NO}_x]$ was determined through reduction with V(III) to NO and chemiluminescence detection of the NO (Braman and Hendrix, 1989; Cox, 1980; Garside, 1982). The detection limit for NO_x concentration measurements was 0.02 $\mu\text{mol L}^{-1}$. This study focuses on the hypolimnetic RTZ where NO_2^- concentrations were below the detection limit of 0.02 $\mu\text{mol L}^{-1}$ (Wenk et al., 2013). Hence, NO_x will hereafter be referred to as NO_3^- .

The N and O isotopic composition of NO_3^- was determined using the denitrifier method (Casciotti et al., 2002; Sigman et al., 2001). Briefly, 20 nmoles of sample NO_3^- were converted to N_2O by cultured denitrifying bacteria (*Pseudomonas chlororaphis* ATCC 43928, and *Pseudomonas chlororaphis* ATCC 13985 (formerly *Pseudomonas aureofaciens*)) lacking the enzyme responsible for N_2O reduction. Produced N_2O was automatically extracted, purified, and subsequently analyzed on an isotope ratio mass spectrometer (Thermo Finnigan DELTA^{plus} XP). Blank contribution was less than 2% of the target sample size. Correction for O isotope exchange with H_2O during the reduction of NO_3^- to N_2O (determined according to Casciotti et al., 2002) was always

less than 5‰ and corrected for by standard bracketing. N and O isotope ratios are reported as δ values in ‰ relative to air N₂ and Vienna Standard Mean Ocean Water (VSMOW), respectively.

$$\delta = \left(\frac{R_{\text{sample}}}{R_{\text{standard}}} - 1 \right) 1000 \quad (3.2)$$

where $R = {}^{15}\text{N}/{}^{14}\text{N}$ or ${}^{18}\text{O}/{}^{16}\text{O}$. For isotope value calibration, we used internal ($\delta^{15}\text{N} = 12.15\text{‰}$) and international KNO₃ reference materials with reported $\delta^{15}\text{N}$ and $\delta^{18}\text{O}$ values of 4.7‰ and 25.6‰ (IAEA-N3), and -1.8‰ and -27.9‰ (USGS 34), respectively (Böhlke et al., 2003; Gonfiantini et al., 1995). Replicate reproducibility was generally better than 0.3‰ for $\delta^{15}\text{N}$ and 0.4‰ for $\delta^{18}\text{O}$.

The N isotopic composition of NH₄⁺ was determined using a combination of the ammonia diffusion (Sigman et al., 1997), the persulfate oxidation (Knapp et al., 2005), and the denitrifier methods (Sigman et al., 2001) as described in Houlton et al. (2007) and adapted by Bourbonnais et al. (2012). Briefly, >100 nmoles of sample NH₄⁺ were converted to NH₃ (g) under alkaline conditions after MgO addition. The product NH₃ (g) was trapped as NH₄⁺ on combusted and acidified glass fiber discs (Whatman #1823010) sandwiched between two Teflon membranes (Millipore LCWP 01300). The NH₄⁺ trapped on the glass fiber discs was then chemically oxidized to NO₃⁻ in a sodium persulfate solution. After adjusting the pH to 4, the isotope composition of the product NO₃⁻ was determined using the denitrifier method as described above. Isotope values were calibrated using two (NH₄)₂SO₄ reference materials (IAEA-N1 and IAEA-N2) with assigned $\delta^{15}\text{N}$ values of 0.4‰ and 20.3‰, respectively. Reproducibility for repeated analyses of standards and samples was $\pm 1.0\text{‰}$.

3.3 Results

During summer and fall, photosynthetic activity led to an O₂ maximum at about 10 m water depth (Fig. 3.1a) and to nitrate-limiting conditions in the surface water (Fig. 3.1b). Thermal stratification during this time caused a density gradient between 10 and 20 m depth and an associated NO₃⁻ concentration maximum due to organic matter (OM) remineralization and NO₃⁻ regeneration below the photic zone (Wenk et al., 2013). In the epilimnion, $\delta^{15}\text{N}\text{-NO}_3^-$ ranged between 0.2‰ (September 2009) and 4.8‰ (January 2010; Fig. 3.1c), whereas $\delta^{18}\text{O}\text{-NO}_3^-$ showed an opposite but less pronounced seasonal trend (from 1.7‰ in August 2009 to 0.7‰ in January 2010; Fig. 3.1d). In the hypolimnion, O₂ concentrations systematically decreased with depth and reached concentrations < 1 $\mu\text{mol L}^{-1}$ between 125 m and 130 m depth

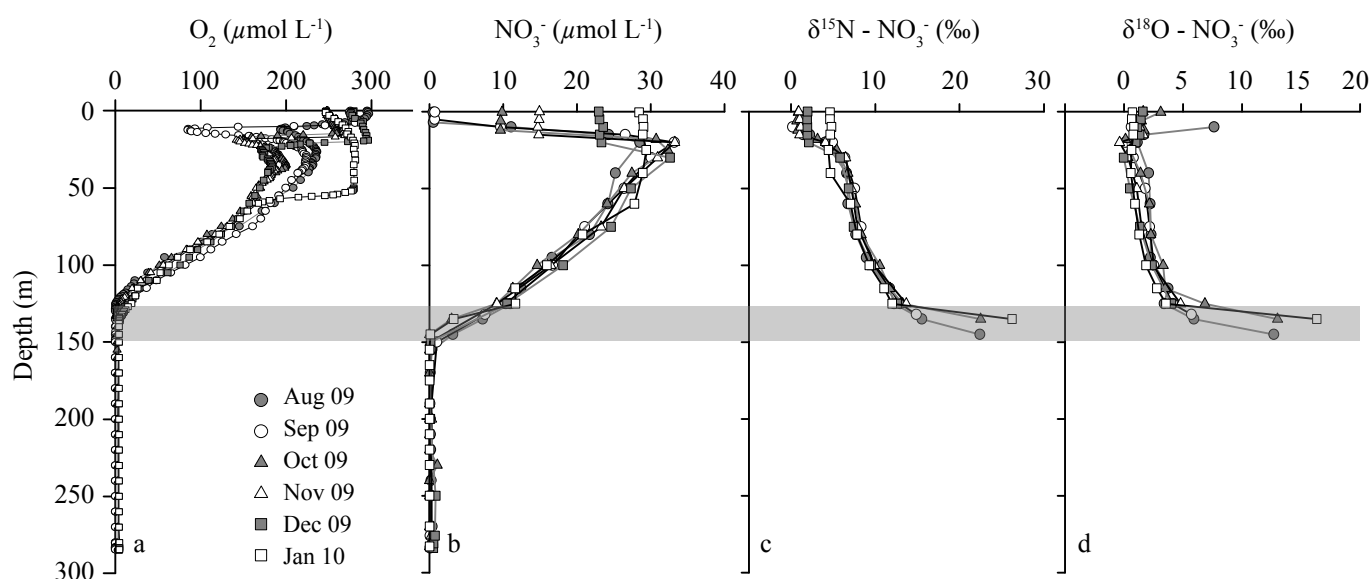


Figure 3.1: Water column profiles of (a) dissolved oxygen and (b) nitrate concentrations, as well as (c) N and (d) O isotopic composition of NO_3^- in the northern basin of Lake Lugano. The anoxic (i.e., $[\text{O}_2] < 1 \mu\text{mol L}^{-1}$), non-sulfidic (i.e., $[\text{H}_2\text{S}] < 0.2 \mu\text{mol L}^{-1}$) water layer is indicated by a grey bar. Concentration data from Wenk et al. (2013).

(Fig. 3.1a). The anoxic deeper hypolimnion below 150 m depth was sulfidic with H_2S concentrations of up to $12 \mu\text{mol L}^{-1}$ (Wenk et al., 2013). Independently of the sampling period, NO_3^- concentrations decreased from approximately $30 \mu\text{mol L}^{-1}$ at 15 m depth to undetectable levels just below the oxic-anoxic interface at 150 m depth. Concomitantly with the NO_3^- concentration decrease, we always observed an increase in both the $\delta^{15}\text{N} - \text{NO}_3^-$ and $\delta^{18}\text{O} - \text{NO}_3^-$ from approximately 5‰ to >20‰ and from 0‰ to >10‰, respectively (Fig. 3.1b-d), indicating N and O isotope fractionation due to the preferential removal of ^{14}N - and ^{16}O -containing NO_3^- by NO_3^- reducing organisms. Ammonium concentrations were highest ($\sim 40 \mu\text{mol L}^{-1}$) in near-bottom waters, and decreased upward toward the RTZ (Fig. 3.2a). Just below the oxic-anoxic interface (i.e., $[\text{O}_2] < 1 \mu\text{mol L}^{-1}$) NH_4^+ concentrations were below the detection limit. Ammonium consumption below that depth must hence be due to anammox or microaerobic ammonium oxidation (Wenk et al., 2013). Near-bottom ammonium displayed a $\delta^{15}\text{N} - \text{NH}_4^+$ of $6.7 \pm 0.8\text{‰}$ (Fig. 3.2b). In association with the upward decrease in $[\text{NH}_4^+]$ toward the oxic-anoxic interface, we observed an increase in $\delta^{15}\text{N} - \text{NH}_4^+$ to approximately 15‰.

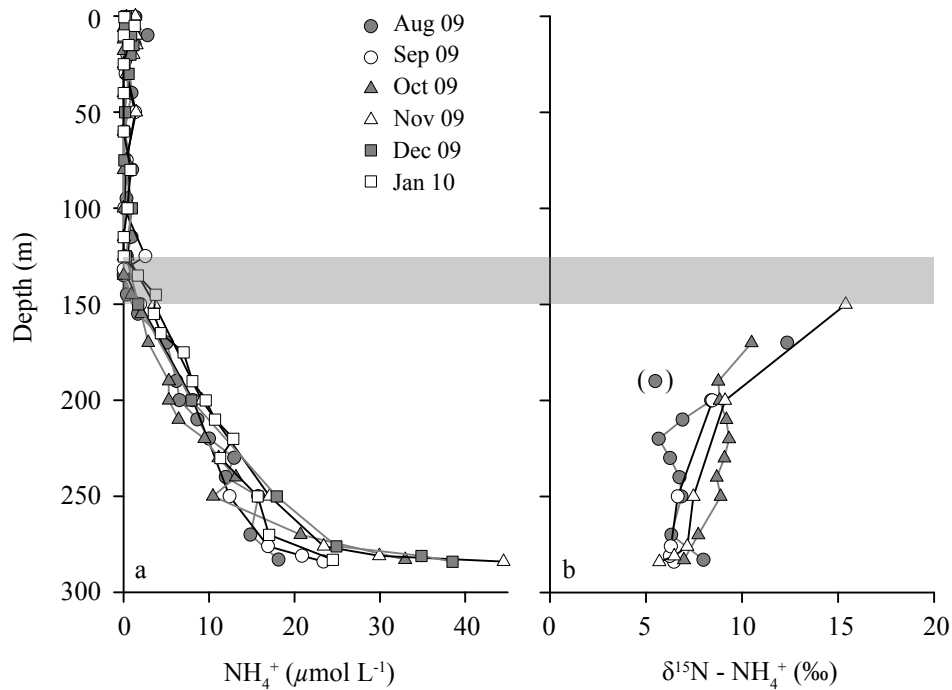


Figure 3.2: Water column profiles of (a) ammonium concentration and (b) its isotopic composition in the northern basin of Lake Lugano. The data point in brackets was not considered in further model analyses. The anoxic and non-sulfidic water layer is indicated by a grey bar. Concentration data from Wenk et al. (2013).

3.4 Discussion

In a previous study, where we used a combination of molecular analyses and ^{15}N -label incubations, we demonstrated that chemolithotrophic denitrification coupled to sulfide (H_2S) oxidation was the dominant process responsible for fixed N elimination. Furthermore, we showed that anammox bacteria coexist with sulfide-dependent denitrifiers in the RTZ, and that N_2 production by organotrophic denitrification is negligible (Wenk et al., 2013). The observed community N isotope effects, which we discuss below, can thus be considered as typical signature for N_2 loss in a lacustrine RTZ environment where chemolithotrophic denitrification and anammox co-occur, but where microaerobic NO_3^- regeneration may also play a significant role in determining the observed N (and O) isotope dynamics.

3.4.1 Low community isotope enrichment factor for NO_3^- reduction in the water column

Analogous to Sigman et al. (2003), we first estimated the isotope enrichment factors associated with NO_3^- (and NH_4^+) consumption in the RTZ, using a closed system model (Rayleigh model). The model assumes the gradual consumption of NO_3^- (and NH_4^+) with insignificant diffusive exchange with surrounding waters and a constant isotope enrichment factor. In this model, the isotopic composition ($\delta^{15}\text{N}$ and $\delta^{18}\text{O}$) of the residual substrate is approximated by the equation (Mariotti et al., 1981):

$$\delta_s = \delta_{s,0} - \varepsilon \times \ln(f) \quad (3.3)$$

where δ_s is the isotopic composition of the residual substrate, $\delta_{s,0}$ is the isotopic composition of the source substrate, and f is the fraction of the remaining substrate (i.e., $[\text{NO}_3^-]_s : [\text{NO}_3^-]_{s,0}$ and $[\text{NH}_4^+]_s : [\text{NH}_4^+]_{s,0}$, respectively). The $\delta_{s,0}$, $[\text{NO}_3^-]_{s,0}$, and $[\text{NH}_4^+]_{s,0}$ are assigned according to the isotopic and concentration analyses of samples at approximately 20 m depth, i.e., the upper boundary of the hypolimnion (for $\delta^{15}\text{N}$ - and $\delta^{18}\text{O}$ - NO_3^- in Fig. 3.3a), or at 125 m depth, i.e., the upper boundary of the denitrifying zone (for $\delta^{15}\text{N}$ - and $\delta^{18}\text{O}$ - NO_3^- in Fig. 3.3b), and at 200 m water depth (for $\delta^{15}\text{N}$ - NH_4^+). The isotope enrichment factor, ε , is approximated by the slope of the linear regression line ± 1 standard error (Mariotti et al., 1981). Including all hypolimnetic NO_3^- data, the Rayleigh model yields N and O isotope enrichment factors for NO_3^- reduction of $^{15}\varepsilon = 7.6 \pm 0.3\text{‰}$ and $^{18}\varepsilon = 5.1 \pm 0.3\text{‰}$ (Fig. 3.3a). However, the Rayleigh model fit to the complete data set is not perfect, suggesting that one single isotope effect (for N and O, respectively) only insufficiently predicts the community NO_3^- isotope fractionation in the water column (i.e., indicating slightly reduced NO_3^- isotope effects at low NO_3^- concentrations). We thus divided the hypolimnion into two parts: The upper, oxic zone, where NO_3^- concentrations are probably only influenced by diffusive mixing and by NO_3^- production through nitrification, and the RTZ, i.e., the water column below the depth of O_2 disappearance (at ~ 125 m depth), where most NO_3^- reduction occurs. The measured NO_3^- concentration and isotope data from the RTZ follow clear Rayleigh-type trends, indicating community isotope enrichment factors associated with NO_3^- consumption of $^{15}\varepsilon = 9.1 \pm 0.6\text{‰}$ and $^{18}\varepsilon = 8.0 \pm 0.8\text{‰}$ (Fig. 3.3b). These values are significantly lower than the 25‰ generally assumed for canonical denitrification (Brandes et al., 1998; Sigman et al., 2005; Voss et al., 2001). Thus far, similarly low water column N isotope enrichment factors for NO_3^- reduction have been measured only in the Cariaco Basin (Thunell et al., 2004), the Santa Barbara Basin (Sigman et al., 2003), the Eastern Tropical South Pacific (Ryabenko et al., 2012), or the southern basin of Lake Lugano (Lehmann et al., 2003). For some of these environments, a significant contribution from sedimentary denitrification, which barely fractionates the nitrate N and O isotopes (Brandes and

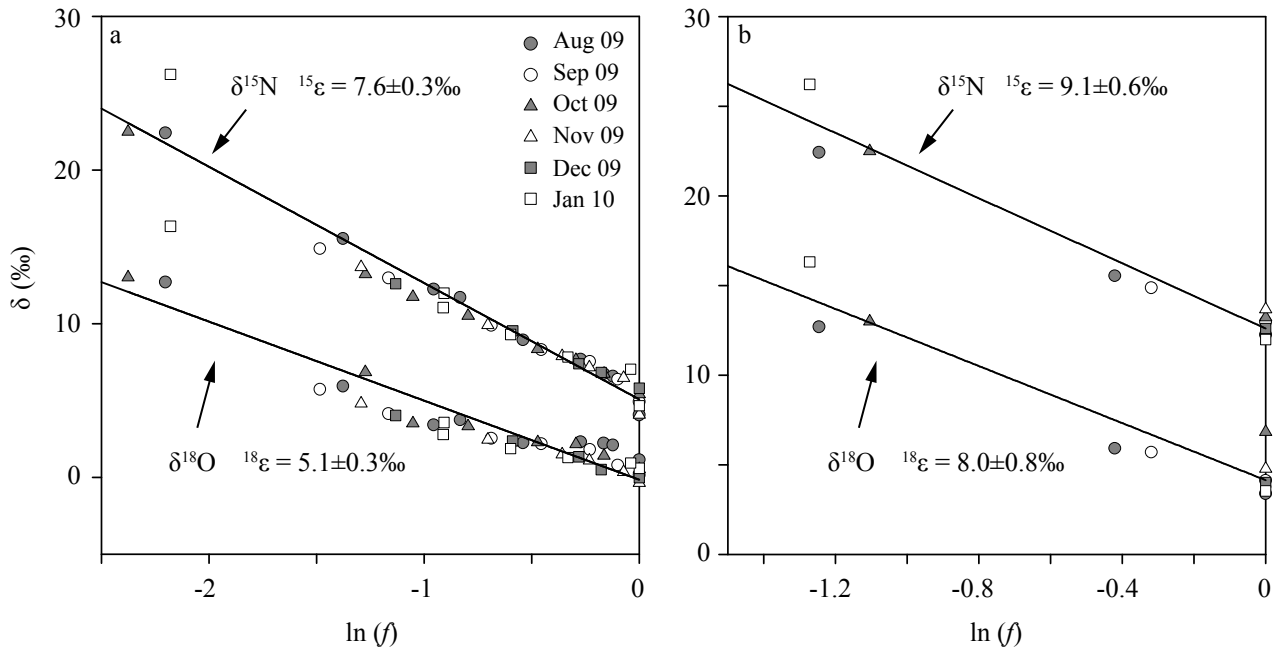


Figure 3.3: Rayleigh plots for nitrate consumption in the RTZ of the Lake Lugano north basin. $\delta^{15}\text{N}$ - and $\delta^{18}\text{O}$ - NO_3^- values are plotted against $\ln(f)$, where f represents the remaining nitrate fraction with respect to the concentration (a) below the metalimnion, i.e., at ~ 20 m water depth, and (b) at the upper boundary of the denitrifying zone, i.e., at 125 m water depth.

Devol, 1997; Lehmann et al., 2003, 2004, 2007; Sigman et al., 2003), has been invoked to explain the observed under-expression of the nitrate N isotope fractionation in the anoxic water column. In the Lake Lugano north basin, however, ^{15}N -label rate measurements of denitrification were consistent with dissolved inorganic nitrogen (DIN) flux calculations, suggesting that concentration gradients, and therefore also the isotopic signatures, can be attributed to water column processes alone (Wenk et al., 2013).

There are several plausible explanations for the reduced apparent nitrate N (and O) isotope enrichment factors, which we will discuss in the subsequent Sections: (1) Reduced emanation of the isotope fractionation signatures through the water column (ϵ_{app}) due to diffusion limitation of NO_3^- consumption in the denitrifying zone, (2) reduced isotope fractionation at the cellular level (ϵ_{cell}) under nitrate-limiting conditions, (3) low organism-specific fractionation by chemolithotrophic nitrate reducers, and (4) overprinting effects by other N transformations (i.e., N-regeneration, anammox).

Reduced isotope fractionation due to diffusion limitation of NO_3^- consumption in the water column

The closed system model above provides only a rough estimation of the isotope enrichment factors, because turbulent diffusion and substrate exchange throughout the water column are not considered. In particular, when substrate utilization is strong (almost complete consumption), it tends to significantly underestimate the intrinsic N isotope fractionation (ϵ_{cell}) of the biological processes at work (Thunell et al., 2004). A simple Rayleigh approach may also be biased by potential NO_3^- production, changing the overall NO_3^- concentration to $\delta^{15}\text{N}$ relationship. We thus applied a reaction-diffusion model akin to the one previously described by Lehmann et al. (2003, 2007) to determine the intrinsic (ϵ_{cell}) N and O isotope effects of NO_3^- reduction. Our model simulates downward turbulent diffusion of NO_3^- , sulfide-dependent denitrification, NO_3^- production through nitrification, upward turbulent diffusion of NH_4^+ , and consumption through anammox and nitrification. The model distinguishes between the concentrations of $^{14}\text{N}^{16}\text{O}_3^-$, $^{15}\text{N}^{16}\text{O}_3^-$, $^{14}\text{N}^{18}\text{O}^{16}\text{O}_2^-$, $^{14}\text{NH}_4^+$, and $^{15}\text{NH}_4^+$ and was computed using the AQUASIM software (Reichert, 1994). Resolving the vertical dimension only, this leads to five coupled differential equations:

$$\begin{aligned} \frac{\partial C_{^{14}\text{N}^{16}\text{O}_3^-}}{\partial t} = & K_z \frac{\partial^2 C_{^{14}\text{N}^{16}\text{O}_3^-}}{\partial z^2} \\ & - v_{\text{den}} \frac{K_{\text{O}_2, \text{inhib}}}{K_{\text{O}_2, \text{inhib}} + C_{\text{O}_2, \text{meas}}} \frac{C_{\text{H}_2\text{S}, \text{meas}}}{K_{\text{H}_2\text{S}} + C_{\text{H}_2\text{S}, \text{meas}}} \frac{C_{^{14}\text{N}^{16}\text{O}_3^-}}{K_{\text{NO}_3, \text{den}} + C_{\text{NO}_3^-}} \\ & + v_{\text{nit}} \frac{C_{\text{O}_2, \text{meas}}}{K_{\text{O}_2, \text{nit}} + C_{\text{O}_2, \text{meas}}} \frac{C_{^{14}\text{NH}_4^+}}{K_{\text{NH}_4, \text{nit}} + C_{\text{NH}_4^+}} \quad (3.4) \end{aligned}$$

$$\begin{aligned} \frac{\partial C_{^{15}\text{N}^{16}\text{O}_3^-}}{\partial t} = & K_z \frac{\partial^2 C_{^{15}\text{N}^{16}\text{O}_3^-}}{\partial z^2} \\ & - \left(1 - \frac{^{15}\epsilon_{\text{den}}}{1000}\right) v_{\text{den}} \frac{K_{\text{O}_2, \text{inhib}}}{K_{\text{O}_2, \text{inhib}} + C_{\text{O}_2, \text{meas}}} \frac{C_{\text{H}_2\text{S}, \text{meas}}}{K_{\text{H}_2\text{S}} + C_{\text{H}_2\text{S}, \text{meas}}} \frac{C_{^{15}\text{N}^{16}\text{O}_3^-}}{K_{\text{NO}_3, \text{den}} + C_{\text{NO}_3^-}} \\ & + \left(1 - \frac{^{15}\epsilon_{\text{nit}}}{1000}\right) v_{\text{nit}} \frac{C_{\text{O}_2, \text{meas}}}{K_{\text{O}_2, \text{nit}} + C_{\text{O}_2, \text{meas}}} \frac{C_{^{14}\text{NH}_4^+}}{K_{\text{NH}_4, \text{nit}} + C_{\text{NH}_4^+}} \quad (3.5) \end{aligned}$$

$$\begin{aligned}
\frac{\partial C_{14N^{18}O^{16}O_2}}{\partial t} &= K_z \frac{\partial^2 C_{14N^{18}O^{16}O_2}}{\partial z^2} \\
&- \left(1 - \frac{^{18}\varepsilon_{\text{den}}}{1000}\right) v_{\text{den}} \frac{K_{O_2,\text{inhib}}}{K_{O_2,\text{inhib}} + C_{O_2,\text{meas}}} \frac{C_{H_2S,\text{meas}}}{K_{H_2S} + C_{H_2S,\text{meas}}} \frac{C_{^{15}N^{18}O^{16}O_2}}{K_{NO_3,\text{den}} + C_{NO_3}} \\
&\quad + ^{18}R_{\text{source}} ^{18}\alpha_{\text{nit}} v_{\text{nit}} \frac{C_{O_2,\text{meas}}}{K_{O_2,\text{nit}} + C_{O_2,\text{meas}}} \frac{C_{^{14}NH_4}}{K_{NH_4,\text{nit}} + C_{NH_4}} \quad (3.6)
\end{aligned}$$

$$\begin{aligned}
\frac{\partial C_{^{14}NH_4}}{\partial t} &= K_z \frac{\partial^2 C_{^{14}NH_4}}{\partial z^2} \\
&- v_{\text{nit}} \frac{C_{O_2,\text{meas}}}{K_{O_2,\text{nit}} + C_{O_2,\text{meas}}} \frac{C_{^{14}NH_4}}{K_{NH_4} + C_{NH_4}} \\
&\quad - v_{\text{anmx}} \frac{K_{O_2,\text{inhib}}}{K_{O_2,\text{inhib}} + C_{O_2,\text{meas}}} \frac{C_{NO_3}}{K_{NO_3,\text{anmx}} + C_{NO_3}} \frac{C_{^{14}NH_4}}{K_{NH_4,\text{anmx}} + C_{NH_4}} \quad (3.7)
\end{aligned}$$

$$\begin{aligned}
\frac{\partial C_{^{15}NH_4}}{\partial t} &= K_z \frac{\partial^2 C_{^{15}NH_4}}{\partial z^2} \\
&- \left(1 - \frac{^{15}\varepsilon_{\text{nit}}}{1000}\right) v_{\text{nit}} \frac{C_{O_2,\text{meas}}}{K_{O_2,\text{nit}} + C_{O_2,\text{meas}}} \frac{C_{^{15}NH_4}}{K_{NH_4} + C_{NH_4}} \\
&- \left(1 - \frac{^{15}\varepsilon_{\text{anmx}}}{1000}\right) v_{\text{anmx}} \frac{K_{O_2,\text{inhib}}}{K_{O_2,\text{inhib}} + C_{O_2,\text{meas}}} \frac{C_{NO_3}}{K_{NO_3,\text{anmx}} + C_{NO_3}} \frac{C_{^{15}NH_4}}{K_{NH_4,\text{anmx}} + C_{NH_4}} \quad (3.8)
\end{aligned}$$

where t is the time, z is the water depth, and C is the concentration of the compound given in the index. $^{18}R_{\text{source}}$ denotes the isotope ratio of the oxygen source for nitrification, with a $\delta^{18}O$ range of -3‰ to +3‰. The associated fractionation factor ($^{18}\alpha_{\text{nit}}$) was set to 1. In order to keep the model as simple as possible several assumptions were made: The turbulent diffusion coefficient (K_z) was estimated as described by Wenk et al. (2013) and was considered constant for the depth range above and below the RTZ, respectively. The half-saturation and inhibition constants (K_i) were defined within the range of previous studies (Lehmann et al. (2007) and references therein) and the final values are listed in Table 3.1. Measured profiles of dissolved oxygen ($C_{O_2,\text{meas}}$) and sulfide ($C_{H_2S,\text{meas}}$) concentrations were used and the NO_3^- and NH_4^+ concentrations and isotope compositions were kept constant at 50 m and at 250 m water depth, respectively. In a first scenario (A) we used the measured NO_3^- concentration data to fit the maximum reaction rates (v_i). This parameter fit yielded high NO_3^- reduction rates in close vicinity of the sulfidic water

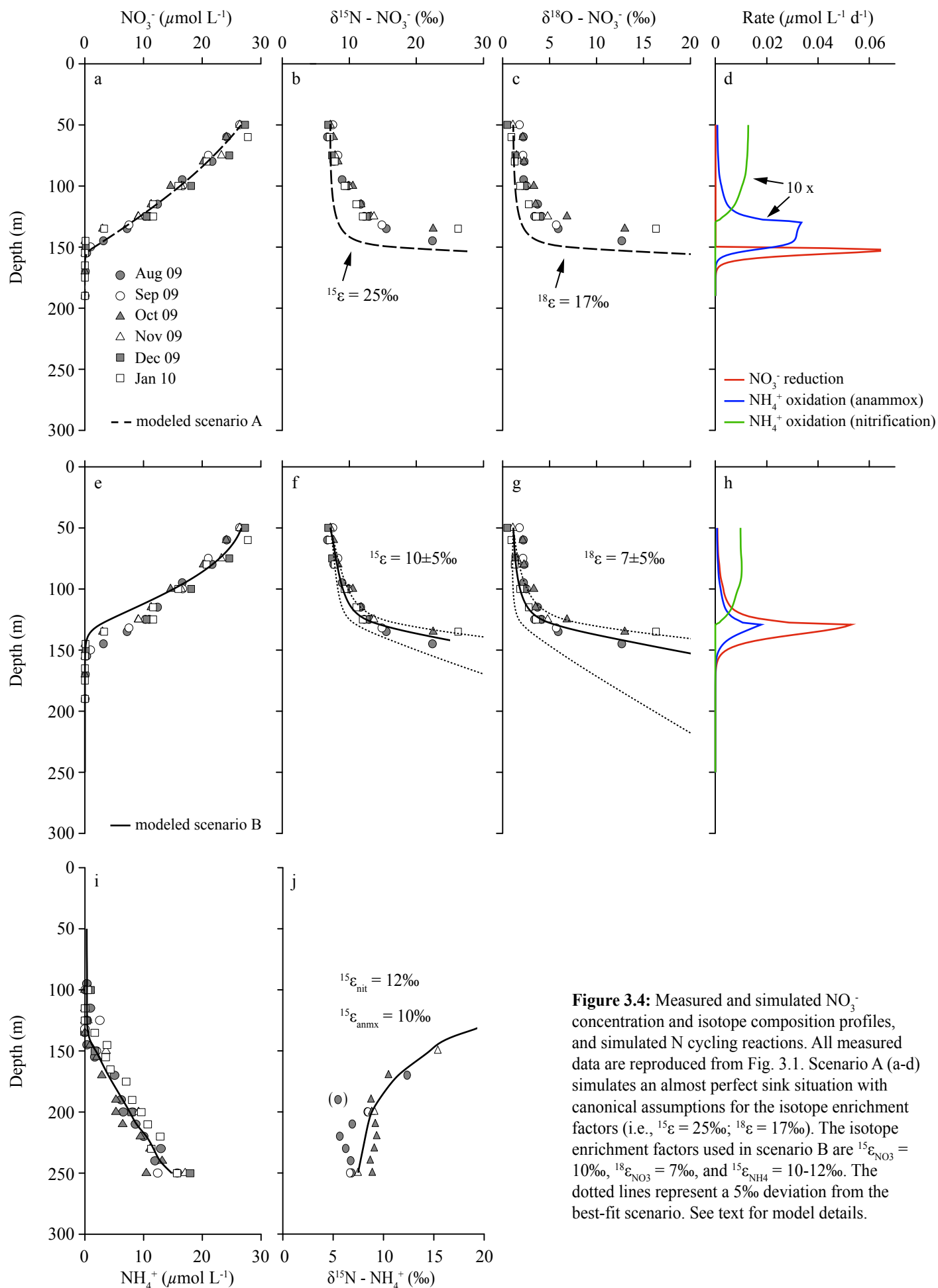


Figure 3.4: Measured and simulated NO_3^- concentration and isotope composition profiles, and simulated N cycling reactions. All measured data are reproduced from Fig. 3.1. Scenario A (a-d) simulates an almost perfect sink situation with canonical assumptions for the isotope enrichment factors (i.e., $^{15}\epsilon = 25\text{‰}$; $^{18}\epsilon = 17\text{‰}$). The isotope enrichment factors used in scenario B are $^{15}\epsilon_{\text{NO}_3} = 10\text{‰}$, $^{18}\epsilon_{\text{NO}_3} = 7\text{‰}$, and $^{15}\epsilon_{\text{NH}_4} = 10\text{--}12\text{‰}$. The dotted lines represent a 5‰ deviation from the best-fit scenario. See text for model details.

column and negligible NO_3^- production through nitrification (Figs. 3.4a, d). Although this simplified model predicts the measured NO_3^- concentration data quite well, it is not suitable to explain the observed $\delta^{15}\text{N}$ - and $\delta^{18}\text{O}$ - NO_3^- profiles (Figs. 3.4b, c). An unrealistically high intrinsic N isotope enrichment factor, much greater than 25‰, would be needed to simulate the observed values. Hence we conclude that diffusive mixing and complete NO_3^- consumption within a narrow denitrifying zone may contribute to an under-expression of the N (and O) isotope signature in the water column, but cannot fully explain the observed $[\text{NO}_3^-]$ vs. $\delta^{15}\text{N}$ - NO_3^- profiles in the Lake Lugano north basin.

In a second attempt (scenario B) to fit the model to the combined NO_3^- concentration and isotope data set, we amended the model by including higher rates of anammox and nitrification, as well as lower maximum denitrification rates than in scenario A. We also slightly changed the zonation of the active processes by varying the sulfide, nitrate, and ammonium half-saturation concentrations of denitrification and nitrification, respectively (Table 3.1). For an overall best fit with the measured NO_3^- isotope data, we computed biological N and O isotope enrichment factors of 10‰ and 7‰, respectively for NO_3^- consumption (Figs. 3.4e-j). N isotope enrichment factors of NH_4^+ consumption by anammox and nitrification were 10‰ and 12‰, respectively (see Section 3.4.3 for a discussion of the NH_4^+ consumption processes). While these model results are sensitive to the choice of the biogeochemical parameters, our results indicate that comparatively low intrinsic N (and O) isotope enrichment factors (i.e., 10‰ and 7‰, respectively) for NO_3^- consumption describe the distribution of the NO_3^- isotopes in the Lake Lugano water column quite well. We are aware that our model still mimics the natural conditions insufficiently. Yet, excluding diffusion limitation as sole explanation for an under-expression of the biological N and O isotope fractionation at the ecosystem level, we argue that the under-expression of N and O isotope enrichment must happen in parts on other dimensional levels (cellular, enzyme), or is due to overprinting effects by other N transformations not included in our model.

Reduced isotope fractionation under low cell specific nitrate reduction rates and NO_3^- limitation

Isotope fractionation on the cellular level (ϵ_{cell}) can be reduced under low cell specific nitrate reduction (CSNR) rates (Kritee et al., 2012), if NO_3^- reduction is catalyzed by the membrane-bound dissimilatory nitrate reductase (Nar). Such low CSNR rates do generally not affect the enzyme-level isotope fractionation (ϵ_{Nar}). It is rather the expression of ϵ_{Nar} outside the cell, which is reduced and which is a function of the NO_3^- efflux to uptake ratio. Under low CSNR rates, this ratio must be low according to the “efflux model” (Shearer et al., 1991) and thus ϵ_{Nar} is under-expressed outside the cell. Our NO_3^- N isotope data suggest that such a condition may well apply to the

Table 3.1: Parameters used in model scenarios A and B presented in Fig. 3.4.

Parameter	Scenario A	Scenario B	Unit	Description
$K_{O_2, \text{inhib}}$	3	3	$\mu\text{mol L}^{-1}$	Inhibition constant for nitrate reduction due to oxygen
$K_{NO_3, \text{den}}$	15	2	$\mu\text{mol L}^{-1}$	Nitrate half-saturation concentration for denitrification
$K_{O_2, \text{nit}}$	20	20	$\mu\text{mol L}^{-1}$	Oxygen half-saturation concentration for nitrification
$K_{NH_4, \text{nit}}$	15	5	$\mu\text{mol L}^{-1}$	Ammonium half-saturation concentration for nitrification
$K_{NO_3, \text{anmx}}$	5	5	$\mu\text{mol L}^{-1}$	Nitrate half-saturation concentration for anammox
$K_{NH_4, \text{anmx}}$	1	1	$\mu\text{mol L}^{-1}$	Ammonium half-saturation concentration for anammox
K_{H_2S}	1	0.5	$\mu\text{mol L}^{-1}$	Sulfide half-saturation concentration for denitrification

denitrification zone of the Lake Lugano north basin. Here we previously found high copy numbers of *nirS* genes (responsible for NO_2^- reduction) throughout the anoxic water column with a maximum value of 4.5×10^6 copies mL^{-1} (Wenk et al., 2013). Maximum potential denitrification rates, determined in ex situ ^{15}N -label experiments, were 91.5 ± 32 $nmol N_2 L^{-1} d^{-1}$. If we assume that all bacteria containing a *nirS* gene also reduce NO_3^- , we obtain an estimated CSNR rate of 2.8×10^{-14} $\mu\text{mol cell}^{-1} \text{min}^{-1}$. Although this rate is only a rough estimate of the in situ CSNR, it is at least two orders of magnitude lower than the lowest CSNR rate reported from culture experiments (Kritee et al., 2012), which yielded effective N isotope effects of only 10 - 15‰. With the low CSNR rates determined for Lake Lugano, it is reasonable to assume that the NO_3^- efflux to uptake ratio during NO_3^- reduction is very low, and ϵ_{cell} is even more reduced relative to ϵ_{Nar} .

Moreover, in the northern basin of Lake Lugano, active denitrification is most probably confined to water layers below 125 m depth, where NO_3^- concentrations are always $< 5 \mu\text{mol L}^{-1}$. If ambient NO_3^- concentrations are this low, NO_3^- uptake by the cell can become the rate limiting, and thus the first irreversible step of denitrification. Since cellular NO_3^- uptake is thought to cause negligible isotope fractionation, ϵ_{cell} would be further reduced.

Finally, Granger et al. (2008) and Kritee et al. (2012) found evidence for the regulation of ϵ_{cell} by ambient dissolved O_2 concentrations, which reduced N isotope enrichment in the presence of micromolar O_2 (compared to truly anoxic conditions). Although in the Lake Lugano north basin O_2 concentrations were always $< 1 \mu\text{mol L}^{-1}$ below 130 m depth, there is putative evidence for episodic O_2 intrusions not directly detected by our sampling scheme (Wenk et al., 2013).

Although, we do not know the exact mechanisms that may be responsible for a lowered ϵ_{cell} , we suggest that the environmental conditions in the water column (low CSNR rates, substrate limitation, possible O_2 intrusion) are highly conducive to the under-expression of ϵ_{Nar} in the ambient water column. However, we cannot exclude

the possibility that it is actually ϵ_{Nar} (and not only its expression in the environment) that is lower compared to previous culture and field based estimates, or that NO_3^- reduction is partly catalyzed by a different enzyme.

Unknown isotope fractionation by chemolithotrophic denitrifiers

The low community isotope enrichment factors observed in the Lake Lugano north basin may also reflect true organism-specific fractionation. Unfortunately, no culture study has yet addressed the isotope effects associated with NO_3^- consumption by chemolithotrophs. It is possible that the enzymatic machinery for NO_3^- reduction differs between chemolithotrophic and organotrophic denitrifiers. However, there is no systematic difference in N isotope fractionation among different organotrophic denitrifiers (Granger et al., 2008). The highest variability in N isotope fractionation was actually observed between cultures of the same strain, indicating that under-expression of ϵ_{Nar} happens rather on the cellular level (as described in Section 3.4.1). However, there is putative evidence that NO_3^- reduction in the Lake Lugano north basin is partly catalyzed by Nap (see Section 3.4.2), possibly with a N isotope effect much closer to our modeled value of $\sim 10\text{‰}$ (Granger et al., 2008).

Overprinting isotope effects by nitrate production in the RTZ

Potential NO_3^- production by anammox (Strous et al., 1999) was not included in our diffusion-reaction model. Nevertheless, anammox-derived NO_3^- may have an effect on the N isotope composition of the ambient NO_3^- . From recent culture experiments we have evidence that the NO_2^- oxidation by anammox is associated with a strong inverse N isotope fractionation (Brunner et al., 2013). However, although the N isotope effects of anammox (equilibrium and kinetic) were relatively well constrained in the enrichment culture experiments by Brunner et al. (2013), their expression in the natural environment remained uncertain. It is uncertain (1) what the $\delta^{15}\text{N}$ of NO_3^- from the oxidation of NO_2^- by anammox is, and (2) what the lifetime of anammox-regenerated NO_3^- in the RTZ ambient water is. Its immediate and complete consumption by other microorganisms is likely, because the denitrifying zone in the Lake Lugano north basin is extremely NO_3^- limited.

Although we did not directly measure potential aerobic nitrification rates, the concentration profiles of dissolved NH_4^+ and O_2 suggest that NH_4^+ is consumed mainly anaerobically (Wenk et al., 2013). Furthermore, potential anammox rates measured in ex situ ^{15}N label experiments agreed very well with estimated NH_4^+ oxidation rates based on flux calculations (Wenk et al., 2013). Nevertheless, we cannot exclude that part of the NH_4^+ is oxidized to NO_3^- through microaerobic nitrification. This process could add NO_3^- to the denitrifying zone with a significantly lower $\delta^{15}\text{N}$ compared to the upper hypolimnetic NO_3^- . This dilution, or overprinting effect could in turn lead to

an apparently reduced community N isotope fractionation for net NO_3^- consumption. In contrast, the N isotope effects associated with NO_2^- oxidation should not play a role, in the case where NO_2^- is not accumulating.

3.4.2 Oxygen vs. nitrogen isotope enrichment during NO_3^- reduction in the RTZ

Freshwater denitrification seems to occur with an O to N isotope enrichment ratio significantly lower than unity (Lehmann et al. (2003) and references therein), whereas marine denitrification and assimilatory NO_3^- reduction fractionate the N and O isotopes with a 1:1 ratio (Casciotti et al., 2002; Granger et al., 2004, 2008, 2010; Sigman et al., 2005). In qualitative agreement with observations from other freshwater studies, the ^{18}O to ^{15}N enrichment ratio associated with NO_3^- consumption in the RTZ of the Lake Lugano north basin was 0.89 (Fig. 3.5). As discussed in Section 3.4.1, the expression of both the N and O isotope fractionation in the water column can be significantly reduced at multiple spatial scales. The degree of the under-expression, however, should not be different for the ^{15}N and ^{18}O enrichment at the ecosystem and at the cellular level, so that $^{18}\epsilon_{\text{app}} : ^{15}\epsilon_{\text{app}} = ^{18}\epsilon_{\text{cell}} : ^{15}\epsilon_{\text{cell}}$. A possible explanation for $^{18}\epsilon$ to $^{15}\epsilon$ ratios lower than 1 could be related to the differential expression of N vs. O isotope fractionation at the enzyme level. There are four types of nitrate reductases: Bacterial membrane-bound dissimilatory Nar, periplasmic dissimilatory Nap, cytoplasmic assimilatory Nas, and the eukaryotic assimilatory eukNR. Nitrate reduction catalyzed by Nar, Nas, and eukNR fractionates N and O isotopes near unity (Granger et al., 2008, 2010; Karsh et al., 2012). However, NO_3^- reduction by *Rhodobacter sphaeroides*, which utilize Nap, was found to proceed with an $^{18}\epsilon$ to $^{15}\epsilon$ ratio of ~ 0.62 , independent of whether freshwater or seawater was used as growth medium (Granger et al., 2008). It has been shown that Nap can be essential for NO_3^- reduction under certain conditions, such as during aerobic denitrification, but also for growth under anaerobic and NO_3^- limited conditions (reviews in Richardson, 2000; Morozkina and Zvyagilskaya, 2007). Competition experiments with different *E. coli* strains for instance showed that the Nar-expressing strain was out-competed by the Nap-expressing strain under NO_3^- limited cultivation (Potter et al., 1999). Richardson (2000) concluded from this observation that under nitrate-limited conditions, bacteria might sacrifice energy conservation efficiency in favor of substrate affinity. The overall energetic loss associated with the use of Nap vs. Nar during denitrification can be as low as 8% (Richardson et al., 2001). In agreement with this interpretation of a selective advantage for Nap under nitrate-limited conditions, Dong et al. (2009) found that the relative abundance of *napA* genes (vs. *narG* genes) increased with decreasing NO_3^- concentrations along an estuarine nutrient gradient, suggesting that Nap may indeed be more important under nitrate-limited conditions, such as found

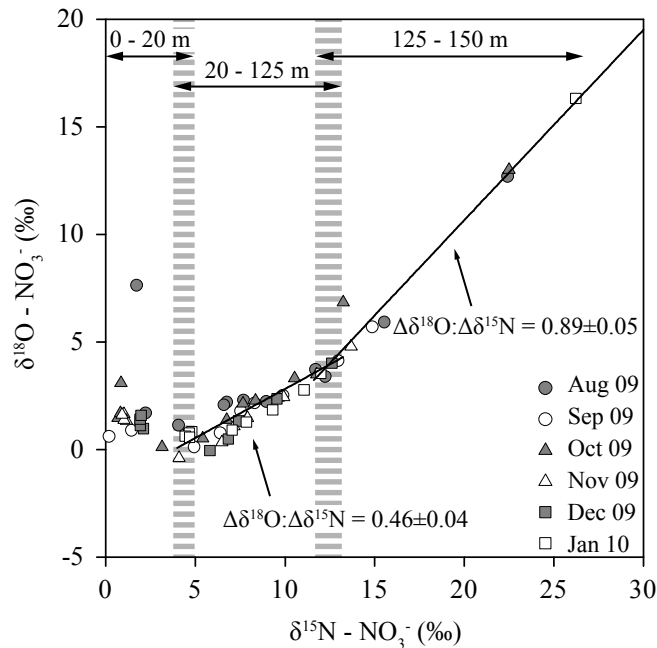


Figure 3.5: Nitrate $\Delta\delta^{18}\text{O}$ -to- $\Delta\delta^{15}\text{N}$ relationship in the Lake Lugano north basin. $\Delta\delta^{18}\text{O}:\Delta\delta^{15}\text{N}$ values denote the mean slopes (± 1 standard error) of the linear regression lines for all data from the RTZ (125-150 m depth; 0.89 ± 0.05), and from the oxic hypolimnion (20-125 m depth; 0.46 ± 0.04). The vertical dashed lines mark the boundaries between the epilimnion (0-20 m depth), the oxic hypolimnion (20-125 m depth), and the RTZ (125-150 m depth).

in the Lake Lugano RTZ.

Little is known about sulfide-dependent denitrification in freshwater ecosystems, but genome analysis of sulfur oxidizing, NO_3^- reducing bacteria revealed that at least two of them, *Sulfurovum* sp. NBC37-1 and *Sulfurimonas denitrificans*, contain only the genes for the Nap system (Nakagawa et al., 2007; Sievert et al., 2008). Given the relatively low $^{18}\epsilon$ to $^{15}\epsilon$ ratio observed in this study and for cultured denitrifiers expressing Nap, we hypothesize that Nap is catalyzing part of the NO_3^- reduction in the Lake Lugano north basin (and maybe other freshwater environments).

Another explanation for a relatively low $^{18}\epsilon$ to $^{15}\epsilon$ ratio in the RTZ could be some overprinting effect by anammox or microaerobic nitrification. Interestingly, in the oxic hypolimnion, we observed a reduced ^{18}O to ^{15}N enrichment ratio of only ~ 0.5 (Fig. 3.5). The reduced ratio can possibly be explained by NO_3^- production through coupled mineralization-nitrification. Previous work has predicted that nitrification would lead to a decoupling of the $\delta^{18}\text{O}$ and $\delta^{15}\text{N}$ signals (Lehmann et al., 2003; Sigman et al., 2005) in net NO_3^- consuming (i.e., uptake or denitrification) zones. The possible effect

of nitrification on the NO_3^- pool is highlighted by the NO_3^- isotope signatures in the epilimnion, where the NO_3^- concentration decrease was associated with a decrease in $\delta^{15}\text{N-NO}_3^-$ but a slight increase in $\delta^{18}\text{O-NO}_3^-$ (Figs. 3.1, 3.5). At this point it is unclear as to what the possible NO_3^- $\delta^{15}\text{N}$ vs. $\delta^{18}\text{O}$ patterns caused by nitrification and anammox under different environmental conditions could be, and these patterns almost certainly depend on the relative rates of NO_3^- production and consumption, as well as the isotopic composition of the source N and O atoms during NO_3^- production (so that nitrification may have a completely different effect on the NO_3^- pool in marine vs. freshwater environments). We speculate, that (microaerobic) NO_3^- production does not necessarily lead to a significant deviation from a linear $\delta^{18}\text{O-}$ vs. $\delta^{15}\text{N-NO}_3^-$ trend in general, but that it instead can shift the apparent $^{18}\epsilon$ to $^{15}\epsilon$ ratio to lower values, as observed in the Lake Lugano north basin. Independent of the effect of nitrification and anammox on the NO_3^- N to O isotope dynamics in the Lake Lugano RTZ, it is obvious that the oxidation of NH_4^+ represents an important constraint on the overall N isotope effect of N loss by N_2 production in the water column.

3.4.3 Low community isotope enrichment for NH_4^+ consumption in the RTZ

In the RTZ of the Lake Lugano north basin we have identified anammox as the main NH_4^+ sink (Wenk et al., 2013). The Rayleigh model-derived isotope enrichment factor associated with NH_4^+ consumption was $5.9 \pm 0.8\%$ (Fig. 3.6). There is experimental evidence that anaerobic NH_4^+ oxidation catalyzed by the enzyme hydrazine hydrolase (Hh) occurs with a relatively strong isotope effect (Brunner et al., 2013). If this assumption of a high $^{15}\epsilon_{\text{Hh}}$ holds true, it begs the question as to why we observe such a low N isotope enrichment factor for NH_4^+ consumption in the Lake Lugano water column. Similar to the argumentation in Section 3.4.1, the fact that NH_4^+ is consumed almost completely within a well-defined layer can reduce the expression of the biological N isotope effect of NH_4^+ oxidation in the water column. At this point it is difficult to derive a robust estimate for this biological N isotope effect from our diffusion-reaction model. Firstly, it needs to be noted that the isotope enrichment factor would represent a combined N isotope effect for NH_4^+ oxidation by anammox and microaerobic nitrification, and we only have incomplete information with regard to the partitioning between these two NH_4^+ consuming processes in the Lake Lugano RTZ. Secondly, and even more importantly, we lack $\delta^{15}\text{N-NH}_4^+$ measurements from low- $[\text{NH}_4^+]$ samples close to the active NH_4^+ oxidizing site, where the $\delta^{15}\text{N-NH}_4^+$ distribution is most sensitive to the biological N isotope effect, rendering the parameter estimation problematic. Nevertheless, N isotope enrichment factors of 10‰ and 12‰ for NH_4^+ consumption by anammox and nitrification, respectively, yielded a good model fit with the available observational data (Figs. 3.4e-j). The model-derived estimates

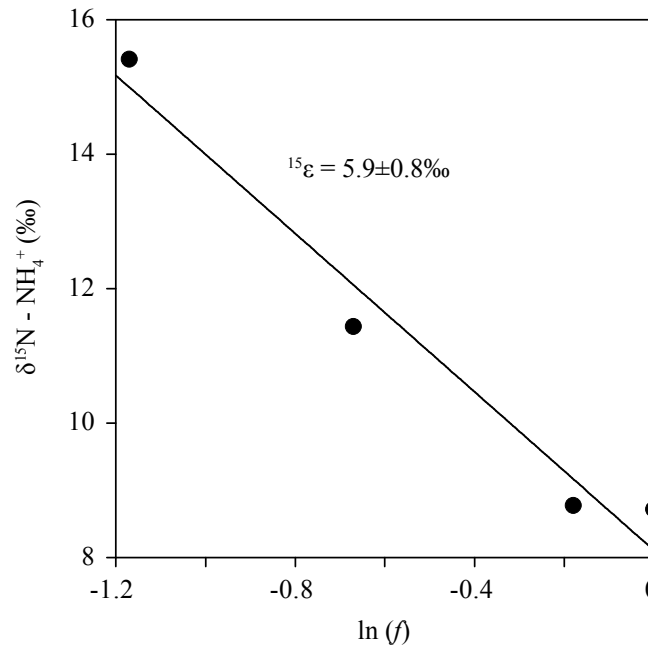


Figure 3.6: Rayleigh plot for ammonium consumption in the RTZ. Concentration and $\delta^{15}\text{N}-\text{NH}_4^+$ data were averaged for each depth. The slope (± 1 standard error) of the linear regression line is $5.9 \pm 0.8\text{‰}$. f denotes the remaining ammonium fraction with respect to the average ammonium concentration at 200 m water depth.

for $^{15}\epsilon_{\text{NH}_4}$ are afflicted with relatively large uncertainties. They do, however, provide putative evidence that the cellular-level N isotope effect of anammox may indeed be relatively low. If true, it is likely that the expression of the enzymatic isotope effect by anammox is reduced outside the cell due to a relatively low efflux-to-uptake ratio. Under-expression of the N isotope fractionation could thus happen in analogy to the nitrate efflux model discussed in Section 3.4.1. The peculiar cell compartmentalization in anammox bacteria may make them particularly prone to such an under-expression. In the case of anammox bacteria, most catabolic processes take place within a unique compartment called the anammoxosome (Lindsay et al., 2001). The anammoxosome is surrounded by a very dense membrane composed of ladderane lipids. Specific transporters are needed to regulate the internal concentrations of NH_4^+ and NO_2^- (van Niftrik and Jetten, 2012). It is therefore very likely that the energy-dependence of NH_4^+ uptake, efflux, and oxidation is characteristic for anammox bacteria, at least under natural conditions.

3.5 Summary and implications for N isotope budgets

We present the first putative report on the community N and O isotope effects for sulfide-dependent denitrifiers and anammox bacteria in a natural environment. Although the model results bear some uncertainties, they indicate that the N isotope enrichment factors for sulfide-dependent denitrification and NH_4^+ oxidation by anammox in the Lake Lugano north basin are low compared to the canonical assumptions for organotrophic denitrification and nitrification. At what spatial level the isotope effects are under-expressed remains uncertain. Given the environmental conditions in the Lake Lugano RTZ, the efflux model (Kritee et al., 2012; Shearer et al., 1991) provides a compelling explanation for the under-expression of ϵ at the cellular level, requiring, however, that most NO_3^- reduction is catalyzed by the membrane-bound nitrate reductase Nar. This seems inconsistent with evidence from the coupled N and O isotope measurements. The ^{18}O to ^{15}N isotope enrichment associated with NO_3^- reduction in the RTZ is lower than 1, in contrast to measurements in marine settings and in most laboratory experiments. While it is possible that the lowered ^{18}O to ^{15}N isotope enrichment ratio is partly due to NO_3^- regeneration by microaerobic nitrification or anammox, we speculate that NO_3^- reduction in the RTZ was partly catalyzed by the periplasmic Nap instead of the membrane-bound Nar. While this conclusion awaits confirmation from independent molecular data, we suggest that Nap may play a much more important role in driving NO_3^- reduction in aquatic ecosystems than previously assumed.

We conclude that the expression of the N (and O) isotope fractionation during NO_3^- reduction and NH_4^+ oxidation can be variable in nature and likely depends on the pathways of NO_3^- dissimilation (organotrophic vs. chemolithotrophic), the main catalyzing enzymes (Nar vs. Nap), the pathways of NH_4^+ oxidation (nitrification vs. anammox), and the controlling environmental conditions (e.g., substrate limitation, cell specific N transformation rates). Our study implies that the community isotope effects associated with NO_3^- and NH_4^+ consumption can be significantly lower in a natural ecosystem than traditionally assumed in N isotope balances and biogeochemical models. We are aware that the data presented here originate from a lake, and our findings can thus not be directly extrapolated to the ocean. Also, the exact mechanisms behind the relatively low N isotope effects are uncertain. Still, our results support the suggestion by Kritee et al. (2012) to refrain from a canonical assumption of a robust $^{15}\epsilon = 25\%$ for pelagic denitrification in N isotope budgets. Given the increasingly acknowledged role of chemolithotrophic fixed N elimination pathways in aquatic ecosystems, future experimental studies need to address these pathways specifically. More precisely, culture experiments with anammox bacteria and chemolithotrophic denitrifiers are vital to validate the here-reported community N (and O) isotope effects and their potential variability in response to changing

environmental conditions.

3 - References

- M. Alkhatib, M. F. Lehmann, and P. A. del Giorgio. The nitrogen isotope effect of benthic remineralization-nitrification-denitrification coupling in an estuarine environment. *Biogeosciences*, 9:1633–1646, 2012.
- M. A. Altabet. Constraints on oceanic N balance/imbalance from sedimentary ^{15}N records. *Biogeosciences*, 4:75–86, 2007.
- A. Barbieri and B. Polli. Description of Lake Lugano. *Aquatic Sciences*, 54:181–183, 1992.
- C. C. Barford, J. P. Montoya, M. A. Altabet, and R. Mitchell. Steady-state nitrogen isotope effects of N_2 and N_2O production in *Paracoccus denitrificans*. *Applied and Environmental Microbiology*, 65:989–994, 1999.
- J. K. Böhlke, S. J. Mroczkowski, and T. B. Coplen. Oxygen isotopes in nitrate: New reference materials for ^{18}O : ^{17}O : ^{16}O measurements and observations on nitrate-water equilibration. *Rapid Communications in Mass Spectrometry*, 17:1835–1846, 2003.
- A. Bourbonnais, M. F. Lehmann, D. A. Butterfield, and S. K. Juniper. Subseafloor nitrogen transformations in diffuse hydrothermal vent fluids of the Juan de Fuca Ridge evidenced by the isotopic composition of nitrate and ammonium. *Geochemistry Geophysics Geosystems*, 13, 2012.
- R. S. Braman and S. A. Hendrix. Nanogram nitrite and nitrate determination in environmental and biological materials by vanadium(III) reduction with chemiluminescence detection. *Analytical Chemistry*, 61:2715–2718, 1989.
- J. A. Brandes and A. H. Devol. Isotopic fractionation of oxygen and nitrogen in coastal marine sediments. *Geochimica et Cosmochimica Acta*, 61:1793–1801, 1997.
- J. A. Brandes, A. H. Devol, T. Yoshinari, D. A. Jayakumar, and S. W. A. Naqvi. Isotopic composition of nitrate in the central Arabian Sea and Eastern Tropical North Pacific: A tracer for mixing and nitrogen cycles. *Limnology and Oceanography*, 43:1680–1689, 1998.

- I. Brettar and G. Rheinheimer. Denitrification in the Central Baltic: Evidence for H₂S-oxidation as motor of denitrification at the oxic-anoxic interface. *Marine Ecology Progress Series*, 77:157–169, 1991.
- B. Brunner, S. Contreras, M. F. Lehmann, O. Matantseva, M. Rollog, T. Kalvelage, G. Klockgether, G. Lavik, M. S. M. Jetten, B. Kartal, and M. M. M. Kuypers. Nitrogen isotope effects induced by anammox bacteria. *PNAS Proceedings of the National Academy of Sciences*, 110:18994–18999, 2013.
- D. E. Canfield, F. J. Stewart, B. Thamdrup, L. De Brabandere, T. Dalsgaard, E. F. Delong, N. P. Revsbech, and O. Ulloa. A cryptic sulfur cycle in oxygen-minimum-zone waters off the Chilean coast. *Science*, 330:1375–1378, 2010.
- K. L. Casciotti and M. R. McIlvin. Isotopic analyses of nitrate and nitrite from reference mixtures and application to Eastern Tropical North Pacific waters. *Marine Chemistry*, 107:184–201, 2007.
- K. L. Casciotti, D. M. Sigman, M. Galanter Hastings, J. K. Böhlke, and A. Hilkert. Measurement of the oxygen isotopic composition of nitrate in seawater and freshwater using the denitrifier method. *Analytical Chemistry*, 74:4905–4912, 2002.
- K. L. Casciotti, D. M. Sigman, and B. B. Ward. Linking diversity and stable isotope fractionation in ammonia-oxidizing bacteria. *Geomicrobiology Journal*, 20:335–353, 2003.
- R. D. Cox. Determination of nitrate and nitrite at the parts per billion level by chemiluminescence. *Analytical Chemistry*, 52:332–335, 1980.
- T. Dalsgaard, D. E. Canfield, J. Petersen, B. Thamdrup, and J. Acuña González. N₂ production by the anammox reaction in the anoxic water column of Golfo Dulce, Costa Rica. *Nature*, 422:606–608, 2003.
- C. Deutsch, D. M. Sigman, R. C. Thunell, A. N. Meckler, and G. H. Haug. Isotopic constraints on glacial/interglacial changes in the oceanic nitrogen budget. *Global Biogeochemical Cycles*, 18, 2004.
- L. F. Dong, C. J. Smith, S. Papaspyrou, A. Stott, A. M. Osborn, and D. B. Nedwell. Changes in benthic denitrification, nitrate ammonification, and anammox process rates and nitrate and nitrite reductase gene abundances along an estuarine nutrient gradient (the Colne Estuary, United Kingdom). *Applied and Environmental Microbiology*, 75:3171–3179, 2009.
- C. Garside. A chemiluminescent technique for the determination of nanomolar concentrations of nitrate and nitrite in seawater. *Marine Chemistry*, 11:159–167, 1982.

- R. Gonfiantini, W. Stichler, and K. Rosanski. Standards and intercomparison materials distributed by the IAEA for stable isotope measurements. *IAEA-TECDOC-825*, IAEA, Vienna, pages 13–31, 1995.
- J. Granger, D. M. Sigman, J. A. Needoba, and P. J. Harrison. Coupled nitrogen and oxygen isotope fractionation of nitrate during assimilation by cultures of marine phytoplankton. *Limnology and Oceanography*, 49:1763–1773, 2004.
- J. Granger, D. M. Sigman, M. F. Lehmann, and P. D. Tortell. Nitrogen and oxygen isotope fractionation during dissimilatory nitrate reduction by denitrifying bacteria. *Limnology and Oceanography*, 53:2533–2545, 2008.
- J. Granger, D. M. Sigman, M. M. Rohde, M. T. Maldonado, and P. D. Tortell. N and O isotope effects during nitrate assimilation by unicellular prokaryotic and eukaryotic plankton cultures. *Geochimica et Cosmochimica Acta*, 74:1030–1040, 2010.
- C. P. Holzner, W. Aeschbach-Hertig, M. Simona, M. Veronesi, D. M. Imboden, and R. Kipfer. Exceptional mixing events in meromictic Lake Lugano (Switzerland/Italy), studied using environmental tracers. *Limnology and Oceanography*, 54:1113–1124, 2009.
- S. G. Horrigan, J. P. Montoya, J. L. Nevins, and J. J. McCarthy. Natural isotopic composition of dissolved inorganic nitrogen in the Chesapeake Bay. *Estuarine, Coastal and Shelf Science*, 30:393–410, 1990.
- B. Z. Houlton, D. M. Sigman, E. A. G. Schuur, and L. O. Hedin. A climate-driven switch in plant nitrogen acquisition within tropical forest communities. *Proceedings of the National Academy of Sciences of the United States of America (PNAS)*, 104:8902–8906, 2007.
- K. L. Karsh, J. Granger, K. Kritee, and D. M. Sigman. Eukaryotic assimilatory nitrate reductase fractionates N and O isotopes with a ratio near unity. *Environmental Science and Technology*, 46:5727–5735, 2012.
- A. N. Knapp, D. M. Sigman, and F. Lipschultz. N isotopic composition of dissolved organic nitrogen and nitrate at the Bermuda Atlantic time-series study site. *Global Biogeochemical Cycles*, 19, 2005.
- F. Koroleff. *Determination of ammonia*. In: K. Grasshoff [ed.], *Methods of Seawater Analysis*, pages 126–133. Verlag Chemie, 1976.
- K. Kritee, D. M. Sigman, J. Granger, B. B. Ward, A. Jayakumar, and C. Deutsch. Reduced isotope fractionation by denitrification under conditions relevant to the ocean. *Geochimica et Cosmochimica Acta*, 92:243–259, 2012.

- M. M. M. Kuypers, A. O. Sliemers, G. Lavik, M. Schmid, B. B. Jørgensen, J. G. Kuenen, J. S. S. Damsté, M. Strous, and M. S. M. Jetten. Anaerobic ammonium oxidation by anammox bacteria in the Black Sea. *Nature*, 422:608–611, 2003.
- G. Lavik, T. Stuhmann, V. Brochert, A. van der Plas, V. Mohrholz, P. Lam, M. Mussmann, B. M. Fuchs, R. Amann, U. Lass, and M. M. M. Kuypers. Detoxification of sulphidic African shelf waters by blooming chemolithotrophs. *Nature*, 457:581–584, 2009.
- M. F. Lehmann, P. Reichert, S. M. Bernasconi, A. Barbieri, and J. A. McKenzie. Modelling nitrogen and oxygen isotope fractionation during denitrification in a lacustrine redox-transition zone. *Geochimica Et Cosmochimica Acta*, 67:2529–2542, 2003.
- M. F. Lehmann, D. M. Sigman, and W. M. Berelson. Coupling the $^{15}\text{N}/^{14}\text{N}$ and $^{18}\text{O}/^{16}\text{O}$ of nitrate as a constraint on benthic nitrogen cycling. *Marine Chemistry*, 88:1–20, 2004.
- M. F. Lehmann, D. M. Sigman, D. C. McCorkle, J. Granger, S. Hoffmann, G. Cane, and B. G. Brunelle. The distribution of nitrate $^{15}\text{N}/^{14}\text{N}$ in marine sediments and the impact of benthic nitrogen loss on the isotopic composition of oceanic nitrate. *Geochimica et Cosmochimica Acta*, 71:5384–5404, 2007.
- M. R. Lindsay, R. I. Webb, M. Strous, M. S. M. Jetten, M. K. Butler, R. J. Forde, and J. A. Fuerst. Cell compartmentalisation in planctomycetes: Novel types of structural organisation for the bacterial cell. *Archives of Microbiology*, 175:413–429, 2001.
- A. Mariotti, J. C. Germon, P. Hubert, P. Kaiser, R. Letolle, A. Tardieux, and P. Tardieux. Experimental determination of nitrogen kinetic isotope fractionation: Some principles; Illustration for the denitrification and nitrification processes. *Plant and Soil*, 62:413–430, 1981.
- E. V. Morozkina and R. A. Zvyagilskaya. Nitrate reductases: Structure, functions, and effect of stress factors. *Biochemistry*, 72:1151–1160, 2007.
- S. Nakagawa, Y. Takaki, S. Shimamura, A.-L. Reysenbach, K. Takai, and K. Horikoshi. Deep-sea vent ϵ -proteobacterial genomes provide insights into emergence of pathogens. *Proceedings of the National Academy of Sciences of the United States of America*, 104:12146–12150, 2007.
- S. Otte, J. G. Kuenen, L. P. Nielsen, H. W. Paerl, J. Zopfi, H. N. Schulz, A. Teske, B. Strotmann, V. A. Gallardo, and B. B. Jørgensen. Nitrogen, carbon, and sulfur

- metabolism in natural *Thioploca* samples. *Applied and Environmental Microbiology*, 65:3148–3157, 1999.
- L. C. Potter, P. Millington, L. Griffiths, G. H. Thomas, and J. A. Cole. Competition between *Escherichia coli* strains expressing either a periplasmic or a membrane-bound nitrate reductase: Does Nap confer a selective advantage during nitrate-limited growth? *Biochemical Journal*, 344:77–84, 1999.
- P. Reichert. AQUASIM - A tool for simulation and data analysis of aquatic systems. *Water Science and Technology*, 30:21–30, 1994.
- D. J. Richardson. Bacterial respiration: A flexible process for a changing environment. *Microbiology*, 146:551–571, 2000.
- D. J. Richardson, B. C. Berks, D. A. Russell, S. Spiro, and C. J. Taylor. Functional, biochemical and genetic diversity of prokaryotic nitrate reductases. *Cellular and Molecular Life Sciences*, 58:165–178, 2001.
- E. Ryabenko, A. Kock, H. W. Bange, M. A. Altabet, and D. W. R. Wallace. Contrasting biogeochemistry of nitrogen in the Atlantic and Pacific oxygen minimum zones. *Biogeosciences*, 9:203–215, 2012.
- G. Shearer, J. D. Schneider, and D. H. Kohl. Separating the efflux and influx components of net nitrate uptake by *Synechococcus* R2 under steady-state conditions. *Journal of General Microbiology*, 137:1179–1184, 1991.
- S. M. Sievert, K. A. Scott, M. G. Klotz, P. S. G. Chain, L. J. Hauser, J. Hemp, M. Hügl, M. Land, A. Lapidus, F. W. Larimer, S. Lucas, S. A. Malfatti, F. Meyer, I. T. Paulsen, Q. Ren, and J. Simon. Genome of the epsilonproteobacterial chemolithoautotroph *Sulfurimonas denitrificans*. *Applied and Environmental Microbiology*, 74:1145–1156, 2008.
- D. M. Sigman, M. A. Altabet, R. Michener, D. C. McCorkle, B. Fry, and R. M. Holmes. Natural abundance-level measurement of the nitrogen isotopic composition of oceanic nitrate: An adaptation of the ammonia diffusion method. *Marine Chemistry*, 57:227–242, 1997.
- D. M. Sigman, K. L. Casciotti, M. Andreani, C. Barford, M. Galanter, and J. K. Böhlke. A bacterial method for the nitrogen isotopic analysis of nitrate in seawater and freshwater. *Analytical Chemistry*, 73:4145–4153, 2001.
- D. M. Sigman, R. Robinson, A. N. Knapp, A. van Geen, D. C. McCorkle, J. A. Brandes, and R. C. Thunell. Distinguishing between water column and sedimentary denitrification in the Santa Barbara Basin using the stable isotopes of nitrate. *Geochemistry Geophysics Geosystems*, 4, 2003.

- D. M. Sigman, J. Granger, P. J. DiFiore, M. F. Lehmann, R. Ho, G. Cane, and A. van Geen. Coupled nitrogen and oxygen isotope measurements of nitrate along the eastern North Pacific margin. *Global Biogeochemical Cycles*, 19, 2005.
- D. M. Sigman, P. J. DiFiore, M. P. Hain, C. Deutsch, Y. Wang, D. M. Karl, A. N. Knapp, M. F. Lehmann, and S. Pantoja. The dual isotopes of deep nitrate as a constraint on the cycle and budget of oceanic fixed nitrogen. *Deep-Sea Research*, 56:1419–1439, 2009.
- M. Strous, J. A. Fuerst, E. H. M. Kramer, S. Logemann, G. Muyzer, K. T. van de Pas-Schoonen, R. Webb, J. G. Kuenen, and M. S. M. Jetten. Missing lithotroph identified as new planctomycete. *Nature*, 400:446–449, 1999.
- B. Thamdrup, T. Dalsgaard, M. M. Jensen, O. Ulloa, L. Farías, and R. Escibano. Anaerobic ammonium oxidation in the oxygen-deficient waters off northern Chile. *Limnology and Oceanography*, 51:2145–2156, 2006.
- R. C. Thunell, D. M. Sigman, F. Muller-Karger, Y. Astor, and R. Varela. Nitrogen isotope dynamics of the Cariaco Basin, Venezuela. *Global Biogeochemical Cycles*, 18, 2004.
- L. van Niftrik and M. S. M. Jetten. Anaerobic ammonium-oxidizing bacteria: Unique microorganisms with exceptional properties. *Microbiology and Molecular Biology Reviews*, 76:585–596, 2012.
- M. Voss, J. W. Dippner, and J. P. Montoya. Nitrogen isotope patterns in the oxygen-deficient waters of the Eastern Tropical North Pacific Ocean. *Deep-Sea Research*, 48:1905–1921, 2001.
- S. D. Wankel, C. Kendall, and A. Paytan. Using nitrate dual isotopic composition ($\delta^{15}\text{N}$ and $\delta^{18}\text{O}$) as a tool for exploring sources and cycling of nitrate in an estuarine system: Elkhorn Slough, California. *Journal of Geophysical Research*, 114, 2009.
- R. P. Wellman, F. D. Cook, and H. R. Krouse. Nitrogen-15: Microbiological alteration of abundance. *Science*, 161:269–270, 1968.
- C. B. Wenk, J. Blees, J. Zopfi, M. Veronesi, A. Bourbonnais, C. J. Schubert, H. Niemann, and M. F. Lehmann. Anaerobic ammonium oxidation (anammox) bacteria and sulfide-dependent denitrifiers coexist in the water column of a meromictic south-alpine lake. *Limnology and Oceanography*, 58:1–12, 2013.

CHAPTER 4

Partitioning between benthic and pelagic nitrate reduction in the Lake Lugano south basin

C. B. Wenk, J. Zopfi, W. S. Gardner, M. J. McCarthy, H. Niemann, M. Veronesi,
and M. F. Lehmann

submitted to:
Limnology and Oceanography

Abstract

We evaluated the seasonal variation of denitrification, anaerobic ammonium oxidation (anammox), and dissimilatory nitrate reduction to ammonium (DNRA) rates in the sediments and the integrative N (and O) isotopic signatures of dissolved inorganic nitrogen (DIN) compounds in the overlying water column of the monomictic Lake Lugano south basin. Denitrification was the dominant NO_3^- reduction pathway, whereas the contribution of anammox and DNRA to total benthic NO_3^- reduction was <6% and <12%, respectively. Sedimentary denitrification rates were highest (up to $57.2 \pm 16.8 \mu\text{mol N m}^{-2} \text{ h}^{-1}$) during fully oxic bottom water conditions. With the formation of seasonal bottom water anoxia, NO_3^- reduction was partitioned between water column and sedimentary processes. Total benthic NO_3^- reduction rates determined in ^{15}N label experiments and sediment-water interface N_2 fluxes as calculated from water column $\text{N}_2:\text{Ar}$ gradients revealed that sedimentary denitrification still accounted for $\sim 40\%$ of total N_2 production during bottom water anoxia. The partitioning between water column and sedimentary denitrification was further evaluated by the natural abundance stable N isotope composition of dissolved NO_3^- in the water column. With anaerobic bottom water conditions, water column NO_3^- concentrations gradually decreased, paralleled by an increase in $\delta^{15}\text{N}$ - and $\delta^{18}\text{O}-\text{NO}_3^-$ from approximately 7‰ to 20‰ and from 2‰ to 14‰, respectively. Using a closed-system (Rayleigh) model, the N and O isotope effects associated with community NO_3^- consumption were $^{15}\epsilon \approx 14\%$ and $^{18}\epsilon \approx 11\%$, respectively. With the assumptions of a relatively low net N isotope effect associated with sedimentary denitrification (i.e., $^{15}\epsilon_{\text{sed}} = 1.5\text{--}3\%$) vs. a fully expressed biological N isotope fractionation during water column denitrification (i.e., $^{15}\epsilon_{\text{water}} = 20\text{--}25\%$), our results confirm that 36–51% of NO_3^- reduction occurred within the sediment. The general agreement between the indirect (isotopic) approach and the flux and rate measurements suggests that water column nitrate isotope measurements can be used to distinguish between benthic and pelagic denitrification quantitatively.

4.1 Introduction

Redox transition zones (RTZs) in the water column and sediments of lakes represent hot spots of nitrogen (N) transformations and are important microbe-driven sinks for fixed N. For instance, organotrophic denitrification, the stepwise reduction of nitrate (NO_3^-) to nitrite (NO_2^-), nitric oxide (NO), nitrous oxide (N_2O), and dinitrogen gas (N_2), coupled to the oxidation of organic matter (OM), is the dominant fixed N elimination pathway in many lacustrine ecosystems. On the other hand, microbes are also capable of reducing NO_3^- to NH_4^+ , resulting in fixed N recycling instead of elimination (Koike and Hattori, 1978; Zopfi et al., 2001; An and Gardner, 2002). This pathway, dissimilatory nitrate reduction to ammonium (DNRA), can be important in some lacustrine environments (McCarthy et al., 2007). Recently, additional pathways for fixed N removal have been identified; for example, chemolithotrophic microorganisms thriving in lacustrine RTZs are capable of using reduced sulfur compounds as electron donors for denitrification (Burgin et al., 2012; Wenk et al., 2013). Furthermore, anaerobic ammonium oxidation (anammox), the oxidation of NH_4^+ with NO_2^- , is also an important fixed N removal process in some freshwater environments (Schubert et al., 2006; Hamersley et al., 2009; Wenk et al., 2013).

To constrain N budgets, it is essential to understand the quantitative importance of N transformations, to identify where most of the N turnover occurs (e.g., water column vs. sediment), and to determine whether and how much fixed N is lost from the ecosystem. The controlling environmental factors can be multifold and are often ambiguous with regard to the dominant N transforming process (see e.g., Burgin and Hamilton, 2007). The ^{15}N isotope pairing technique, which has been proven useful for determining denitrification and anammox rates, is based on the enrichment of incubated sediment or water samples with ^{15}N -labeled NO_3^- or NH_4^+ and the isotopic analysis of the produced N_2 by isotope ratio mass spectrometry (IRMS) (Nielsen, 1992; Steingruber et al., 2001; Thamdrup and Dalsgaard, 2002). This approach was applied successfully to water column measurements, e.g., the Black Sea (Kuypers et al., 2003) and Lake Tanganyika (Schubert et al., 2006). A modified isotope approach to disentangle denitrification and DNRA rates, using membrane inlet mass spectrometry (MIMS) and high performance liquid chromatography (HPLC), respectively, was applied in Corpus Christi Bay, Texas (McCarthy et al., 2008), Lake Taihu in China (McCarthy et al., 2007), and other aquatic systems. A less direct, more integrative approach to assess N transformations at the ecosystem level is to measure the natural abundance stable isotope composition of N compounds. While nitrification, the aerobic oxidation of NH_4^+ to NO_2^- and NO_3^- , leads to NO_3^- depleted in ^{15}N , denitrification has an opposite effect on the NO_3^- pool. To quantify such

observations, the kinetic N isotope effect for a given reaction, $^{15}\epsilon$, is defined as

$$^{15}\epsilon = \left(\frac{^{14}k}{^{15}k} - 1 \right) 1000 \quad (4.1)$$

where ^{14}k and ^{15}k are the reaction rates of ^{14}N and ^{15}N bearing isotopologues, respectively. For instance, many studies report an N isotope enrichment factor associated with organotrophic denitrification of $25 \pm 5\text{‰}$ (e.g., Wellman et al., 1968; Voss et al., 2001; Granger et al., 2008). Such high N isotope fractionation seems to be intrinsic to NO_3^- reduction catalyzed by the membrane-bound dissimilatory nitrate reductase (Nar), but does not necessarily translate into an equivalent N isotopic imprint on the ecosystem level (Lehmann et al., 2007; Kritee et al., 2012; Wenk et al., 2014). For instance, the ecosystem-level isotope effect (ϵ_{app}) of denitrification can be reduced relative to the cellular-level isotope effect (ϵ_{cell}) if, for example, denitrification is limited by NO_3^- supply rates to the denitrifying zone, and NO_3^- consumption is complete. Such a scenario often applies to sedimentary environments, where expressed denitrification N isotope effects can be as low as 0‰ to 4‰ (Brandes and Devol, 1997; Lehmann et al., 2007). While the exact controls on ϵ_{app} are complex (Lehmann et al., 2007; Alkhatib et al., 2012; Wenk et al., 2014), the relatively large discrepancy between sedimentary and water column N isotope effects of denitrification ($\sim 1.5\text{‰}$ vs. $\sim 25\text{‰}$, respectively), was used in an end-member approach to quantitatively distinguish between the two NO_3^- reduction sites (Sigman et al., 2003; Lehmann et al., 2005). Combined measurements of concentrations and isotopologues of various N species in a lacustrine water column may yield integrative (in space and time) information on N transformations co-occurring in the same environment, if the respective isotope effects of the involved biogeochemical reactions are known. Natural abundance N isotope measurements are particularly valuable when calibrated with discrete measurements of reaction rates. However, studies using natural abundance measurements in tandem with ^{15}N tracer experiments to constrain N cycle reactions are scarce.

In this study, we examine the relative importance and dynamics of fixed N elimination and recycling pathways, such as denitrification, anammox, and DNRA, in the monomictic southern basin of Lake Lugano (Switzerland). We combine continuous-flow sediment core incubations with ^{15}N isotope labeling experiments, water column profiles and flux calculations of dissolved inorganic nitrogen (DIN) compounds, with measurements of natural abundance stable N and O isotope composition of DIN to: (1) determine seasonal variations of benthic DIN fluxes and denitrification, anammox, and DNRA rates; (2) assess the expression of the N (and O) isotope effects by these processes at the ecosystem level; and (3) test the applicability of the end-member isotope approach to determine water column vs. benthic denitrification rates in a lake basin with seasonal hypolimnetic anoxia.

4.2 Methods

4.2.1 Study site and sampling

Lake Lugano is located on the border between Switzerland and Italy on the southern slopes of the Alps at 271 m above sea level (Fig. 4.1). The lake is separated into a permanently stratified northern basin and a monomictic southern basin by a natural dam. This study focuses on the shallower southern basin. Samples were collected at a site (45.95°N, 8.90°E) west of the village of Figino, close to the point of maximum water depth (95 m). Water column profiles of temperature and dissolved oxygen (O₂) concentration were obtained with a conductivity, temperature, depth (CTD) device equipped with an O₂ sensor (Ocean Seven 316Plus, Idronaut). O₂ concentrations were calibrated against Winkler titrations, with a detection limit of 1 μmol L⁻¹. Water samples for hydrochemical and natural abundance stable isotope analyses were collected using 5 L or 10 L Niskin bottles during sampling campaigns in 2009 (March, June, August, September, October, November, December). Hydrochemical profiling (without sampling for stable isotope analyses) was also performed in 2010 (January, March, August, October), and 2011 (January, May). Sample aliquots were filtered (0.45 μm) and stored frozen until analysis in the laboratory. For dissolved N₂:Ar measurements, water from Niskin bottles was filled directly into 12 mL exetainers (Labco). Overflow of at least three exetainer volumes was assured before sealing and poisoning with HgCl₂. Samples were taken in triplicate and stored underwater at ~6.5°C before analysis within 3 days. For ex situ ¹⁵N continuous-flow incubations,

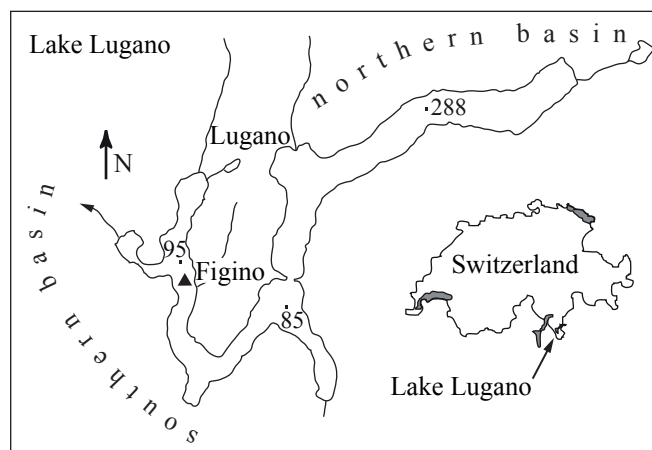


Figure 4.1: Location and map of Lake Lugano. The sampling station (black triangle) is located close to the point of maximum water depth in the southern basin. (Map adapted from Barbieri and Polli, 1992).

bottom water was collected in open ~ 20 L carboys during oxic conditions (April 2010, May 2011) or directly into gas-tight collapsible bags at times of hypolimnetic anoxia (August 2010, October 2010, January 2011). These bags were stored under water to minimize the risk of O_2 contamination. Six intact sediment cores (~ 50 cm long) with 20 cm overlying bottom water were collected using a mini gravity corer during each sampling campaign in 2010 (April, August, October) and 2011 (January, May).

4.2.2 Continuous-flow sediment core incubations

Within 6 hours after sampling, the continuous-flow sediment core incubations were set up in a cold room at near in situ temperature (6.5°C), as described previously (Lavrentyev et al., 2000; McCarthy and Gardner, 2003). Briefly, gas-tight plungers containing two holes were positioned ~ 10 cm above the sediment surface to yield ~ 255 mL of overlying water volume. Inflow water from the reservoirs was pumped with a multi-channel peristaltic pump through gas-tight tubes (0.8 mm inner diameter) and through the overlying water at a constant flow rate of ~ 1 mL min^{-1} . A total of 6 sediment core incubations were set up after each sampling campaign, and three inflow water reservoirs were installed, each feeding two duplicate sediment cores. One of the reservoirs was amended with $^{15}\text{NH}_4^+$ ($>99\%$ ^{15}N - NH_4Cl , Spectra Stable Isotopes), one with $^{15}\text{NO}_3^-$ ($>99\%$ ^{15}N - KNO_3 , Spectra Stable Isotopes), and one was left un-amended as a control. The labeled substrates were added to yield final concentrations approximately twice the in situ levels (41% - 73% ^{15}N), except for the aerobic incubations, where the background NH_4^+ concentrations were <1 $\mu\text{mol L}^{-1}$. Here, 10 $\mu\text{mol L}^{-1}$ $^{15}\text{NH}_4^+$ label was added ($\sim 97\%$ ^{15}N). After a >24 hours pre-conditioning period to re-establish steady-state, in- and outflow samples were collected daily for up to three days. Separate aliquots of filtered (0.22 μm) water were frozen for subsequent nutrient analysis (see below). Samples for ^{15}N - N_2 analyses were taken in triplicate during each sampling day and analyzed immediately by membrane inlet mass spectrometry (MIMS) as described below. Potential O_2 contamination was monitored daily in the in- and outflowing water with an optical sensor system (PreSens Dipping Probe; detection limit 0.5 $\mu\text{mol L}^{-1}$).

4.2.3 Hydrochemical analyses

NO_x (i.e., $\text{NO}_3^- + \text{NO}_2^-$) and NO_2^- concentrations were determined with a NO_x -Analyzer (Antek Model 745) after reduction to nitric oxide (NO) in an acidic V^{3+} or sodium iodide solution, respectively (Garside, 1982; Braman and Hendrix, 1989). $[\text{NO}_3^-]$ was calculated from the difference of $[\text{NO}_x]$ and $[\text{NO}_2^-]$. NH_4^+ was determined photometrically using the indophenol method (Koroleff, 1976). For sediment core incubation samples, $[\text{NH}_4^+]$ was additionally measured on a HPLC system together with its ^{15}N isotope composition (see below) (Gardner et al., 1991). Total phosphorous

(P), iron (Fe), and manganese (Mn) concentrations were determined by inductively coupled plasma optical emission spectrometry (ICP-OES). N_2 :Ar ratios (water column samples) and ^{15}N - N_2 (incubation samples) were measured using a MIMS system (Pfeiffer Vacuum PrismaTM) as described by Kana et al. (1994). The MIMS setup included a copper furnace at 650°C to scavenge O_2 , which otherwise would be ionized and react with N_2 , thereby artificially lowering the N_2 signals and producing mass 30 through NO generation (Eyre et al., 2002). N_2 saturation is reported as the N_2 :Ar ratio of the sample divided by the N_2 :Ar ratio at equilibrium with the atmosphere at a given temperature (Weiss, 1970).

4.2.4 Stable isotope analyses

Prior to NO_3^- N and O isotope analyses, NO_2^- , where present, was removed by sulfamic acid addition (Granger and Sigman, 2009). The natural abundance N and O isotopic composition of NO_3^- was then determined using the denitrifier method (Sigman et al., 2001; Casciotti et al., 2002). Briefly, 20 nmoles of sample NO_3^- were converted to N_2O by cultured denitrifying bacteria (*Pseudomonas chlororaphis* strains ATCC 43928 and ATCC 13985), which lack the enzyme responsible for N_2O reduction. Produced N_2O was automatically extracted, purified, and subsequently analyzed using IRMS (Thermo Finnigan DELTA^{plus} XP). Blank contribution was generally less than 2% of the target sample size. N and O isotope ratios are reported as δ values in ‰ relative to air N_2 and Vienna Standard Mean Ocean Water (VSMOW), respectively. $\delta = (R_{\text{sample}} : R_{\text{standard}} - 1) \times 1000$, where $R = ^{15}N:^{14}N$ or $^{18}O:^{16}O$. Isotope values were calibrated using internal ($\delta^{15}N = 12.15\text{‰}$) and international KNO_3 reference materials with reported $\delta^{15}N$ and $\delta^{18}O$ values of 4.7‰ and 25.6‰ (IAEA-N3) and -1.8‰ and -27.9‰ (USGS 34), respectively (Gonfiantini et al., 1995; Böhlke et al., 2003). Replicate reproducibility was generally better than 0.3‰ for $\delta^{15}N$ and 0.5‰ for $\delta^{18}O$.

The natural abundance N isotopic composition of NH_4^+ was determined using a combination of the ammonia diffusion method (Sigman et al., 1997), persulfate oxidation (Knapp et al., 2005), and the denitrifier method (Sigman et al., 2001) as described by Houlton et al. (2007) and adapted by Bourbonnais et al. (2012). Briefly, >100 nmoles of sample NH_4^+ were converted to NH_3 (g) under alkaline conditions after MgO addition. The product NH_3 (g) was trapped as NH_4^+ on combusted and acidified glass fiber discs (Whatman No. 1823010) sandwiched between two Teflon membranes (Millipore LCWP 01300). The NH_4^+ trapped on the glass fiber discs was then oxidized chemically to NO_3^- in a sodium persulfate solution. After adjusting the solution to pH 4, the isotope composition of the product NO_3^- was determined using the denitrifier method. Isotope values were calibrated using two $(NH_4)_2SO_4$ reference materials (IAEA-N1 and IAEA-N2) with $\delta^{15}N$ values of 0.4‰ and 20.3‰, respectively. Reproducibility for repeated analyses of standards was $\pm 1.0\text{‰}$.

For the ^{15}N -label incubation experiments, $^{15}\text{NH}_4^+$ was analyzed on a HPLC system in Texas (Gardner et al., 1991, 1995). Briefly, sample water was pumped at constant pressure through a heated, stainless steel column (30 cm x 4 mm inner diameter) containing a strong cation exchange resin and an assembled post-column reaction system. Ammonium was analyzed on a Gilson 121 Fluorometric detector, and the ^{15}N content was calculated based on the retention time shift between the signals of the heavier and lighter isotopologues.

4.2.5 Benthic flux calculations and N transformation rates

Benthic solute fluxes (J) were calculated as:

$$J_C = (C_{\text{out}} - C_{\text{in}}) \times \frac{Q}{S} \quad (4.2)$$

where C_{out} is the outflow concentration of any given solute in $\mu\text{mol L}^{-1}$, C_{in} is the inflow concentration, Q is the flow rate ($\sim 0.06 \text{ L h}^{-1}$), and S is the sediment surface area (0.00255 m^2). Negative values indicate solute fluxes into the sediment.

Total potential benthic denitrification rates (i.e., $D_{\text{total}} = D_{14} + D_{15}$) were determined from ^{15}N - N_2 production in the ^{15}N - NO_3^- experiments and calculated according to An et al. (2001), based on isotope pairing considerations by Nielsen (1992). The denitrification rates based on the added $^{15}\text{NO}_3^-$ (D_{15}) and based on $^{14}\text{NO}_3^-$ (D_{14}) were calculated as:

$$D_{15} = 2 \times P(15,15) + P(14,15) \quad (4.3)$$

$$D_{14} = \frac{P(14,15)}{2 \times P(15,15)} \times D_{15} \quad (4.4)$$

where $P(14,15)$ and $P(15,15)$ are the net $^{14}\text{N}^{15}\text{N}$ and $^{15}\text{N}^{15}\text{N}$ production rates, respectively.

Potential benthic anammox rates (A_{total}) were estimated from two individual approaches. First, they were derived from $^{14}\text{N}^{15}\text{N}$ production in the ^{15}N - NH_4^+ amended experiments (Thamdrup et al., 2006) and calculated as:

$$A_{\text{total}} = \frac{P(14,15)}{F_A} \quad (4.5)$$

where F_A is the mole fraction of ^{15}N in total NH_4^+ . In a second approach, and when oxygen was absent, we calculated potential anammox rates from the production of $^{14}\text{N}^{15}\text{N}$ and $^{15}\text{N}^{15}\text{N}$ in the ^{15}N - NO_3^- experiments (Thamdrup and Dalsgaard, 2002;

Thamdrup et al., 2006):

$$A_{\text{total}} = \frac{1}{F_{\text{N}}} \times \left(P(14,15) + 2 \times P(15,15) \times \left(1 - \frac{1}{F_{\text{N}}} \right) \right) \quad (4.6)$$

where F_{N} is the mole fraction of ^{15}N in NO_3^- . Anammox was only detectable in October 2010 and January 2011. In both months, the two approaches yielded comparable results, within the reported error.

A potential rate for benthic DNRA was calculated based on the production of $^{15}\text{NH}_4^+$ in the $^{15}\text{NO}_3^-$ amended experiments (An and Gardner, 2002), but that approach is conservative because it does not account for the production of $^{14}\text{NH}_4^+$ from natural abundance NO_3^- in the system. All benthic fluxes and N transformation rates are reported as the mean value (± 1 standard deviation) of 4 to 6 measurements performed in two parallel sediment core incubations on 2 to 3 consecutive days.

4.3 Results

4.3.1 Dissolved concentrations and natural abundance stable N and O isotope profiles in the water column

During summer and fall, thermal stratification led to a pronounced density gradient between 12 and 16 m depth. Ongoing phototrophic primary production caused a decline in surface NO_3^- concentrations from $\sim 80 \mu\text{mol L}^{-1}$ (winter months) to $< 40 \mu\text{mol L}^{-1}$ (August 2009 and 2010), paralleled by a systematic increase in both $\delta^{15}\text{N-NO}_3^-$ and $\delta^{18}\text{O-NO}_3^-$ (Figs. 4.2-4.4). In association with the maximum density gradient, O_2 concentrations reached a local minimum ($< 25 \mu\text{mol L}^{-1}$ in September 2009), indicating enhanced OM mineralization and nutrient turnover via microbial respiration (Fig. 4.2b, d). OM remineralization in subsurface waters was indicated by increased NO_3^- (and NO_2^-) concentrations corresponding to a pronounced $\delta^{15}\text{N-NO}_3^-$ minimum of 5‰, which was not observed for $\delta^{18}\text{O-NO}_3^-$ (Fig. 4.4a, b). Here, however, we focus on the hypolimnetic waters, the RTZ, and N transformation processes at the sediment-water interface. Enhanced OM mineralization led to the formation of an anoxic layer at the bottom of the lake basin between June and August (Fig. 4.2b, d), which expanded into the water column during summer and fall, reaching a maximum thickness of approximately 20 m in December 2009. The rise of the oxycline into the water column was paralleled by NH_4^+ accumulation in the anoxic bottom water (Fig. 4.3c, g) and the development of a bacterial benthic nepheloid layer (BNL) (Lehmann et al., 2004). Ammonium concentrations were always highest at the sediment-water interface (up to $80 \mu\text{mol L}^{-1}$ in October 2009) and decreased toward the oxic-anoxic interface, indicating turbulent diffusive mixing, its aerobic or anaerobic consumption, or uptake

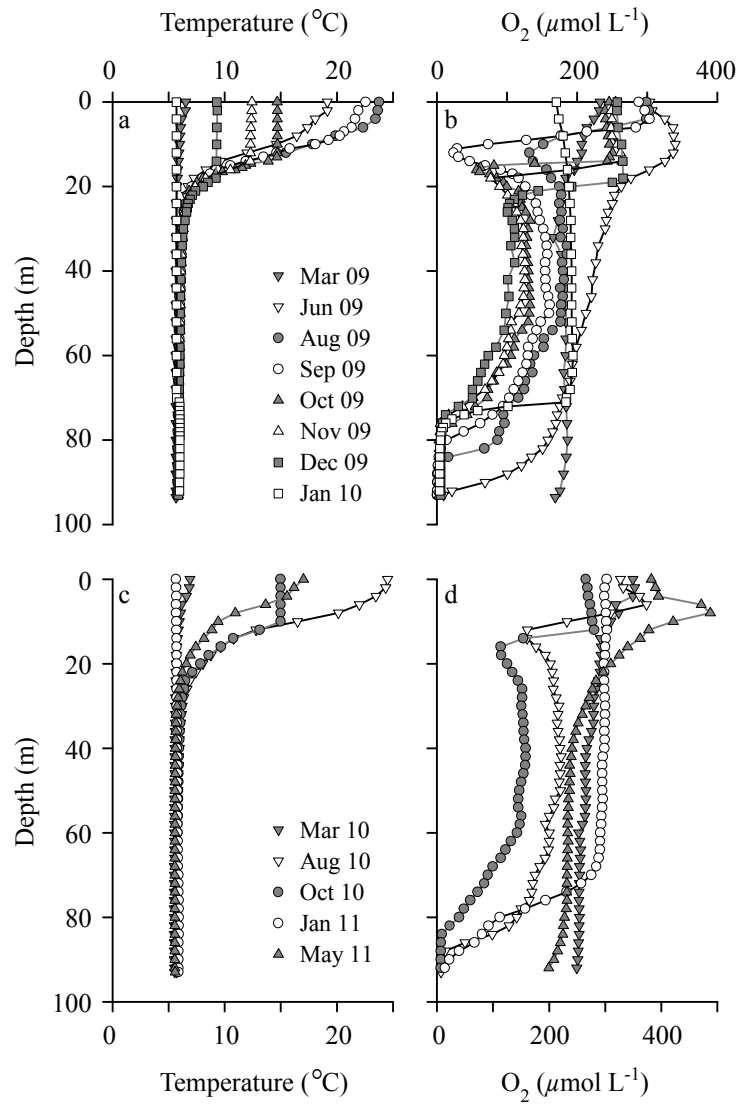


Figure 4.2: Water column profiles of (a, c) temperature and (b, d) dissolved oxygen concentrations in the southern basin of Lake Lugano in 2009-2010 (upper panel), and 2010-2011 (lower panel).

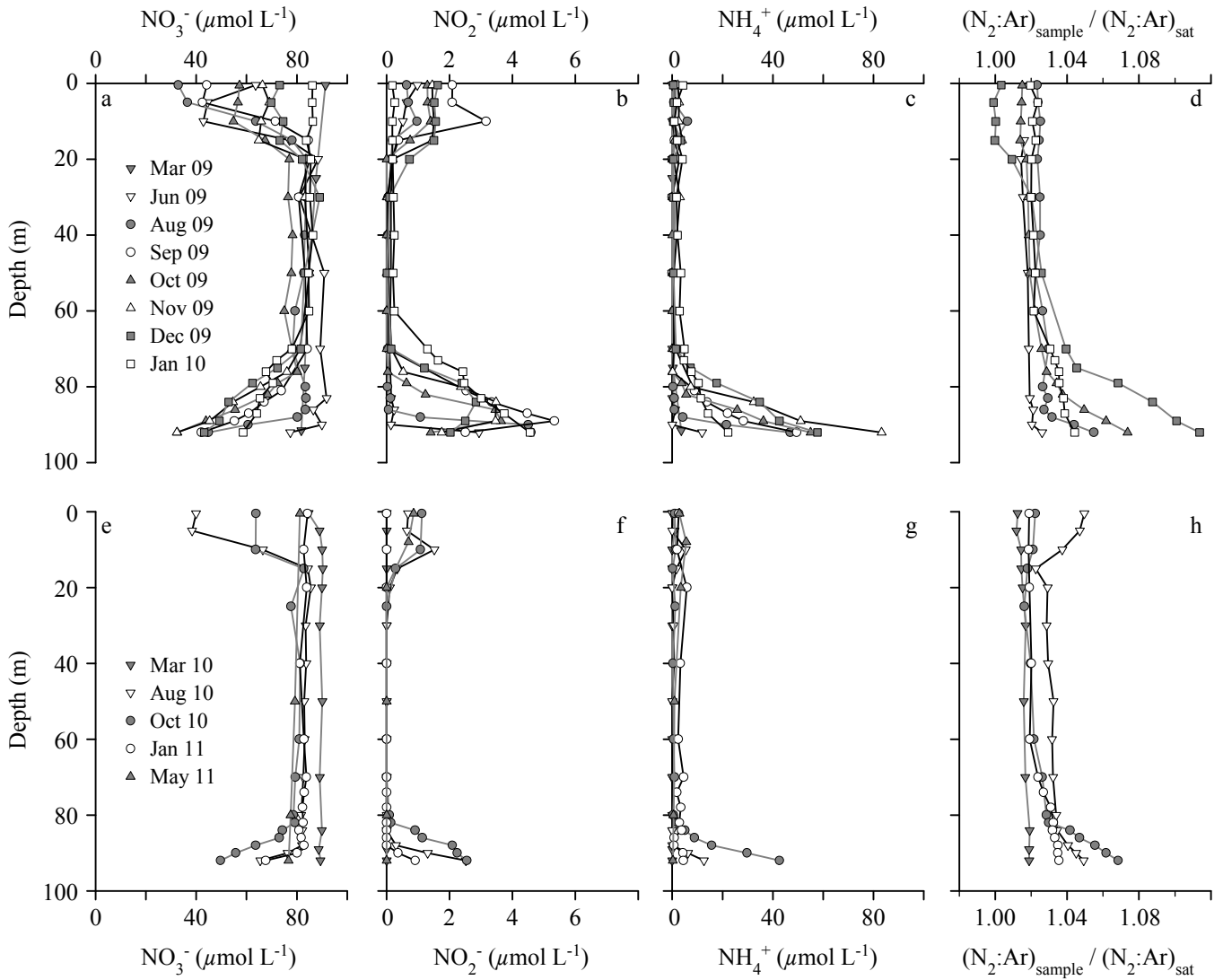


Figure 4.3: Water column concentrations of (a, e) dissolved nitrate, (b, f) nitrite, and (c, g) ammonium, and (d, h) $\text{N}_2:\text{Ar}$ ratios in 2009-2010 (upper panel) and 2010-2011 (lower panel).

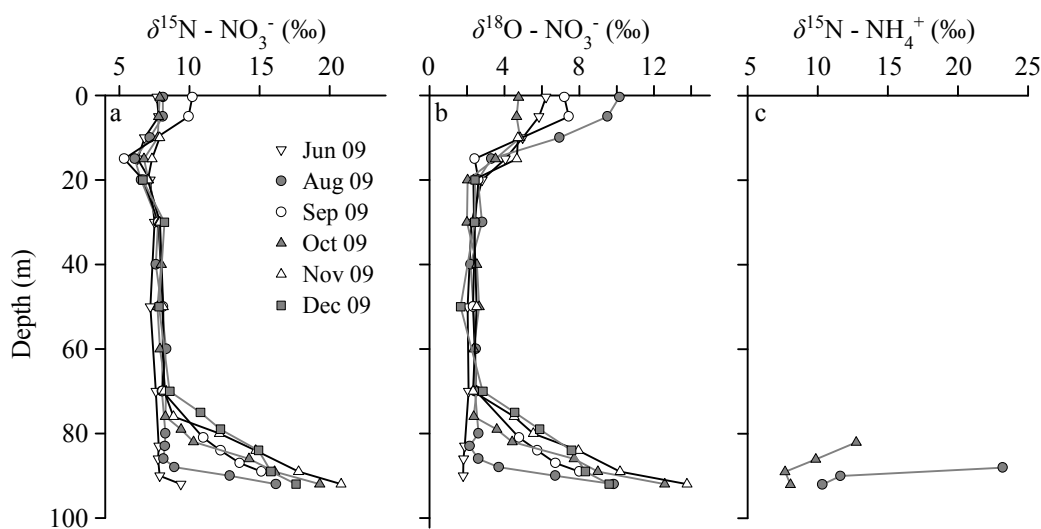


Figure 4.4: Water column profiles of (a) $\delta^{15}\text{N}$ -, (b) $\delta^{18}\text{O}\text{-NO}_3^-$, and (c) $\delta^{15}\text{N}\text{-NH}_4^+$ in the Lake Lugano south basin in 2009.

by microorganisms within the BNL. In tandem with the NH_4^+ concentration decrease, the $\delta^{15}\text{N}\text{-NH}_4^+$ increased from 8‰ to 13‰ in October 2009 and from 10‰ to 23‰ in August 2009 (Fig. 4.4c). Nitrate concentrations decreased from $80 \mu\text{mol L}^{-1}$ above the oxycline to $<40 \mu\text{mol L}^{-1}$ at the sediment-water interface (Fig. 4.3a, e). This concentration decrease was paralleled by an increase in $\delta^{15}\text{N}$ - and $\delta^{18}\text{O}\text{-NO}_3^-$ from 7‰ to 20‰ and from 2‰ to 14‰, respectively (Fig. 4.4a, b), indicating N and O isotope fractionation during NO_3^- reduction. With continuous expansion of the RTZ into the water column, NO_2^- accumulated in the anoxic bottom water (Fig. 4.3b, f). The NO_2^- concentration peak was most pronounced from September to November 2009. Measured $\text{N}_2\text{:Ar}$ profiles revealed that the anoxic bottom water was oversaturated with respect to N_2 (relative to equilibrium saturation with the atmosphere) (Fig. 4.3d, h). In December 2009, oversaturation was highest and reached levels ($>10\%$) significantly exceeding measurements from other natural aquatic systems (Fuchsman et al., 2008), including the neighboring north basin (Wenk et al., 2013). With thermal destratification in January, and subsequent holomixis, bottom water masses were re-oxygenated and all concentration and isotope ratio gradients collapsed (Figs. 4.2-4.4).

4.3.2 Benthic N transformation rates and fluxes at the sediment-water interface

Sedimentary denitrification rates were highest ($57.2 \pm 16.8 \mu\text{mol N m}^{-2} \text{ h}^{-1}$) during oxic bottom water conditions in April 2010 (Table 4.1). During this time, benthic anammox and DNRA rates were undetectable. With the development of water column anoxia, benthic denitrification rates decreased to $7.8 \pm 3.1 \mu\text{mol N m}^{-2} \text{ h}^{-1}$ (August 2010). As anoxic bottom water conditions prevailed, anammox rates increased and contributed to total fixed N removal within the sediment (October 2010). However, canonical denitrification remained the dominant N_2 production pathway (Table 4.1). In January 2011, when the first signs of deep water ventilations could be discerned in the physico-chemical profiles, and bottom water O_2 concentrations rose to $13 \mu\text{mol L}^{-1}$, benthic denitrification as well as anammox rates decreased to $5.9 \pm 2.7 \mu\text{mol N m}^{-2} \text{ h}^{-1}$ and $0.7 \pm 0.6 \mu\text{mol N m}^{-2} \text{ h}^{-1}$, respectively. In May 2011, benthic denitrification rates returned to the values similar to those measured in the previous year ($48.4 \pm 20.8 \mu\text{mol N m}^{-2} \text{ h}^{-1}$). DNRA rates were generally low and exceeded the detection limit only in August 2010 and January 2011, when anammox was not observed.

There were no systematic differences between nutrient fluxes in control and NH_4^+ - or NO_3^- -amendment experiments (Fig. 4.5). Net sedimentary NO_3^- fluxes ranged from $-29.1 \pm 24.1 \mu\text{mol N m}^{-2} \text{ h}^{-1}$ to $-98.9 \pm 62.1 \mu\text{mol N m}^{-2} \text{ h}^{-1}$ and always balanced, or significantly exceeded, sedimentary denitrification (Fig. 4.5a, Table 4.1). Net sediment-water NO_2^- fluxes were generally low and reached $12.5 \pm 6.7 \mu\text{mol N m}^{-2} \text{ h}^{-1}$ in January 2011 (Fig. 4.5b). Net NH_4^+ fluxes out of the sediments were lowest during aerobic bottom water conditions ($72.0 \pm 9.5 \mu\text{mol N m}^{-2} \text{ h}^{-1}$) and increased to $192.0 \pm 96.5 \mu\text{mol N m}^{-2} \text{ h}^{-1}$ (October 2010) with ongoing bottom water anoxia (Fig. 4.5c). Net water-sediment P fluxes were only significantly different from 0 during anoxic bottom water conditions and reached $-13.0 \pm 5.4 \mu\text{mol P m}^{-2} \text{ h}^{-1}$ in October 2010 (Fig. 4.5d). In the same month, dissolved Fe and Mn fluxes out of the sediment were highest, with $6.6 \pm 3.0 \mu\text{mol Fe m}^{-2} \text{ h}^{-1}$ (Fig. 4.5e) and $202.7 \pm 97.7 \mu\text{mol Mn m}^{-2} \text{ h}^{-1}$ (Fig. 5f), respectively.

4.4 Discussion

In contrast to the meromictic north basin of Lake Lugano, the south basin mixes completely every year in winter. The formation of a seasonally developing anoxic bottom water layer during summer and fall was described by Lehmann et al. (2004). Hydrochemical data, together with the measurement of elevated suspended particle concentrations in the anoxic zone, indicate the presence of a benthic nepheloid layer (BNL). The development of a BNL is common for lakes, but the identity of the

Table 4.1: Benthic denitrification, anammox, and DNRA rates in the Lake Lugano south basin determined in ^{15}N -label continuous-flow sediment core incubation experiments. Rates are given in $\mu\text{mol N m}^{-2} \text{h}^{-1}$ (± 1 standard deviation of replicate analyses). nd = not detectable.

Sampling date	Benthic N transformation rates ($\mu\text{mol N m}^{-2} \text{h}^{-1}$)		
	Denitrification	Anammox	DNRA
April 2010	52.2 ± 16.8	nd	nd
August 2010	7.8 ± 3.1	nd	0.7 ± 0.6
October 2010	28.2 ± 23.7	3.8 ± 2.4	nd
January 2011	5.9 ± 2.7	0.7 ± 0.6	nd
May 2011	48.4 ± 20.8	nd	6.2 ± 5.5

suspended particles is often uncertain. In the Lake Lugano south basin, compelling evidence indicates that the suspended particles of the BNL are of bacterial origin (Lehmann et al., 2004), and our hydrochemical profiles indicate that intensive N cycling occurs within the BNL. In the next sections, we will first discuss the seasonal variations in benthic solute fluxes and sedimentary N transformation pathways and rates. Results from the continuous-flow sediment core incubation experiments will then be integrated with observations made in the water column (concentration gradients and isotopic composition of DIN) to provide a coherent picture of the modes, rates, and sites of fixed N elimination in the lake basin.

4.4.1 N_2 production during hypolimnetic anoxia

Our data show that the sediments represent a sink for NO_3^- throughout the year, as indicated by the high benthic NO_3^- uptake of $-29.1 \mu\text{mol N m}^{-2} \text{h}^{-1}$ (May 2011) to $-98.9 \mu\text{mol N m}^{-2} \text{h}^{-1}$ (August 2010). If NO_3^- from the water column is reduced completely to N_2 , then benthic denitrification rates should approximately balance or exceed (in case of nitrification-denitrification coupling) the measured NO_3^- fluxes. However, NO_3^- fluxes into the sediment significantly exceeded benthic N_2 production rates through denitrification in all incubations with anoxic bottom water (August, October, January) (Fig. 4.5, Table 4.1). A possible explanation for this phenomenon is that benthic NO_3^- reduction during these months was incomplete, and that significant portions of the reduced N accumulated as N_2O . However, benthic N_2O fluxes ranging between 0.4 and $1.2 \mu\text{mol N m}^{-2} \text{h}^{-1}$ (Freymond et al., 2013) did not account for more than 15% of total benthic NO_3^- reduction, even during periods of maximum N_2O production ($5 \mu\text{mol N m}^{-2} \text{h}^{-1}$ in October 2010). Another potential pathway for benthic NO_3^- reduction, which could explain the imbalance between observed NO_3^- fluxes and N_2 production through denitrification, is its reduction to NO_2^- and

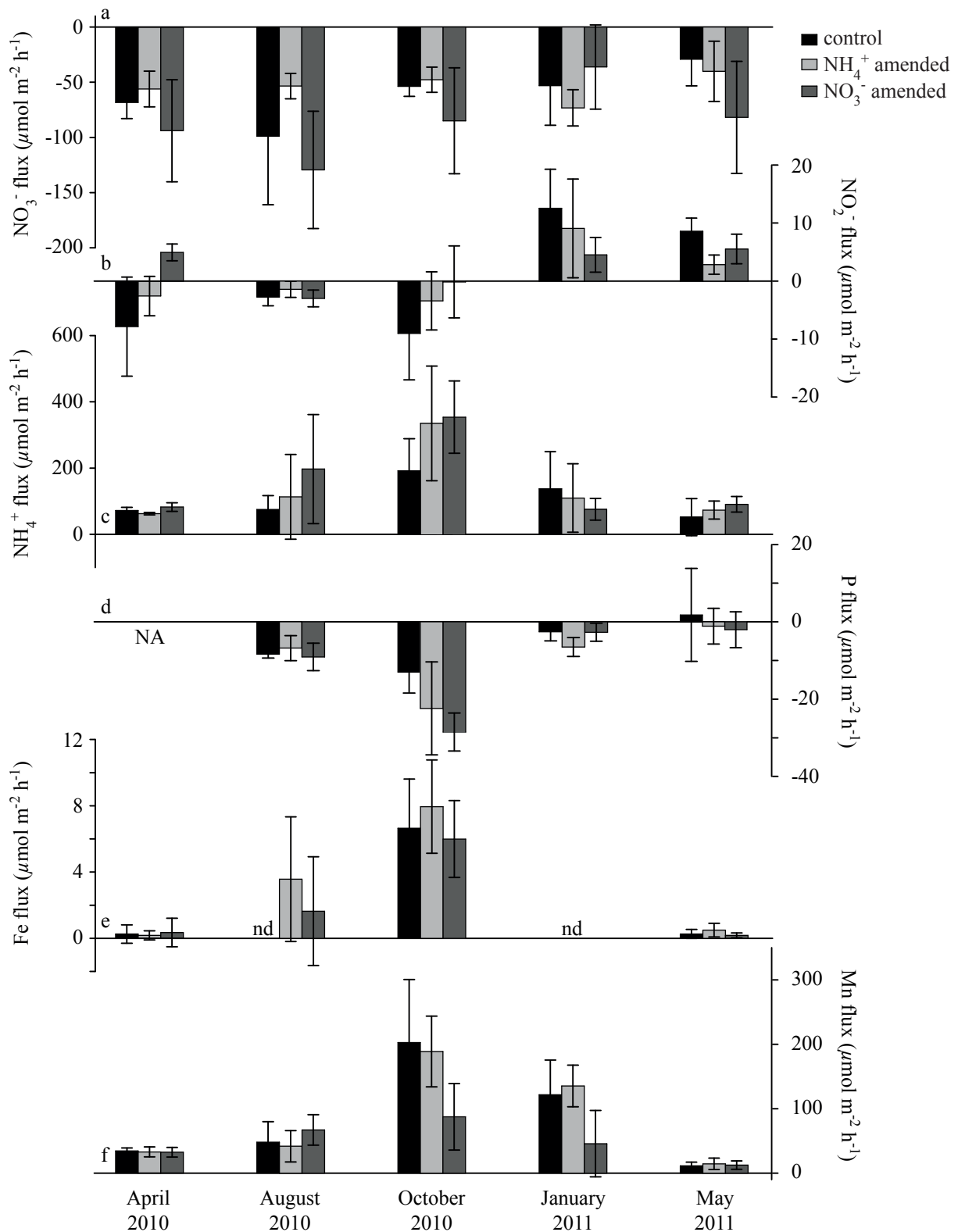


Figure 4.5: Benthic fluxes of (a) dissolved nitrate, (b) nitrite, (c) ammonium, (d) phosphorus, (e) iron, and (f) manganese determined in continuous-flow sediment core incubations. Positive numbers represent sediment-water fluxes, negative numbers signify fluxes into the sediment. NA = not analyzed; nd = not detectable.

subsequent consumption by anammox. Potential anammox rates were only above detection limit in October 2010 and January 2011. However, the rates were low (Table 4.1), and anammox always contributed less than 6% to total NO_3^- reduction. Alternatively, NO_3^- can be reduced to NH_4^+ in sediments by DNRA coupled to OM or inorganic substrate oxidation. For example, sulfide-dependent DNRA contributed up to 75% of total NO_3^- reduction in marine sediments off the coast of Texas (An and Gardner, 2002). Furthermore, Wang et al. (2003) observed a similar imbalance between benthic NO_3^- uptake and denitrification rates in the St. Lawrence Estuary and argued that DNRA coupled to Mn-oxidation could have been responsible for the additional NO_3^- removal. However, DNRA rates were not measured directly by Wang et al. (2003). In the Lake Lugano south basin, we measured Mn fluxes of up to $200 \mu\text{mol N m}^{-2} \text{ h}^{-1}$ during anoxic conditions in October 2010 (Fig. 4.5). Although the environmental conditions in the Lake Lugano south basin therefore seem to be conducive to DNRA coupled to Mn oxidation, potential DNRA rates remained below or close to the detection limit in all our incubations and contributed less than 12% (May 2011) to total benthic NO_3^- reduction (Table 4.1). Hence, the sum of all mentioned benthic NO_3^- sinks (denitrification to N_2 , reduction to N_2O , anammox, and DNRA) amounted to NO_3^- reduction rates of $10 \mu\text{mol N m}^{-2} \text{ h}^{-1}$ in August 2010, $35 \mu\text{mol N m}^{-2} \text{ h}^{-1}$ in October 2010, and $7 \mu\text{mol N m}^{-2} \text{ h}^{-1}$ in January 2011. These rates are significantly lower than the measured average NO_3^- fluxes into the sediment of $-99 \pm 62 \mu\text{mol N m}^{-2} \text{ h}^{-1}$ (August 2010), $-54 \pm 9 \mu\text{mol N m}^{-2} \text{ h}^{-1}$ (October 2010), and $-53 \pm 36 \mu\text{mol N m}^{-2} \text{ h}^{-1}$ (January 2011) (Fig. 4.5). The discussed fluxes and rates, and the apparent imbalance in benthic N cycling, are schematically visualized for October 2010 (Fig. 4.6).

Natural sediment heterogeneity cannot be invoked to explain the discrepancy between the NO_3^- flux and the potential NO_3^- reduction rates, because both parameters were estimated from the same set of experiments. It has to be noted however, that all benthic N transformation rate measurements (i.e., denitrification, anammox, and DNRA) are potential rates based on ^{15}N label addition experiments (dashed, black arrows in Fig. 4.6). A potential disadvantage of the continuous-flow sediment core incubations is that not all of the ^{15}N -labeled products of the investigated N-transformations diffuse across the sediment-water interface as there may be some diffusive loss of produced $^{15}\text{N-N}_2$ (and analogously $^{15}\text{N-NH}_4^+$) downward from the reaction zone. The here reported rates might thus slightly underestimate the actual rates. However, denitrification in the sediments of the Lake Lugano south basin is expected to occur very close to the sediment surface due to the strong redox gradients. The diffusive distance from the denitrification or DNRA sites to the sediment surface is on the order of mm. Thus the concentration gradient and isotope exchange would be greater toward the surface than into the sediments, and underestimation of the rates should be minimal. However, the DNRA rates reported here are likely underestimates of the actual rates, because they are based on $^{15}\text{NH}_4^+$ production in $^{15}\text{NO}_3^-$ -labeling

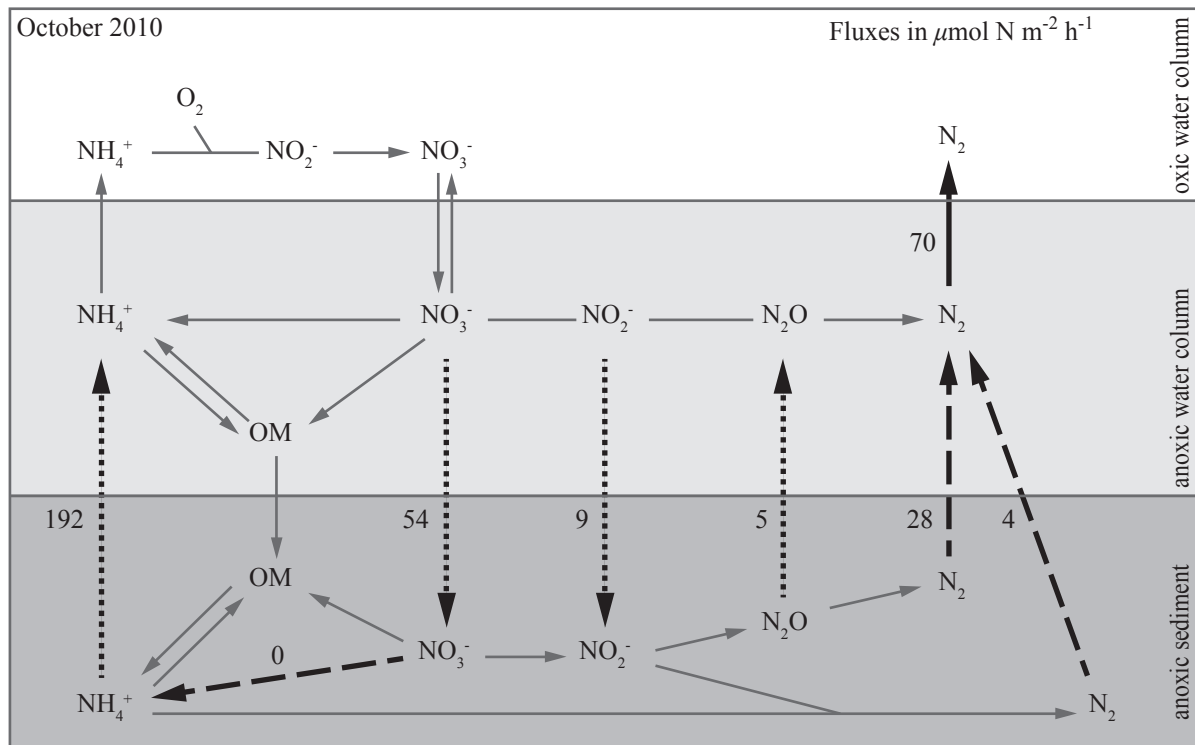


Figure 4.6: Schematic illustration of benthic and hypolimnetic N fluxes in October 2010. The dotted, black arrows indicate net fluxes measured in continuous-flow sediment core incubations, the dashed, black arrows are sedimentary N transformation rates determined from ^{15}N -label experiments, and the solid, black arrow marks the N_2 flux determined from water column $\text{N}_2:\text{Ar}$ profiles. The numbers next to the arrows are net fluxes in $\mu\text{mol N m}^{-2} \text{h}^{-1}$.

experiments only, without considering the reaction of naturally abundant $^{14}\text{NO}_3^-$. In an independent approach to assess the potential for DNRA, we estimated OM mineralization and compared the expected NH_4^+ flux to the experimentally determined one. Benthic O_2 consumption rates were approximately $500 \mu\text{mol m}^{-2} \text{h}^{-1}$ during oxic bottom water conditions in April 2010 and May 2011 (data not shown). With a C:N ratio of 9 for sinking OM in the Lake Lugano south basin (Lehmann et al., 2004), this rate translates into an approximate NH_4^+ mineralization rate of $55 \mu\text{mol m}^{-2} \text{h}^{-1}$, which corresponds to the sediment-water NH_4^+ fluxes measured in these months (Fig. 4.5). This balance between the minimum NH_4^+ mineralization rate and the measured sediment-water NH_4^+ flux confirms that DNRA rates were rather low. During anoxic bottom water conditions, however, NH_4^+ fluxes increased. This change could be associated with increased DNRA rates, but more likely may be due to increased OM mineralization and the inhibition of benthic nitrification.

Nitrate consumption and associated N_2 production rates were investigated further by quantifying N_2 fluxes from the water column $N_2:Ar$ profiles (Fig. 4.3). Using estimated K_z values of $0.49 \text{ m}^2 \text{ d}^{-1}$ (August 2010) and $0.34 \text{ m}^2 \text{ d}^{-1}$ (October 2010) for the bottom water of the Lake Lugano south basin (Lehmann et al., 2003; Wenk et al., 2013), we calculated N_2 fluxes of $54 \mu\text{mol N m}^{-2} \text{ h}^{-1}$ (August 2010) and $70 \mu\text{mol N m}^{-2} \text{ h}^{-1}$ (October 2010) at the sediment water interface. These fluxes are, again, significantly higher than the N_2 production rates determined in the ^{15}N -label sediment core incubation experiments and, within the error, more consistent with the observed NO_3^- fluxes into the sediments. Nevertheless, it is important to understand that the observed excess N_2 in the water column is the result not only of benthic N_2 production but also of NO_3^- reduction within the anoxic water column (Fig. 4.6). Hence, we can compare the total N_2 flux in the anoxic water column (determined from water column $N_2:Ar$ ratio profiles) to the sedimentary N_2 production rates (determined in the ^{15}N -label experiments). This comparison allows a quantitative assessment of the relative contribution of water column and sedimentary processes to total N_2 production. During stratification in 2010, a large fraction (i.e., 85% in August 2010 and 55% in October 2010) of the anoxic N_2 production was due to water column processes. In the next section, we will use the water column NO_3^- N-isotopic data from 2009 to gain further insights into the partitioning between water column and sedimentary denitrification.

4.4.2 Isotopic constraints on denitrification in the sediment and the anoxic water column

To estimate the isotope enrichment factors associated with NO_3^- (and NH_4^+) consumption in the RTZ, we used a closed system model (Rayleigh model). In this approach, the isotope enrichment factor is approximated by the following equation (Mariotti et al., 1981):

$$\delta_s = \delta_{s,0} - \varepsilon \times \ln(f) \quad (4.7)$$

where δ_s is the isotopic composition of the residual substrate (i.e., NO_3^- or NH_4^+), $\delta_{s,0}$ is the isotopic composition of the source substrate, and f is the fraction of the remaining substrate, relative to the concentrations at mid-water depths for NO_3^- and above the sediment for NH_4^+ , respectively. The isotope enrichment factor, ε , is approximated by the slope of the linear regression line ± 1 standard error (Mariotti et al., 1981). Using this approach, the estimated apparent N isotope enrichment factor associated with NO_3^- consumption was $13.7 \pm 0.5\text{‰}$ at the ecosystem level (Fig. 4.7a). This value, which seems to be independent of the time of the year is consistent with previous observations in Lake Lugano (Lehmann et al., 2003) but significantly lower than the canonical assumption of $^{15}\varepsilon = 25\text{‰}$ for water column

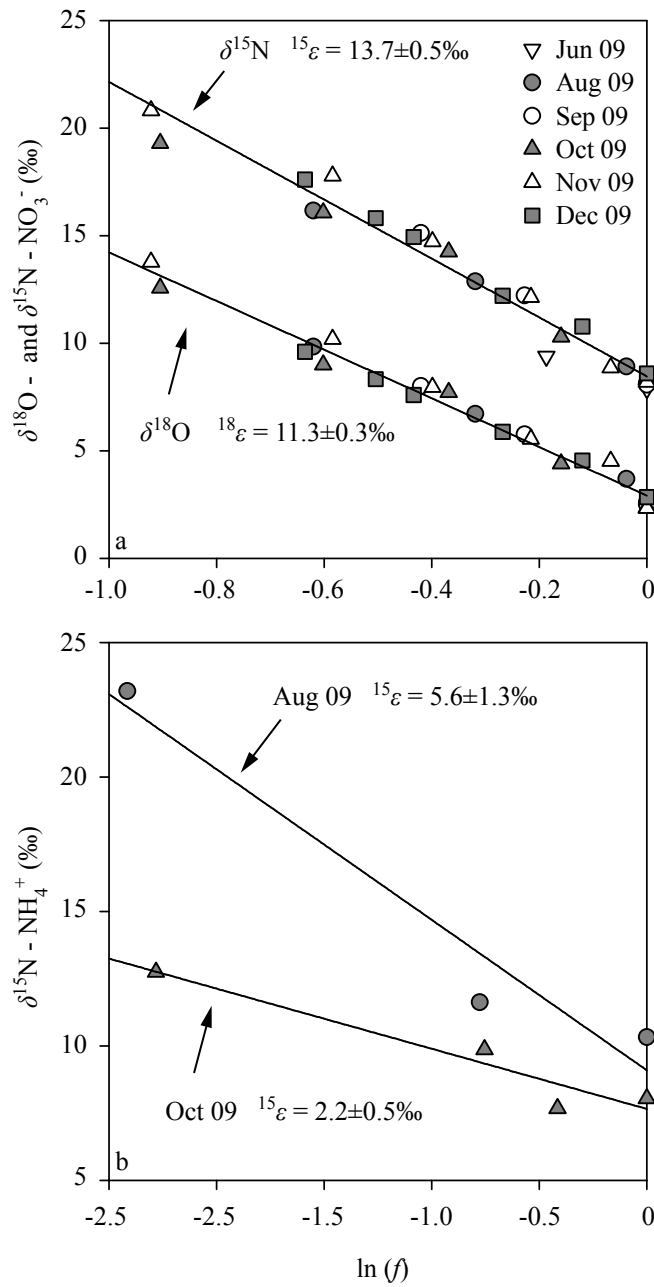


Figure 4.7: Rayleigh plots for (a) nitrate, and (b) ammonium consumption in the BNL in the southern basin of Lake Lugano. The N (and O) isotope composition is plotted against $\ln(f)$, where f denotes the remaining NO_3^- and NH_4^+ fraction with respect to the concentrations at mid-water depth and at the sediment-water interface, respectively.

denitrification. Time series NO_3^- isotope data from the two lowermost depths yielded similarly low N isotope enrichment factors, confirming the profile-based N isotope effect estimates, and validating the closed system Rayleigh approach. A likely explanation for the relatively low community N isotope effect could be that a significant fraction of the water column NO_3^- is reduced within the sediments with low N (and O) isotope fractionation. Biological N isotope fractionation during sedimentary denitrification is barely expressed in the overlying water column, independent of the aquatic environment and reactivity (Sigman et al., 2003; Lehmann et al., 2007; Alkhatib et al., 2012). In the previous section, we provided clear evidence for benthic NO_3^- reduction in the southern basin. In an independent approach, we can use the apparent difference in isotope fractionation between sedimentary (i.e., $^{15}\epsilon_{\text{sed}} \approx 1.5\text{‰}$) and water column denitrification (i.e., $^{15}\epsilon_{\text{water}} \approx 25\text{‰}$) to distinguish quantitatively between the two NO_3^- reduction sites (Sigman et al., 2003). However, this calculation is afflicted with relatively large uncertainties. It has, for example, been proposed to refrain from the common assumption of 25‰ for the higher end member (Kritee et al., 2012; Wenk et al., 2014). Indeed, a water column N isotope enrichment factor of $20.7 \pm 3.6\text{‰}$ was calculated by applying a diffusion-reaction model to the measured N isotope data in the Lake Lugano south basin (Lehmann et al., 2003). Using values between 20.7‰ and 25‰ as an upper limit, and assuming that benthic denitrification occurs with an apparent N isotope effect of 1.5‰ to 3‰, a simple end-member isotope approach leads to the conclusion that 36% to 51% of the NO_3^- is reduced in the sediments and 49% to 64% of the NO_3^- within the water column. This result agrees with the water column vs. benthic denitrification partitioning in the following year, which was inferred from comparing water column N_2 fluxes to benthic N_2 production rates (previous section; Fig. 4.6). However, the NO_3^- isotope approach does not account for any possible effects of NO_3^- production in the water column via nitrification. Hence, it remains uncertain whether nitrification in the net-denitrification zone can act to lower the overall community N isotope fractionation, so that the calculated water column to benthic denitrification ratio must be seen as conservative estimate. Consumption of NH_4^+ by nitrification at the RTZ will be discussed below.

4.4.3 Ammonium consumption at the oxic-anoxic interface as elucidated by NO_3^- isotope ratios

The $\delta^{15}\text{N}$ values of bottom water NH_4^+ were 10.3‰ and 8.1‰ in August and October 2009, respectively (Fig. 4.4c), similar to, but slightly lower than, previous values of approximately 12.5‰ in July and October 1999 (Lehmann et al., 2001). Assuming that remineralization of organic N to NH_4^+ is associated with insignificant N isotope fractionation and that nitrification is not active within the sediment under strictly

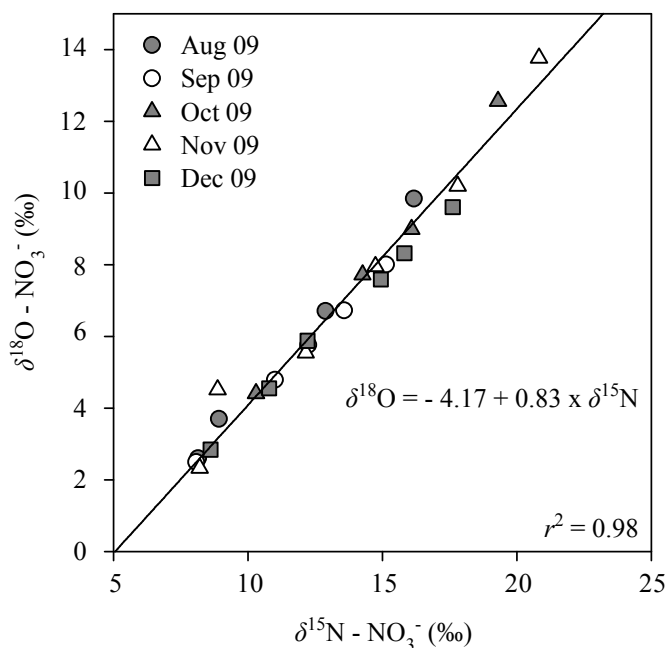


Figure 4.8: Oxygen vs. nitrogen isotope enrichment during nitrate reduction in the BNL. The mean slope of the linear regression line is ~ 0.83 .

anoxic conditions, the $\delta^{15}\text{N}$ value of NH_4^+ diffusing out of the sediment should reflect more or less the $\delta^{15}\text{N}\text{-NH}_4^+$ of the suspended and freshly sedimented particulate organic matter (POM). Indeed, a bottom water $\delta^{15}\text{N}\text{-NH}_4^+$ value of 8.1‰ under anoxic conditions (October 2009) is consistent with the $\delta^{15}\text{N}$ of the sinking OM (i.e., ~ 7 to 8‰; Lehmann et al. (2002)). We also measured $\delta^{15}\text{N}\text{-NH}_4^+$ as a function of depth in the anoxic water column and observed a significant increase in the $\delta^{15}\text{N}$ in association with decreasing NH_4^+ concentrations (Fig. 4.4c). These measured NH_4^+ profiles clearly indicate NH_4^+ consumption rather than simple turbulent mixing. Apparent N isotope enrichment factors associated with NH_4^+ consumption using a closed-system model ranged between $5.6 \pm 1.3\text{‰}$ (August 2009) and $2.2 \pm 0.5\text{‰}$ (October 2009) (Fig. 4.7b). A low N isotope fractionation appears consistent with NH_4^+ uptake during bacterial biosynthesis within the BNL (Hoch et al., 1992, 1994), and argues against nitrification, as N isotope enrichment factors reported for the latter process are typically higher, between 12‰ and 38‰ (Casciotti et al., 2003). However, it is also likely that nitrification occurs, and that the biologic isotope effect associated with nitrification is under-expressed at the ecosystem level due to complete NH_4^+ consumption at the oxic-anoxic interface (Thunell et al., 2004). In fact, from a parallel study on the N_2O isotope dynamics in the Lake Lugano south basin, we have compelling evidence that significant water column N_2O production occurs at the oxic-anoxic interface, most

probably due to NH_2OH decomposition during nitrification (see Chapter 5). Putative evidence for nitrification and in situ NO_3^- production is also provided by the combined $\delta^{15}\text{N}$ - and $\delta^{18}\text{O}$ - NO_3^- signatures in the water column. In marine environments and most culture experiments, the ^{18}O to ^{15}N isotope enrichment ratio ($^{18}\epsilon : ^{15}\epsilon$) during NO_3^- reduction is ~ 1 (Casciotti et al., 2002; Sigman et al., 2005; Granger et al., 2008), whereas it appears to be lower (i.e., $^{18}\epsilon : ^{15}\epsilon = 0.5 - 0.7$) for freshwater denitrification (Böttcher et al., 1990; Mengis et al., 1999; Lehmann et al., 2003). The apparent difference in NO_3^- O vs. N isotope dynamics between freshwater and marine environments represents a conundrum in N isotope biogeochemistry, which is still not fully resolved and awaits further investigation. In this study, we measured an ^{18}O to ^{15}N enrichment ratio of ~ 0.83 (Fig. 4.8), which is similar to the ratio reported for NO_3^- reduction in the Lake Lugano north basin (Wenk et al., 2014), but significantly higher than reported previously for the Lake Lugano south basin (~ 0.57 in 1999; Lehmann et al. (2003)) and for other freshwater environments. We argue that the deviation from a 1:1 ^{18}O to ^{15}N isotope enrichment results, in either case, from NO_3^- regeneration. We speculate that nitrification, if occurring in close proximity to NO_3^- consumption, does not necessarily result in a decoupling of the $\delta^{18}\text{O}$ -to- $\delta^{15}\text{N}$ signature, as observed in surface waters (Fig. 4.4a, b), but can still lead to a co-linearity in ^{18}O to ^{15}N enrichment (Fig. 4.8) at various levels, depending on the ratio of denitrification to nitrification. Such effects may be different for lacustrine environments compared to marine settings, given that the $\delta^{18}\text{O}$ of oxygen in the ambient water (i.e., the main source of added O during NO_3^- regeneration) is generally significantly lower in freshwater than in marine environments. Future modeling work will help to address the potential (variable) effects nitrification can have on the NO_3^- isotope signatures in a net denitrifying environment, and may thus help to resolve the above-mentioned marine and freshwater conundrum.

The sediments of the Lake Lugano south basin represent an effective fixed N sink, with highest N_2 production rates during oxic bottom water conditions. Denitrification is the dominant NO_3^- reduction pathway in the sediments, with only minor contribution from anammox and DNRA. With bottom water anoxia, NO_3^- reduction becomes partitioned between water column and sedimentary processes, and sedimentary denitrification accounts for approximately 40% of total N_2 gas production in the lake basin during fully developed bottom water anoxia (Fig. 4.6). In this study, which combines ^{15}N -tracer applications and natural abundance isotope measurements, a comparison between direct benthic N_2 production rate measurements and water column N_2 fluxes, as well as the indirect estimates based on an end-member N isotope approach, yielded consistent results, suggesting that water column NO_3^- isotope measurements can quantitatively distinguish between benthic and pelagic denitrification. However, using NO_3^- isotopes to constrain denitrification rates in N budget models requires justifiable assumptions regarding the isotopic end-members.

It likely also hinges on the purity of the community denitrification N isotope effect observed in the water column of a lake (or an ocean basin); that is, on the degree to which NO_3^- production affects the community N isotope signature. Our coupled NO_3^- N and O isotope measurements provide evidence for nitrification in close vicinity of the denitrification zone, yet the effect on the community N isotope effect in the RTZ remains elusive. Our study thus underscores the need for additional experiments, field observations, and model simulations to study the potential ability for nitrification to distort the O to N isotope ratio relationship expected for stand-alone denitrification.

4 - References

- M. Alkhatib, M. F. Lehmann, and P. A. del Giorgio. The nitrogen isotope effect of benthic remineralization-nitrification-denitrification coupling in an estuarine environment. *Biogeosciences*, 9:1633–1646, 2012.
- S. M. An and W. S. Gardner. Dissimilatory nitrate reduction to ammonium (DNRA) as a nitrogen link, versus denitrification as a sink in a shallow estuary (Laguna Madre/Baffin Bay, Texas). *Marine Ecology Progress Series*, 237:41–50, 2002.
- S. M. An, W. S. Gardner, and T. Kana. Simultaneous measurement of denitrification and nitrogen fixation using isotope pairing with membrane inlet mass spectrometry analysis. *Applied and Environmental Microbiology*, 67:1171–1178, 2001.
- A. Barbieri and B. Polli. Description of Lake Lugano. *Aquatic Sciences*, 54:181–183, 1992.
- J. K. Böhlke, S. J. Mroczkowski, and T. B. Coplen. Oxygen isotopes in nitrate: New reference materials for ^{18}O : ^{17}O : ^{16}O measurements and observations on nitrate-water equilibration. *Rapid Communications in Mass Spectrometry*, 17:1835–1846, 2003.
- J. Böttcher, O. Strebel, S. Voerkelius, and H.-L. Schmidt. Using isotope fractionation of nitrate-nitrogen and nitrate-oxygen for evaluation of microbial denitrification in a sandy aquifer. *Journal of Hydrology*, 114:413–424, 1990.
- A. Bourbonnais, M. F. Lehmann, D. A. Butterfield, and S. K. Juniper. Subseafloor nitrogen transformations in diffuse hydrothermal vent fluids of the Juan de Fuca Ridge evidenced by the isotopic composition of nitrate and ammonium. *Geochemistry Geophysics Geosystems*, 13, 2012.
- R. S. Braman and S. A. Hendrix. Nanogram nitrite and nitrate determination in environmental and biological materials by vanadium(III) reduction with chemiluminescence detection. *Analytical Chemistry*, 61:2715–2718, 1989.
- J. A. Brandes and A. H. Devol. Isotopic fractionation of oxygen and nitrogen in coastal marine sediments. *Geochimica et Cosmochimica Acta*, 61:1793–1801, 1997.

- A. J. Burgin and S. K. Hamilton. Have we overemphasized the role of denitrification in aquatic ecosystems? A review of nitrate removal pathways. *Frontiers in Ecology*, 5:89–96, 2007.
- A. J. Burgin, S. K. Hamilton, S. E. Jones, and J. T. Lennon. Denitrification by sulfur-oxidizing bacteria in a eutrophic lake. *Aquatic Microbial Ecology*, 66:283–293, 2012.
- K. L. Casciotti, D. M. Sigman, M. Galanter Hastings, J. K. Böhlke, and A. Hillert. Measurement of the oxygen isotopic composition of nitrate in seawater and freshwater using the denitrifier method. *Analytical Chemistry*, 74:4905–4912, 2002.
- K. L. Casciotti, D. M. Sigman, and B. B. Ward. Linking diversity and stable isotope fractionation in ammonia-oxidizing bacteria. *Geomicrobiology Journal*, 20:335–353, 2003.
- B. D. Eyre, S. Rysgaard, T. Dalsgaard, and P. B. Christensen. Comparison of isotope pairing and $N_2:Ar$ methods for measuring sediment denitrification - Assumptions, modifications, and implications. *Estuaries*, 25:1077–1087, 2002.
- C. V. Freymond, C. B. Wenk, C. H. Frame, and M. F. Lehmann. Year-round N_2O production by benthic NO_x reduction in a monomictic south-alpine lake. *Biogeosciences*, 10:8373–8383, 2013.
- C. A. Fuchsman, J. W. Murray, and S. K. Konovalov. Concentration and natural stable isotope profiles of nitrogen species in the Black Sea. *Marine Chemistry*, 111:90–105, 2008.
- W. S. Gardner, L. R. Herche, P. A. S. John, and S. P. Seitzinger. High-performance liquid chromatographic determination of $^{15}NH_4^+ : (^{14}NH_4^+ + ^{15}NH_4^+)$ ion ratios in seawater for isotope dilution experiments. *Analytical Chemistry*, 63:1838–1843, 1991.
- W. S. Gardner, H. A. Bootsma, C. Evans, and P. A. S. John. Improved chromatographic analysis of $^{15}N:^{14}N$ ratios in ammonium or nitrate for isotope addition experiments. *Marine Chemistry*, 48:271–282, 1995.
- C. Garside. A chemiluminescent technique for the determination of nanomolar concentrations of nitrate and nitrite in seawater. *Marine Chemistry*, 11:159–167, 1982.
- R. Gonfiantini, W. Stichler, and K. Rosanski. Standards and intercomparison materials distributed by the IAEA for stable isotope measurements. *IAEA-TECDOC-825*, IAEA, Vienna, pages 13–31, 1995.

- J. Granger and D. M. Sigman. Removal of nitrite with sulfamic acid for nitrate N and O isotope analysis with the denitrifier method. *Rapid Communications in Mass Spectrometry*, 23:3753–3762, 2009.
- J. Granger, D. M. Sigman, M. F. Lehmann, and P. D. Tortell. Nitrogen and oxygen isotope fractionation during dissimilatory nitrate reduction by denitrifying bacteria. *Limnology and Oceanography*, 53:2533–2545, 2008.
- M. R. Hamersley, D. Woebken, B. Boehrer, M. Schultze, G. Lavik, and M. M. M. Kuypers. Water column anammox and denitrification in a temperate permanently stratified lake (Lake Rassnitzer, Germany). *Systematic and Applied Microbiology*, 32:571–582, 2009.
- M. P. Hoch, M. L. Fogel, and D. L. Kirchman. Isotope fractionation associated with ammonium uptake by a marine bacterium. *Limnology and Oceanography*, 37:1447–1459, 1992.
- M. P. Hoch, M. L. Fogel, and D. L. Kirchman. Isotope fractionation during ammonium uptake by marine microbial assemblages. *Geomicrobiology Journal*, 12:113–127, 1994.
- B. Z. Houlton, D. M. Sigman, E. A. G. Schuur, and L. O. Hedin. A climate-driven switch in plant nitrogen acquisition within tropical forest communities. *Proceedings of the National Academy of Sciences of the United States of America (PNAS)*, 104:8902–8906, 2007.
- T. M. Kana, C. Darkangelo, M. D. Hunt, J. B. Oldham, G. E. Bennett, and J. C. Cornwell. Membrane inlet mass spectrometer for rapid high-precision determination of N₂, O₂, and Ar in environmental water samples. *Analytical Chemistry*, 66:4166–4170, 1994.
- A. N. Knapp, D. M. Sigman, and F. Lipschultz. N isotopic composition of dissolved organic nitrogen and nitrate at the Bermuda Atlantic time-series study site. *Global Biogeochemical Cycles*, 19, 2005.
- I. Koike and A. Hattori. Denitrification and ammonia formation in anaerobic coastal sediments. *Applied and Environmental Microbiology*, 35:278–282, 1978.
- F. Koroleff. *Determination of ammonia*. In: K. Grasshoff [ed.], *Methods of Seawater Analysis*, pages 126–133. Verlag Chemie, 1976.
- K. Kritee, D. M. Sigman, J. Granger, B. B. Ward, A. Jayakumar, and C. Deutsch. Reduced isotope fractionation by denitrification under conditions relevant to the ocean. *Geochimica et Cosmochimica Acta*, 92:243–259, 2012.

- M. M. M. Kuypers, A. O. Sliemers, G. Lavik, M. Schmid, B. B. Jørgensen, J. G. Kuenen, J. S. S. Damsté, M. Strous, and M. S. M. Jetten. Anaerobic ammonium oxidation by anammox bacteria in the Black Sea. *Nature*, 422:608–611, 2003.
- P. J. Lavrentyev, W. S. Gardner, and L. Y. Yang. Effects of the zebra mussel on nitrogen dynamics and the microbial community at the sediment-water interface. *Aquatic Microbial Ecology*, 21:187–194, 2000.
- M. F. Lehmann, S. M. Bernasconi, and J. A. McKenzie. A method for the extraction of ammonium from freshwaters for nitrogen isotope analysis. *Analytical Chemistry*, 73:4717–4721, 2001.
- M. F. Lehmann, S. M. Bernasconi, A. Barbieri, and J. A. McKenzie. Preservation of organic matter and alteration of its carbon and nitrogen isotope composition during simulated and in situ early sedimentary diagenesis. *Geochimica et Cosmochimica Acta*, 66:3573–3584, 2002.
- M. F. Lehmann, P. Reichert, S. M. Bernasconi, A. Barbieri, and J. A. McKenzie. Modelling nitrogen and oxygen isotope fractionation during denitrification in a lacustrine redox-transition zone. *Geochimica Et Cosmochimica Acta*, 67:2529–2542, 2003.
- M. F. Lehmann, S. M. Bernasconi, J. A. McKenzie, A. Barbieri, M. Simona, and M. Veronesi. Seasonal variation of the $\delta^{13}\text{C}$ and $\delta^{15}\text{N}$ of particulate and dissolved carbon and nitrogen in Lake Lugano: Constraints on biogeochemical cycling in a eutrophic lake. *Limnology and Oceanography*, 49:415–429, 2004.
- M. F. Lehmann, D. M. Sigman, D. C. McCorkle, B. G. Brunelle, S. Hoffmann, M. Kienast, G. Cane, and J. Clement. Origin of the deep Bering Sea nitrate deficit: Constraints from the nitrogen and oxygen isotopic composition of water column nitrate and benthic nitrate fluxes. *Global Biogeochemical Cycles*, 19, 2005.
- M. F. Lehmann, D. M. Sigman, D. C. McCorkle, J. Granger, S. Hoffmann, G. Cane, and B. G. Brunelle. The distribution of nitrate $^{15}\text{N}/^{14}\text{N}$ in marine sediments and the impact of benthic nitrogen loss on the isotopic composition of oceanic nitrate. *Geochimica et Cosmochimica Acta*, 71:5384–5404, 2007.
- A. Mariotti, J. C. Germon, P. Hubert, P. Kaiser, R. Letolle, A. Tardieux, and P. Tardieux. Experimental determination of nitrogen kinetic isotope fractionation: Some principles; Illustration for the denitrification and nitrification processes. *Plant and Soil*, 62:413–430, 1981.

- M. J. McCarthy and W. S. Gardner. An application of membrane inlet mass spectrometry to measure denitrification in a recirculating mariculture system. *Aquaculture*, 218:341–355, 2003.
- M. J. McCarthy, P. J. Lavrentyev, L. Yang, L. Zhang, Y. Chen, B. Qin, and W. S. Gardner. Nitrogen dynamics and microbial food web structure during a summer cyanobacterial bloom in a subtropical, shallow, well-mixed, eutrophic lake (Lake Taihu, China). *Hydrobiologia*, 581:195–207, 2007.
- M. J. McCarthy, K. S. McNeal, J. W. Morse, and W. S. Gardner. Bottom-water hypoxia effects on sediment-water interface nitrogen transformations in a seasonally hypoxic, shallow bay (Corpus Christi Bay, TX, USA). *Estuaries and Coasts*, 31:521–531, 2008.
- M. Mengis, S. L. Schiff, M. Harris, M. C. English, R. Aravena, R. J. Elgood, and A. MacLean. Multiple geochemical and isotopic approaches for assessing ground water NO_3^- elimination in a riparian zone. *Ground Water*, 37:448–457, 1999.
- L. P. Nielsen. Denitrification in sediment determined from nitrogen isotope pairing. *FEMS Microbiology Ecology*, 86:357–362, 1992.
- C. J. Schubert, E. Durisch-Kaiser, B. Wehrli, B. Thamdrup, P. Lam, and M. M. M. Kuypers. Anaerobic ammonium oxidation in a tropical freshwater system (Lake Tanganyika). *Environmental Microbiology*, 8:1857–1863, 2006.
- D. M. Sigman, M. A. Altabet, R. Michener, D. C. McCorkle, B. Fry, and R. M. Holmes. Natural abundance-level measurement of the nitrogen isotopic composition of oceanic nitrate: An adaptation of the ammonia diffusion method. *Marine Chemistry*, 57:227–242, 1997.
- D. M. Sigman, K. L. Casciotti, M. Andreani, C. Barford, M. Galanter, and J. K. Böhlke. A bacterial method for the nitrogen isotopic analysis of nitrate in seawater and freshwater. *Analytical Chemistry*, 73:4145–4153, 2001.
- D. M. Sigman, R. Robinson, A. N. Knapp, A. van Geen, D. C. McCorkle, J. A. Brandes, and R. C. Thunell. Distinguishing between water column and sedimentary denitrification in the Santa Barbara Basin using the stable isotopes of nitrate. *Geochemistry Geophysics Geosystems*, 4, 2003.
- D. M. Sigman, J. Granger, P. J. DiFiore, M. F. Lehmann, R. Ho, G. Cane, and A. van Geen. Coupled nitrogen and oxygen isotope measurements of nitrate along the eastern North Pacific margin. *Global Biogeochemical Cycles*, 19, 2005.

- S. M. Steingruber, J. Friedrich, R. Gächter, and B. Wehrli. Measurement of denitrification in sediments with the ^{15}N isotope pairing technique. *Applied and Environmental Microbiology*, 67:3771–3778, 2001.
- B. Thamdrup and T. Dalsgaard. Production of N_2 through anaerobic ammonium oxidation coupled to nitrate reduction in marine sediments. *Applied and Environmental Microbiology*, 68:1312–1318, 2002.
- B. Thamdrup, T. Dalsgaard, M. M. Jensen, O. Ulloa, L. Farías, and R. Escribano. Anaerobic ammonium oxidation in the oxygen-deficient waters off northern Chile. *Limnology and Oceanography*, 51:2145–2156, 2006.
- R. C. Thunell, D. M. Sigman, F. Muller-Karger, Y. Astor, and R. Varela. Nitrogen isotope dynamics of the Cariaco Basin, Venezuela. *Global Biogeochemical Cycles*, 18, 2004.
- M. Voss, J. W. Dippner, and J. P. Montoya. Nitrogen isotope patterns in the oxygen-deficient waters of the Eastern Tropical North Pacific Ocean. *Deep-Sea Research*, 48:1905–1921, 2001.
- F. Wang, S. K. Juniper, S. P. Pelegri, and S. A. Macko. Denitrification in sediments of the Laurentian Trough, St. Lawrence Estuary, Québec, Canada. *Estuarine Coastal and Shelf Science*, 57:515–522, 2003.
- R. F. Weiss. The solubility of nitrogen, oxygen and argon in water and seawater. *Deep-Sea Research*, 17:721–735, 1970.
- R. P. Wellman, F. D. Cook, and H. R. Krouse. Nitrogen-15: Microbiological alteration of abundance. *Science*, 161:269–270, 1968.
- C. B. Wenk, J. Blees, J. Zopfi, M. Veronesi, A. Bourbonnais, C. J. Schubert, H. Niemann, and M. F. Lehmann. Anaerobic ammonium oxidation (anammox) bacteria and sulfide-dependent denitrifiers coexist in the water column of a meromictic south-alpine lake. *Limnology and Oceanography*, 58:1–12, 2013.
- C. B. Wenk, J. Zopfi, J. Blees, M. Veronesi, H. Niemann, and M. F. Lehmann. Community N and O isotope fractionation by sulfide-dependent denitrification and anammox in a stratified lacustrine water column. *Geochimica et Cosmochimica Acta*, 125:551–563, 2014.
- J. Zopfi, T. G. Ferdeman, B. B. Jørgensen, A. Teske, and B. Thamdrup. Influence of water column dynamics on sulfide oxidation and other major biogeochemical processes in the chemocline of Mariager Fjord (Denmark). *Marine Chemistry*, 74: 29–51, 2001.

CHAPTER 5

Nitrous oxide cycling in a mono- and a meromictic lake basin
inferred from stable isotope and isotopomer distributions

C. B. Wenk, K. Koba, K. L. Casciotti, J. Zopfi, M. Veronesi, H. Niemann, C. J.
Schubert, C. H. Frame, and M. F. Lehmann

Abstract

Lakes represent a potential source of nitrous oxide (N_2O), but the biogeochemical controls and microbial pathways of lacustrine N_2O production are not well understood. Here we measured water column N_2O concentrations, the N_2O N and O isotope composition, as well as the ^{15}N -site preference (SP) within in the asymmetric N_2O molecule, to trace microbial N_2O production (denitrification, nitrification, and nitrifier denitrification) and consumption processes in two biogeochemically distinct basins of Lake Lugano (Switzerland/Italy). Our results indicate differential net in situ N_2O production in the two basins, with maximum N_2O concentrations between 12 nmol L^{-1} and $>900 \text{ nmol L}^{-1}$ in the monomictic south basin, and significantly lower maximum N_2O concentrations in the meromictic north basin (always $<13 \text{ nmol L}^{-1}$). In the south basin, extreme N_2O concentrations ($>900 \text{ nmol L}^{-1}$) were measured only once, at the beginning of the seasonal stratification period in 2009. Thereafter, maximum N_2O concentrations were generally $<90 \text{ nmol L}^{-1}$. A characteristic N_2O concentration maximum at the oxic-anoxic interface, together with a $\delta^{15}\text{N}\text{-N}_2\text{O}$ minimum of -18‰ and a SP of 32‰ suggested water column nitrification via hydroxylamine (NH_2OH) oxidation as the dominant N_2O source in the south basin. Below the oxic-anoxic interface, decreasing N_2O concentrations together with an increase in SP, bulk $\delta^{15}\text{N}$ - and $\delta^{18}\text{O}\text{-N}_2\text{O}$ indicated net N_2O reduction to N_2 . In the meromictic north basin, a N_2O concentration maximum of 13 nmol L^{-1} was measured in the subsurface water at 20 m depth. This concentration maximum together with a $\delta^{15}\text{N}\text{-N}_2\text{O}$ minimum of 5‰ and a SP of 16‰ was indicative for in situ N_2O production by nitrifier denitrification. In the hypolimnion, the pronounced decrease in N_2O concentrations to undetectable levels within the redox transition zone, again in tandem with an increase in $\delta^{15}\text{N}\text{-N}_2\text{O}$, $\delta^{18}\text{O}\text{-N}_2\text{O}$, and SP, indicated quantitative N_2O consumption by microbial denitrification. The apparent N and O isotope enrichment factors (assuming Rayleigh model kinetics) associated with net N_2O consumption were $^{15}\epsilon \approx 3.2\text{‰}$ and $^{18}\epsilon \approx 8.6\text{‰}$, respectively. From previous work we know that fixed N elimination is primarily driven by sulfide-dependent denitrification (Wenk et al., 2013). Hence, our study presents the first report of stable isotope fractionation associated with N_2O reduction by chemolithotrophic denitrifiers. The observed ^{18}O to ^{15}N isotope enrichment ratio ($^{18}\epsilon : ^{15}\epsilon \approx 2.5$) is consistent with previous reports for N and O isotope fractionation due to N_2O reduction by organotrophic denitrification. Comparison between the two lake basins suggests that the dynamic environmental conditions in the Lake Lugano south basin are more conducive to incomplete denitrification and N_2O accumulation than the rather stable conditions in the north basin.

5.1 Introduction

Nitrous oxide (N_2O) is a potent greenhouse gas and a major ozone-depleting substance in the stratosphere (Forster et al., 2007; Ravishankara et al., 2009). The recent increase in atmospheric N_2O is mainly due to human alteration of the nitrogen (N) cycle, in particular the increased use of synthetic N-based fertilizers (Mosier et al., 1998). Regional watershed N balance studies have revealed that most of the anthropogenic N input is transferred to gaseous forms before reaching the ocean, making terrestrial ecosystems an important fixed N sink, but also a potential N_2O source (Alexander et al., 2000; Howarth et al., 1996). Terrestrial N-load mitigation can partly be attributed to microbial processes in redox transition zones (RTZs) of lakes. The reactions that affect net N_2O production include: Nitrification, denitrification, and nitrifier denitrification. Nitrification, the aerobic oxidation of ammonium (NH_4^+) to nitrite (NO_2^-) and (NO_3^-) via the intermediate hydroxylamine (NH_2OH) produces N_2O as a byproduct through NH_2OH oxidation (Hooper and Terry, 1979). Denitrification is the stepwise dissimilatory reduction of NO_3^- to NO_2^- , nitric oxide (NO), N_2O and dinitrogen gas (N_2) and is the only known pathway for N_2O consumption. Yet, denitrification, if incomplete, can also lead to the accumulation of N_2O (Baumann et al., 1997). Nitrifier denitrification, the reduction of NO_2^- to N_2O by nitrifying bacteria under low-oxygen conditions is another N_2O source (Poth and Focht, 1985). A promising tool to study N_2O production and consumption processes is the measurement of the stable N and O isotope composition of N_2O . The value of such measurements is based on the fact that most of the different N_2O sources display characteristic isotope signatures, which can be used to diagnose the relative importance of N_2O producing reactions (e.g., Wunderlin et al., 2013). It has for example been shown that organotrophic denitrification to N_2O proceeds with a relatively large isotope fractionation, i.e., $\Delta\delta^{15}\text{N}$ ($= \delta^{15}\text{N}_{\text{substrate}} - \text{bulk } \delta^{15}\text{N}_{\text{N}_2\text{O}}$) $\approx 10\text{‰} - 29\text{‰}$ and $\Delta\delta^{18}\text{O}$ ($= \delta^{18}\text{O}_{\text{substrate}} - \delta^{18}\text{O}_{\text{N}_2\text{O}}$) $\approx 37\text{‰} - 43\text{‰}$ (Barford et al., 1999; Snider et al., 2009; Sutka et al., 2006; Toyoda et al., 2005). N_2O production through NH_2OH oxidation is associated with almost no N isotope fractionation, i.e., $\Delta\delta^{15}\text{N} \approx 0\text{‰}$ (Frame and Casciotti, 2010; Sutka et al., 2006, 2003, 2004), whereas N_2O produced through nitrifier denitrification is significantly depleted in ^{15}N relative to the source NH_4^+ ($\Delta\delta^{15}\text{N} \approx 43\text{‰} - 60\text{‰}$) (Frame and Casciotti, 2010; Wunderlin et al., 2013; Yoshida, 1988). While N_2O production yields N_2O that is relatively depleted in the heavy isotopes, microbial N_2O reduction appears to consistently leave the residual N_2O enriched in ^{15}N and ^{18}O . The kinetic isotope effects associated with N_2O reduction are $^{15}\epsilon_{\text{N}_2\text{O} \rightarrow \text{N}_2} \approx 12\text{‰}$ and $^{18}\epsilon_{\text{N}_2\text{O} \rightarrow \text{N}_2} \approx 31\text{‰}$, respectively (Barford et al., 1999; Yamagishi et al., 2007).

Similar to the bulk stable isotope composition of N_2O , measurements of the intramolecular distribution of ^{15}N within the N_2O molecule, provides valuable constraints on

N_2O consumption and production processes. The intramolecular ^{15}N -site preference (SP), which describes the partitioning of ^{15}N between the central (α) and terminal (β) positions within the asymmetric N_2O molecule, defined as $\text{SP} = \delta^{15}\text{N}^\alpha - \delta^{15}\text{N}^\beta$ (Toyoda and Yoshida, 1999) typically ranges from 30‰ - 36‰ for nitrification (Frame and Casciotti, 2010; Sutka et al., 2006, 2003, 2004; Toyoda et al., 2005). During NH_2OH oxidation, NO can be formed, which can further react to hyponitrous acid ($\text{H}_2\text{N}_2\text{O}_2$), and eventually dehydrate to N_2O . The reason for the positive site preference is likely the result of the preferential ^{14}N - ^{16}O bond breakage within the $\text{H}_2\text{N}_2\text{O}_2$ molecule during dehydration, leading to the relative ^{15}N enrichment in the central (α) position of the product N_2O . On the other hand, N_2O production through incomplete denitrification or nitrifier denitrification is catalyzed by enzymatic reactions, yielding SP values of -5‰ to 0 and -11‰ to 0, respectively (Frame and Casciotti, 2010; Sutka et al., 2006, 2003, 2004; Toyoda et al., 2005). Fractionation during N_2O reduction to N_2 increases the SP of the residual N_2O (Ostrom et al., 2007; Yamagishi et al., 2007). This is most probably due to the preferential N-O bond breakage of N_2O molecules with ^{14}N in the α -position, leaving the residual N_2O enriched in ^{15}N on the α -position. In contrast to the bulk N and O isotope composition of N_2O , the SP is independent of the isotopic composition of the precursor substrate. It has been used to trace metabolic N_2O production and consumption processes in environments with mixed microbial communities, such as wastewater treatment plants (Wunderlin et al., 2013), soils (Snider et al., 2009), the ocean (Popp et al., 2002; Westley et al., 2006; Yamagishi et al., 2007), and recently also in Lake Kizaki (Sasaki et al., 2011). Here we make use of N_2O stable isotope and isotopomer measurements to gain insight into the N_2O dynamics in two biogeochemically distinct basins of Lake Lugano in southern Switzerland. The deeper northern basin is stratified throughout the year. Sulfur-driven denitrification is the main sink for fixed N, but anaerobic ammonium oxidation (anammox) contributes up to 30% of total N_2 production (Wenk et al., 2013). The shallower southern basin is monomictic with strong density stratification and bottom water anoxia during summer and fall. The dominant removal process for fixed N appears to be organotrophic denitrification within the sediments (Wenk et al., in prep.). Our objective was to measure N_2O concentrations as well as stable isotope and isotopomer distributions of N_2O in the water column 1) to assess the spatio-temporal variability of N_2O accumulation in the two basins, 2) to identify the dominant modes of N_2O production in Lake Lugano, and 3) to compare the N_2O dynamics between the two basins with respect to the different environmental conditions.

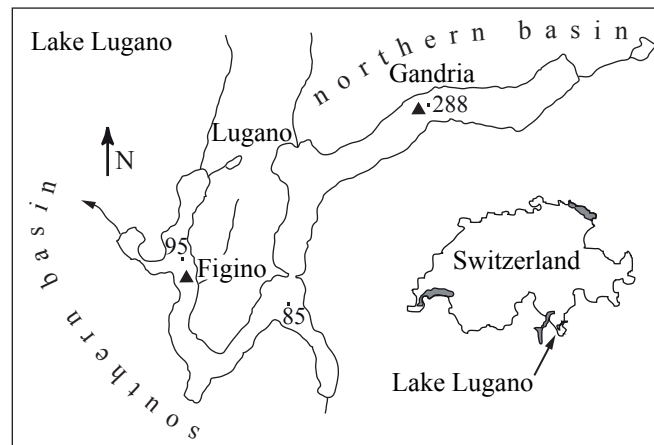


Figure 5.1: Location and map of Lake Lugano. The sampling stations in the northern and the southern basins are marked with black triangles. Map adapted from Barbieri and Polli (1992).

5.2 Methods

5.2.1 Study site and sampling

Lake Lugano is located on the southern slopes of the Alps at 271 m above sea level (Fig. 5.1). A natural dam separates the lake into two main basins. The northern basin has a maximum water depth of 288 m and is permanently stratified. The monomictic southern basin is 95 m deep. Samples were collected from both basins at sites south of the village of Gandria (46.01°N, 9.02°E), and west of the village of Figino (45.95°N, 8.90°E), respectively (Fig. 5.1). Water samples were retrieved by hydrocast, using 5-L and 10-L Niskin bottles during sampling campaigns in 2009 (August, October), and 2010 (January, August, October).

5.2.2 N₂O and nutrient concentrations

For N₂O concentration analyses, water from the Niskin bottle was directly filled into 500 mL glass bottles and immediately sealed with thick butyl rubber stoppers. A 10 mL headspace was introduced, and 10 mL of aqueous NaOH solution (50% w:v) were added in exchange with sample in order to stop microbial activity. N₂O concentrations were determined as described in Diem et al. (2012). Briefly, 40 mL of sample water were replaced with N₂ and equilibrated over night or in an ultrasonic bath for 30 minutes. Headspace measurements were made on a gas chromatograph (GC, Agilent 6890N) equipped with a GS-Carbonplot column (Agilent) and an Electron Capture

Detector (ECD). Dissolved gas N_2O concentrations were calculated according to Weiss and Price (1980). Additionally, N_2O concentrations were determined during stable isotope analysis as described below. All NO_3^- and NH_4^+ concentration data have been published recently in Wenk et al. (2013) (north basin) and in Wenk et al. (in prep.) (south basin). Briefly, separate aliquots of filtered ($0.45 \mu\text{m}$) lake water were frozen for subsequent NO_x (i.e., $\text{NO}_2^- + \text{NO}_3^-$) and NH_4^+ concentration analyses. NO_x and NO_2^- concentrations were determined on a NO_x -Analyzer (Antek Model 745) by reduction to NO in an acidic V^{3+} or sodium iodide solution, respectively, followed by chemiluminescence detection of NO (Braman and Hendrix, 1989; Garside, 1982). $[\text{NO}_3^-]$ was calculated from the difference of $[\text{NO}_x]$ and $[\text{NO}_2^-]$. NH_4^+ concentrations were measured photometrically using the indophenol method (Koroleff, 1976).

5.2.3 N_2O isotope and isotopomer analyses

Water from the Niskin bottle was directly sampled into 160 mL glass bottles. For the August 2009 and August 2010 profiles, the bottles were sealed with butyl rubber stoppers without headspace. To stop microbial activity, 0.5 mL of a HgCl_2 solution (5% w:v) were introduced in exchange with sample water. For the October 2010 profile, 2 mL of sample water were removed, and 0.1 mL of a HgCl_2 solution (5% w:v) were introduced before sealing the vials with butyl rubber stoppers. The samples were stored cooled until analysis. Bulk N_2O isotope and isotopomer analyses of samples from August 2009 and 2010 were conducted at the Tokyo Institute of Technology, Japan, using an online analytical system comprising a 200 mL gas extraction chamber (Koshin Rikagaku Seisakusho, Tokyo, Japan), a stainless-steel gas transfer line, pre-concentration traps, chemical traps for removal of H_2O and CO_2 , and a gas chromatograph / isotope ratio mass spectrometer (MAT 252; Thermo Fisher Scientific Inc.) (Toyoda et al., 2009). Analyses of October 2010 samples were performed at Woods Hole Oceanographic Institution, as described in McIlvin and Casciotti (2010). Briefly, CO_2 was removed from the gas stream by passage through a Carbosorb trap. N_2O was then separated from residual CO_2 using a capillary column (25 m, 0.32 mm) lined with Poraplot-Q before injection into the mass spectrometer (Delta^{PLUS} XP) through an open split. Bulk N and O isotope ratios are reported as δ values in ‰ relative to air N_2 and Vienna Standard Mean Ocean Water (VSMOW), where $\delta = (R_{\text{sample}} / R_{\text{standard}} - 1) \times 1000$, and $R = {}^{15}\text{N} : {}^{14}\text{N}$ or ${}^{18}\text{O} : {}^{16}\text{O}$, respectively. In analogy, $\delta^{15}\text{N}^\alpha$ and $\delta^{15}\text{N}^\beta$ denote the relative enrichment of ${}^{15}\text{N}$ in the central (i.e., ${}^{14}\text{N}{}^{15}\text{N}{}^{16}\text{O} : {}^{14}\text{N}$) and in the terminal (i.e., ${}^{15}\text{N}{}^{14}\text{N}{}^{16}\text{O} : {}^{14}\text{N}$) position with respect to the reference. The measurement precision was usually better than 0.2‰ for bulk $\delta^{15}\text{N}$ - N_2O , better than 0.5‰ for $\delta^{18}\text{O}$ - N_2O , and better than 1.0‰ for the site preference.

5.3 Results

5.3.1 N₂O concentration and isotope composition in the Lake Lugano south basin

The seasonality of hypolimnetic oxygenation and nutrient cycling in the water column has been described in detail in Lehmann et al. (2004) and Wenk et al. (in prep.). Briefly, with the water column overturn in winter, the hypolimnion is ventilated and remains completely oxygenated between February and May. During the spring and summer months, photosynthetic activity and increased primary production in the surface water results in enhanced export of organic matter (OM) and high respiration rates in the hypolimnion, leading to the development of an anoxic layer in the bottom water. Decreasing NO₃⁻ concentrations from mid-water depths toward the sediments indicate active denitrification within the anoxic water column and the sediment. With ongoing water column stratification, the denitrification and redox transition zones rise into the water column, and the anoxic, ammonium-replete bottom water layer reaches a maximum thickness of about 20 m in late fall and winter. In January, the seasonal cycle starts over again, with the destratification of the water column and the collapse of oxygen and nutrient concentration gradients (Fig. 5.2).

In August 2009, huge amounts of dissolved N₂O accumulated in the anoxic bottom water (Fig. 5.2a). A maximum concentration of 918 nmol L⁻¹ (i.e., ~100 times atmospheric equilibrium levels) was measured at the sediment-water interface. Lower N₂O concentrations (96 nmol L⁻¹) were observed just below the depth of O₂ disappearance at 86 m depth, but a secondary N₂O maximum of 163 nmol L⁻¹ was detected at the oxic-anoxic interface (i.e., at 83 m depth). The N₂O peak at the oxic-anoxic interface was a feature, which reoccurred during subsequent sampling campaigns, yet at lower concentration levels. In surface and subsurface waters, the N₂O concentration was ~8 nmol L⁻¹. In October 2009, maximum N₂O concentrations in the near-bottom water (76 nmol L⁻¹) and peak concentrations at the oxic-anoxic interface (20 nmol L⁻¹ at 76 m depth) were significantly reduced relative to August 2009 (Fig. 5.2b). In January 2010, bottom water N₂O accumulation was not observed at all (Fig. 5.2c). At that time, N₂O concentrations decreased from highest values in the oxic water column (12 nmol L⁻¹) to undetectable levels below the oxic-anoxic interface.

The next year, N₂O dynamics showed a different pattern (Fig. 5.3). In August 2010, N₂O concentrations reached a maximum of 90 nmol L⁻¹ at the oxic-anoxic interface (88 m depth), similar to the sampling campaigns before, but, in contrast to 2009, the N₂O concentration dropped to much lower levels (< 19 nmol L⁻¹) in the anoxic bottom water below, without increase toward the sediment-water-interface (Fig. 5.3a). Surface water N₂O concentrations were 11 nmol L⁻¹ in this month. In apparent association with the N₂O concentration peak, a bulk δ¹⁵N-N₂O minimum of

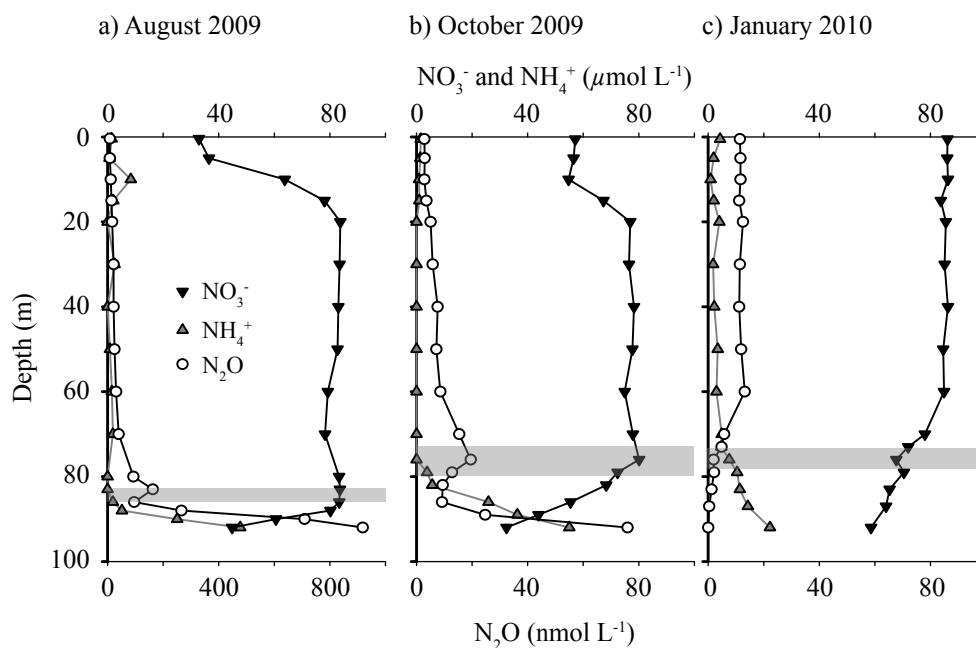


Figure 5.2: Water column profiles of dissolved NO_3^- , NH_4^+ , and N_2O concentrations from the Lake Lugano south basin in a) August 2009, b) October 2009, and c) January 2010. The grey bar marks the oxic-anoxic interface, i.e., $[\text{O}_2]$ from $50 \mu\text{mol L}^{-1}$ to $< 1 \mu\text{mol L}^{-1}$.

-18.0‰ was observed just below the depth of O_2 disappearance (i.e., at 90 m depth). In contrast, the $\delta^{18}\text{O}\text{-N}_2\text{O}$ and the ^{15}N -site preference both increased with depth through the oxic-anoxic interface, from 46.0‰ to 58.7‰ and from 32.3‰ to 42.3‰ , respectively (Fig. 5.3a).

In October 2010, still, a maximum N_2O concentration of 68 nmol L^{-1} was measured at the oxic-anoxic interface (82 m) (Fig. 5.3b). N_2O concentrations steadily decreased to 18 nmol L^{-1} toward the sediment water interface. Similar to the previous sampling, bulk $\delta^{15}\text{N}\text{-N}_2\text{O}$ reached a minimum of -10.8‰ at the depth of O_2 disappearance (i.e., at 84 m depth). Below this depth, $\delta^{15}\text{N}\text{-N}_2\text{O}$ slightly increased to -8.3‰ near the sediment-water interface. SP and $\delta^{18}\text{O}\text{-N}_2\text{O}$ both increased with decreasing N_2O concentrations in the anoxic hypolimnion, reaching maximum values of 44.6‰ and 65.3‰ , respectively, above the sediment-water interface (Fig. 5.3b). The surface water N_2O concentration in this month was 16 nmol L^{-1} .

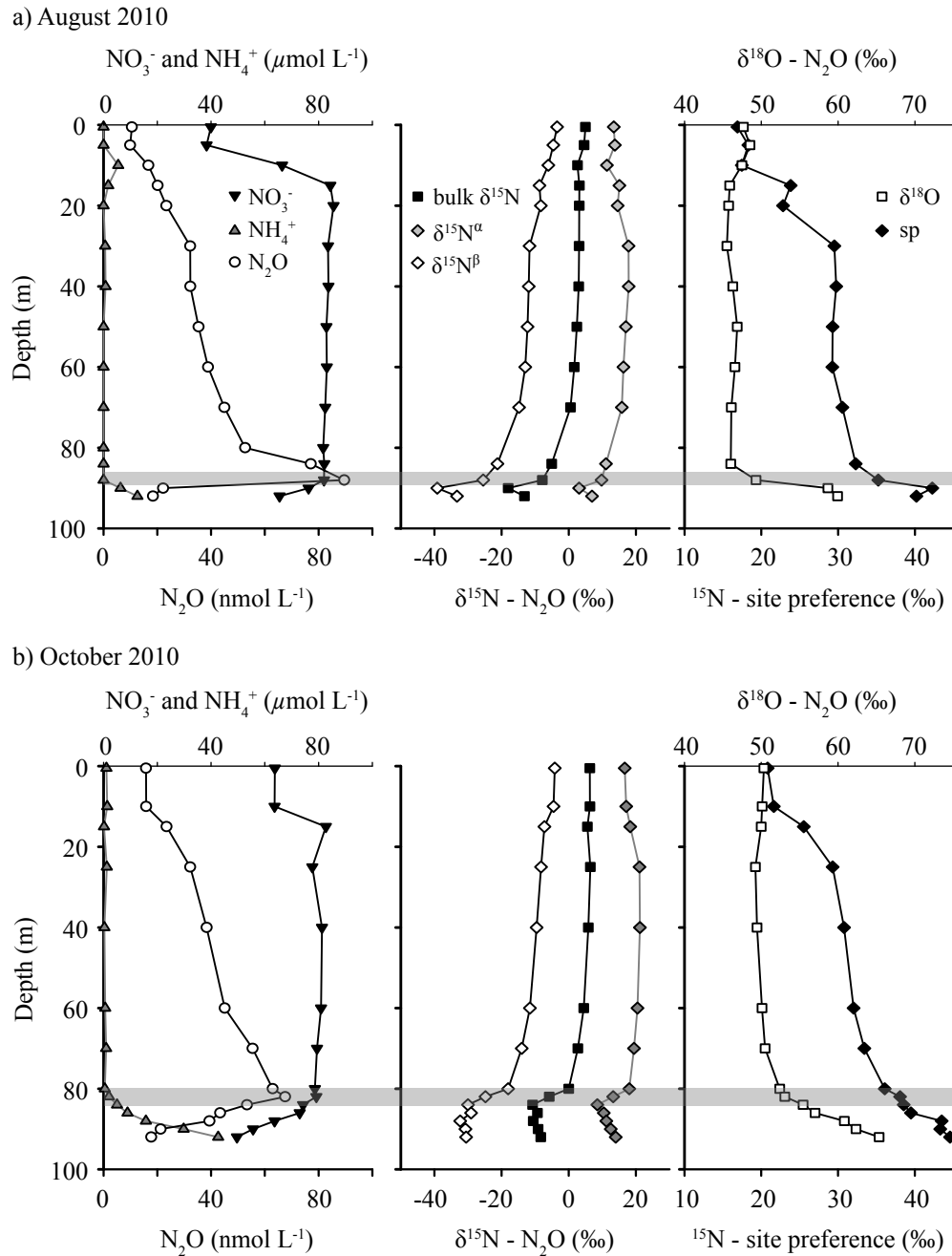


Figure 5.3: Water column profiles of dissolved NO₃⁻, NH₄⁺, and N₂O concentrations as well as bulk δ¹⁵N-, δ¹⁵N^α-, δ¹⁵N^β -, ¹⁵N-site preference (sp), and δ¹⁸O-N₂O for the Lake Lugano south basin in a) August 2010 and b) October 2010. The grey bar marks the depth of the oxic-anoxic interface, i.e., [O₂] from 50 μmol L⁻¹ to < 1 μmol L⁻¹.

5.3.2 N₂O concentration and isotope composition in the Lake Lugano north basin

The nitrogen biogeochemistry of the recent years in this lake basin has been described in detail in Wenk et al. (2013) and Wenk et al. (submitted). Sulfur-driven denitrification is the dominant fixed N removal process in the RTZ and organotrophic denitrification seems to be negligible. Denitrification in the RTZ is indicated by the decrease in NO₃⁻ concentration from ~30 μmol L⁻¹ at 15 m depth to zero levels within the RTZ (Fig. 5.4). Highest NH₄⁺ concentrations (~40 μmol L⁻¹) were found in the anoxic hypolimnion close to the sediment. NH₄⁺ concentrations decrease toward the RTZ, indicating ammonium oxidation below the oxic-anoxic interface. A stable (both in terms of identity and abundance) community of anammox bacteria coexists with sulfide-dependent denitrifiers in the water column at the depth of NO₃⁻ and NH₄⁺ disappearance (Wenk et al., 2013). Anammox bacteria were mainly responsible for NH₄⁺ oxidation, but microaerobic nitrification cannot fully be excluded.

N₂O concentration profiles qualitatively mimic the vertical NO₃⁻ distribution in the water column, with a maximum N₂O concentration of 13 nmol L⁻¹ at 20 m depth and a steady decrease to undetectable levels at 145 m depth, i.e., ~15 m below the depth of O₂ disappearance (Fig. 5.4). The N₂O concentration decrease was paralleled by a rather subtle increase of the bulk δ¹⁵N-N₂O from 5.2‰ at 15 m depth to 10.8‰ in the RTZ. Over the sample depth interval, we observed a systematic increase of the SP from 16.4‰ to 25.7‰ and of δ¹⁸O-N₂O from 43.0‰ to 54.4‰, respectively.

5.4 Discussion

5.4.1 N₂O production and accumulation in the south basin

In August 2009, we observed extreme N₂O oversaturation levels relative to equilibrium with the atmosphere in the anoxic bottom water of the southern basin (Fig 5.2a). The maximum N₂O concentration of >900 nmol L⁻¹ was significantly higher than most peak concentrations reported for other lacustrine (Sasaki et al., 2011) or marine water columns (Popp et al., 2002; Westley et al., 2006; Yamagishi et al., 2007). The hydrochemical profiles suggest a benthic source for the deep-water N₂O, most likely produced by incomplete microbial denitrification within the anoxic sediments. From the observed N₂O concentration gradient in the anoxic bottom water, and based on an average vertical turbulent diffusivity (K_z) of 0.49 m² d⁻¹ (August 2009) (Wenk et al., in prep.), we estimated a sediment-water N₂O flux of 3.1 μmol m⁻² h⁻¹ in August 2009. This flux estimate significantly exceeds N₂O fluxes observed in other lakes, generally ranging between 0.3 μmol m⁻² h⁻¹ and 0.6 μmol m⁻² h⁻¹ (Liikanen and Martikainen, 2003; McCrackin and Elser, 2010; Mengis et al., 1996). The computed

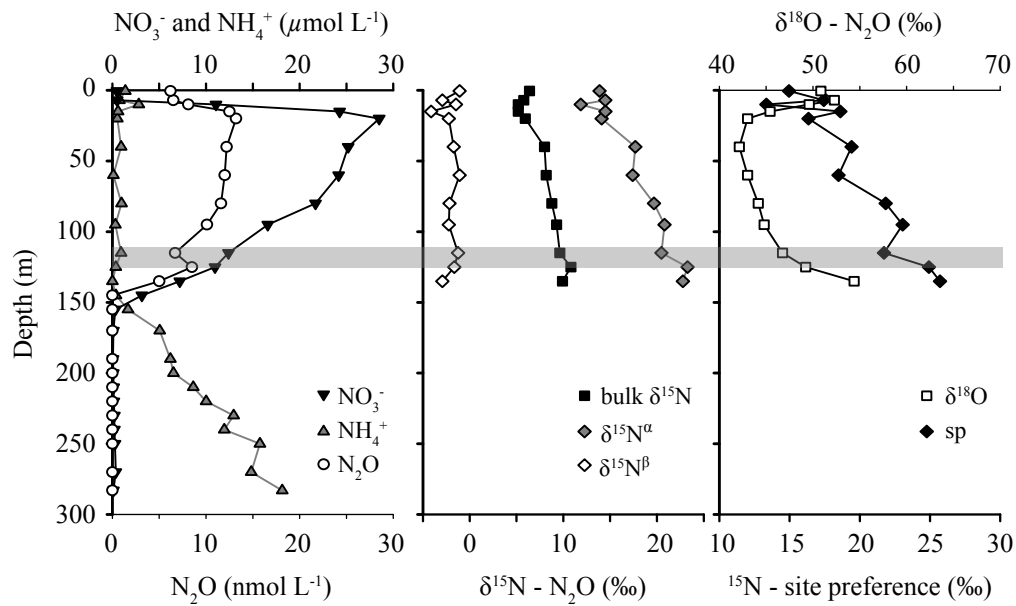


Figure 5.4: NO_3^- , NH_4^+ , and N_2O concentrations in the water column of the Lake Lugano north basin in August 2009. Also shown are bulk $\delta^{15}\text{N}$ -, $\delta^{15}\text{N}^\alpha$ -, $\delta^{15}\text{N}^\beta$ -, ^{15}N -site preference (sp), and $\delta^{18}\text{O}$ - N_2O . The grey bar marks the depth of the oxic-anoxic interface.

N_2O fluxes were also significantly greater than in October 2009 ($0.2 \mu\text{mol m}^{-2} \text{h}^{-1}$ with an average $K_z = 0.34 \text{ m}^2 \text{d}^{-1}$) (Fig. 5.2) and estimates from ex-situ incubations in 2010 (Freymond et al., 2013), suggesting strong variability in benthic N_2O production. In fact, in October 2009, N_2O accumulation in the water column was reduced by an order of magnitude compared to the previous sampling (Fig. 5.2).

The robust, recurrent local N_2O concentration maximum in the water column at the oxic-anoxic interface indicates a pelagic N_2O source in addition to benthic N_2O production. The correspondence between the N_2O concentration peak and the disappearance of both O_2 and NH_4^+ during all sampling campaigns in the southern basin suggests that N_2O production is somehow linked to the oxidation of NH_4^+ by nitrifying bacteria, either through NH_2OH oxidation or NO_2^- reduction during nitrifier denitrification.

At this point, it is uncertain as to what exactly causes the observed seasonal/interannual variability in N_2O production in the Lake Lugano south basin. Meanwhile, it is important to note that the measured N_2O accumulation is the net result of simultaneously occurring N_2O production and consumption processes. In other words, strong N_2O accumulation may not be the result only of enhanced N_2O production rates, but may rather be due to sluggish or absent consumption by denitrifying bacteria. Clear

evidence for N_2O consumption within the RTZ derives from the steep N_2O concentration gradient from the sediment toward the oxic-anoxic interface in August and October 2009, preventing any significant N_2O levels in the upper oxic water column (Fig. 5.2). Furthermore, a comparison between the October 2009 and January 2010 N_2O profiles (Fig. 5.2) reveals that with ongoing bottom water anoxia through the fall months, N_2O concentrations decreased to undetectable levels in the bottom water, indicating net N_2O consumption. This seasonal trend suggests that N_2O production was greater than N_2O reduction (i.e., complete denitrification) at the beginning of the stratification period, i.e., shortly after the establishment of anoxic conditions in near bottom waters. The induction of N_2O reduction is thought to be slow relative to the other steps involved in enzyme-regulated denitrification (Baumann et al., 1997; Otte et al., 1996), so that a sudden increase in denitrification rates (e.g., induced by increased OM inputs due to algal blooms in spring) could result in a lag phase between the expression of N_2O reducing enzymes and the rest of the denitrifying machinery, leading to the short-term accumulation of N_2O . Moreover, N_2O reductase seems most susceptible to O_2 inhibition, so that unstable redox conditions particularly in the initial phase of the anoxic period would tend to hinder the transformation of N_2O to N_2 and foster N_2O accumulation. Independent of the dominant controlling mechanism, we argue that with ongoing, stable anoxia during summer and fall 2009, N_2O reductase became increasingly activated, eventually resulting in the quantitative reduction of the accumulated N_2O (Fig. 5.2).

In 2010, N_2O did not accumulate in the anoxic bottom water to the same extent as observed in August 2009 (Fig. 5.3), although sediment core flow-through incubations revealed that the sediments were a net N_2O source (Freymond et al., 2013). This suggests almost complete N_2O consumption in the RTZ right from the beginning of the stratification period in 2010. The highest N_2O concentrations were detected at the oxic-anoxic interface, suggesting N_2O production by nitrification or nitrifier-denitrification as the main source. The exact controls on the relative importance of N_2O production vs. consumption remains elusive, yet the fundamentally different N_2O concentration dynamics observed in 2009 vs. 2010 suggest that N_2O accumulation may respond in a very sensitive (and possibly unpredictable) way to very subtle changes in environmental conditions (e.g., redox state, OM flux). In the next section, we invoke the vertical distribution of N_2O isotope ratios in the water column to further elucidate and disentangle the various N cycling processes that modulated N_2O accumulation in the deep Lake Lugano south basin in 2010.

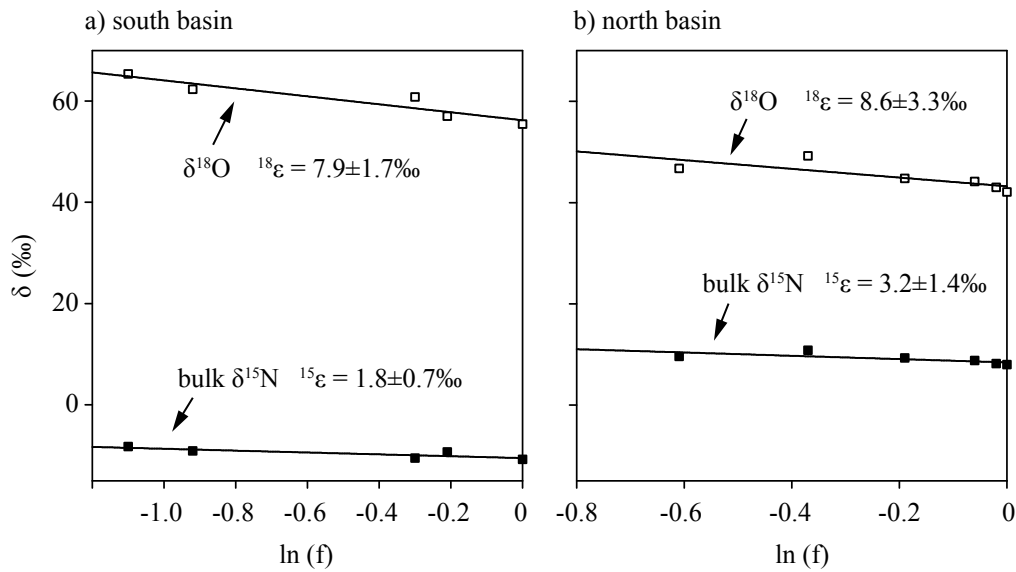


Figure 5.5: Rayleigh plots for N_2O consumption in the RTZ of a) the southern basin in October 2010 and b) the northern basin in August 2009. The bulk $\delta^{15}N$ - and $\delta^{18}O$ - N_2O are plotted against $\ln(f)$, where f denotes the remaining N_2O fraction with respect to the concentrations at 84 m (south basin) and at 40 m (north basin) water depth. The N and O isotope enrichment factors are approximated by the negative slopes of the linear regression lines (± 1 standard error). For the August 2009 profile, the values at 135 m depth were excluded (see text for details).

5.4.2 Isotopic constraints on N_2O formation mechanisms in the south basin

A $\delta^{15}N$ - N_2O of -18.0‰ , as observed at 90 m depth in August 2010 (Fig. 5.3a), is, to our knowledge, by far the lowest value reported for any marine and lacustrine environment (Popp et al., 2002; Sasaki et al., 2011; Westley et al., 2006; Yamagishi et al., 2007). The sharp decrease in $\delta^{15}N$ - N_2O in combination with the N_2O concentration maximum at the oxic-anoxic interface is consistent with N_2O production by nitrifying bacteria, but the bulk isotope signature remains ambivalent with regard to the actual mode of N_2O production (NH_2OH oxidation or nitrite reduction by nitrifier denitrification). Ammonium in the anoxic bottom water has a $\delta^{15}N$ that varies between 8‰ and 23‰ , depending on the extent of partial consumption (Wenk et al. in prep.). The $\delta^{15}N$ of nitrite below the oxic-anoxic interface is approximately -10‰ (Wenk et al. in prep.). N_2O release during NH_2OH oxidation occurs with almost no N isotope fractionation (Frame and Casciotti, 2010; Sutka et al., 2006, 2003, 2004). However, the overall N isotope fractionation with respect to the substrate NH_4^+ is generally quite high, with

a $\Delta\delta^{15}\text{N} \approx 47\text{‰}$ (Sutka et al., 2006). N_2O production by nitrifier-denitrification is associated with an N isotope effect of 43 to 60‰ relative to the source NH_4^+ and of approximately 12‰ relative to the direct precursor NO_2^- (Frame and Casciotti, 2010; Wunderlin et al., 2013; Yoshida, 1988). A $\delta^{15}\text{N}\text{-N}_2\text{O}$ of -18.0‰ as observed at the oxic-anoxic interface in the Lake Lugano south basin can, hence, be explained by either process: Nitrification or nitrifier-denitrification. SP values $>32\text{‰}$ at the depth of N_2O production during both 2010 sampling campaigns (Fig. 5.3), however, are indicative for NH_2OH oxidation rather than N_2O production through nitrifier-denitrification, given that the SP for N_2O from the latter process should be on the order of 0‰ (Frame and Casciotti, 2010; Sutka et al., 2006, 2003, 2004; Toyoda et al., 2005). In a previous study in the Lake Lugano south basin, Lehmann et al. (2003) have argued, based on coupled nitrate N-vs.-O isotope measurements (i.e., the absence of characteristic N-to-O isotope anomalies), that autotrophic nitrification does not play an important role at the oxic-anoxic interface. We do not intend to go into the details of explaining why previously reported NO_3^- isotope data are not necessarily inconsistent with nitrification (based on today's understanding of NO_3^- isotope dynamics). Instead we argue that the here-presented N_2O isotope data provide new conclusive evidence for the presence of ammonium oxidizing bacteria in the deep Lake Lugano south basin, inducing N_2O production through NH_2OH oxidation. We have recently demonstrated that methane-oxidizing bacteria dominate the benthic bacterial community (Blees et al., in prep.). Given that methanotrophic nitrification appears to produce N_2O with an equally high SP as canonical nitrification (Sutka et al., 2006), we speculate that this pathway may be the prime process leading to the observed N_2O concentration peak at the oxic-anoxic interface, yet future work will attempt to verify this hypothesis.

The parallel increase of $\delta^{15}\text{N}$ and $\delta^{18}\text{O}$ toward the sediment, in combination with increasing SP values and decreasing N_2O concentration below the oxic-anoxic interface provides clear evidence for net N_2O reduction to N_2 in the anoxic water column or within the sediment (Fig. 5.3). An estimate of the N and O isotope enrichment factors associated with this net N_2O consumption in the south basin was derived from a closed system (Rayleigh) model (Mariotti et al., 1981). In this model, the N_2O isotope composition ($\delta_{\text{N}_2\text{O}}$) follows a linear trend with $\ln(f)$, where f is the fraction of the remaining N_2O , relative to the concentration at the oxic-anoxic interface:

$$\delta_{\text{N}_2\text{O}} = \delta_{\text{N}_2\text{O},0} - \varepsilon \times \ln(f) \quad (5.1)$$

$\delta_{\text{N}_2\text{O},0}$ is the isotopic composition of the source N_2O at the oxic-anoxic interface and the isotope enrichment factor, ε , is approximated by the slope of the linear regression line. In October 2010, apparent N and O isotope enrichment factors were $^{15}\varepsilon \approx 1.8\text{‰}$ and $^{18}\varepsilon \approx 7.9\text{‰}$, respectively (Fig. 5.5a). These isotope effects are significantly lower than N and O isotope effects reported for N_2O reduction in the Eastern Tropical

North Pacific (ETNP) ($^{15}\epsilon \approx 11.6\text{‰}$ and $^{18}\epsilon \approx 30.5\text{‰}$; Yamagishi et al., 2007) and in culture experiments with *Paracoccus denitrificans* ($^{15}\epsilon \approx 12.9\text{‰}$; Barford et al., 1999). The apparent under-expression of the N and O isotope effects may be explained by simultaneous N_2O production in the anoxic sediments. Denitrification produces N_2O with relatively low $\delta^{15}\text{N}$, $\delta^{18}\text{O}$, and SP, potentially shifting the bulk and site-specific N_2O isotopic composition in the water column to lower values. Furthermore, N_2O reduction is thought to occur with an ^{18}O to ^{15}N enrichment ratio (i.e., $^{18}\epsilon : ^{15}\epsilon$) of ~ 2.5 , independent of the degree of isotope fractionation (Yamagishi et al., 2007) (see below). In the Lake Lugano south basin the ^{18}O to ^{15}N enrichment ratio associated with net N_2O reduction was ~ 4.4 in October 2010 (Figs. 5.5a, 5.6a). This positive deviation from 2.5 suggests that an additional N_2O source with relatively low bulk $\delta^{15}\text{N}\text{-N}_2\text{O}$ values contributed to the N_2O isotope signatures in the RTZ. Indeed, as indicated by the high N_2O concentrations during summer and fall in near bottom waters (see above), and as has been shown by Freymond et al. (2013), the Lake Lugano sediments represent a net N_2O source with denitrification being the main N_2O production pathway. In summary, the isotope and isotopomer profiles in the RTZ reflect an overlapping signature of N_2O production through NH_2OH oxidation at the oxic-anoxic interface, N_2O production through benthic incomplete denitrification, and N_2O reduction to N_2 .

5.4.3 The isotopic signature of N_2O consumption in the Lake Lugano north basin

In the northern basin of Lake Lugano, N_2O concentrations were generally much lower (i.e., $<13 \text{ nmol L}^{-1}$) than in the southern basin and barely exceeded atmospheric equilibrium concentration levels (Fig. 5.4). N_2O in the surface water displays a bulk N isotopic composition ($\sim 6\text{‰}$) and SP ($\sim 17\text{‰}$) that closely reflects background N_2O from exchange with the atmosphere (Yoshida and Toyoda, 2000). Maximum N_2O concentrations were found at 20 m water depth. At the concentration maximum, we observed a bulk $\delta^{15}\text{N}\text{-N}_2\text{O}$ minimum of $\sim 5\text{‰}$, indicating in situ N_2O production within the thermocline by e.g., nitrifying bacteria. Nitrification is also indicated by the NO_3^- concentration peak observed at the same depth, suggesting close links between NO_3^- regeneration and N_2O production by nitrifying bacteria in the subsurface. A relatively low SP of 16‰ at this depth implies that here, in contrast to the RTZ in the south basin, nitrifier denitrification is the main N_2O source. More precisely, the observed SP in the subsurface water is likely the result of N_2O production through nitrifier denitrification with almost no SP, and mixing with atmospheric N_2O (with a SP of 19‰) from overlying and with partly denitrified N_2O (with a SP $<26\text{‰}$) from underlying water masses. Any significant N_2O production through NH_2OH oxidation can be excluded, as this process would produce N_2O with a SP of $30\text{‰} - 36\text{‰}$ (Frame

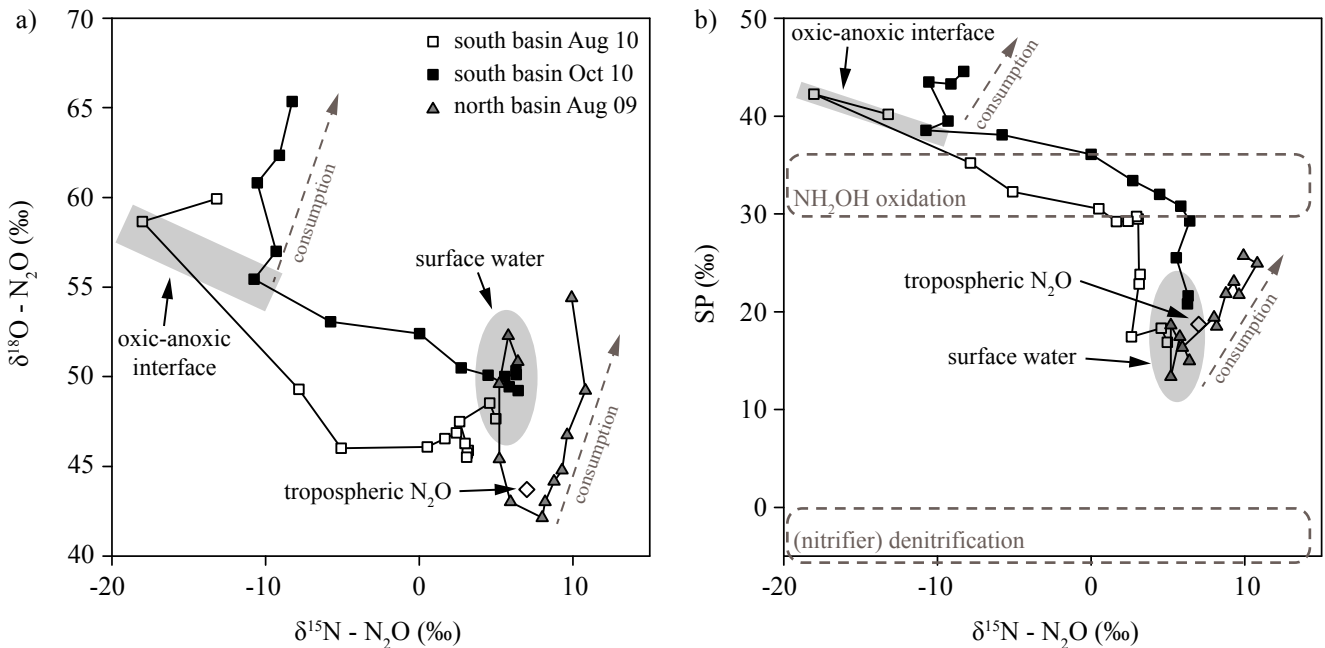


Figure 5.6: a) Oxygen vs. nitrogen isotope composition and b) SP vs. nitrogen isotope composition of N_2O in the Lake Lugano south and north basins. The white diamond indicates the isotope composition of tropospheric background N_2O (Yoshida and Toyoda, 2000). The grey ellipse marks surface water measurements from both basins and the grey bar marks the isotope composition at the oxic-anoxic interface in the Lake Lugano south basin. A theoretical N_2O consumption trend is indicated with grey, dashed arrows. The theoretical SP of N_2O produced through NH_2OH oxidation and (nitrifier) denitrification are indicated by grey, dashed boxes.

and Casciotti, 2010; Sutka et al., 2006, 2003, 2004; Toyoda et al., 2005). Below, in the deeper hypolimnion toward the RTZ, the decreasing N_2O concentrations, in tandem with increasing bulk $\delta^{15}N$ - and $\delta^{18}O$ - N_2O , as well as an increasing SP (up to ~ 26 ‰ in the RTZ) all indicate net N_2O consumption, with the N_2O reduction zone being situated about 15 m below the depth of O_2 disappearance. The characteristic relationship between the N_2O concentration and the N_2O delta values between 40 and 125 m depth (Rayleigh plot; Fig. 5.5b) yields apparent N and O isotope enrichment factors of $^{15}\epsilon \approx 3.2$ ‰ and $^{18}\epsilon \approx 8.6$ ‰, respectively. These isotope effects are again low compared to previous estimates from the ETNP and from a culture study with *Paracoccus denitrificans* (Barford et al., 1999; Yamagishi et al., 2007). This observation can partially be explained by the fact that the Rayleigh model tends to underestimate the biological isotope effects (e.g., Lehmann et al., 2003), particularly if substrate consumption is complete. The apparent under-expression of the isotope effects associated with N_2O consumption in the water column of

the Lake Lugano north basin may hence be the result of complete consumption and N_2O diffusion limitation at the reactive site within the RTZ. Here, similarly low apparent isotope effects (N, O, and C, respectively) have been observed for chemolithotrophic NO_3^- reduction, NH_4^+ oxidation (Wenk et al. submitted), as well as methane oxidation (Blees et al., submitted), and have partially been attributed to the complete consumption of the substrate in a comparatively narrow reaction zone. Low community isotope fractionation may thus be a general feature intrinsic to the northern basin RTZ, independent of the biogeochemical process. However the ratio of ^{18}O vs. ^{15}N enrichment (i.e., the $^{18}\epsilon : ^{15}\epsilon$ ratio) as well as the SP are not affected by open system aspects and may be used to trace N_2O reduction by denitrifying bacteria. Indeed the ^{18}O to ^{15}N enrichment ratio for the northern basin was approximately 2.5 between 40 and 125 m depth (Fig. 5.6a), which is consistent with observations made for N_2O consumption in the ETNP (Yamagishi et al., 2007). Whereas denitrification in the ETNP can be assumed to be organotrophic, recent work has demonstrated that NO_3^- reduction in the Lake Lugano north basin is sulfide-dependent (Wenk et al., 2013). Our study thus presents not only the first report on the coupled community N and O isotope effects for N_2O reduction by sulfide-dependent denitrification, it also suggests that an ^{18}O to ^{15}N enrichment ratio of 2.5 is diagnostic for microbial N_2O reduction, independent of its metabolic mode (organotrophic vs. chemolithotrophic). This in turn is reaffirming our interpretation of the observed N-to-O isotope trends in the south basin, where we regarded a positive deviation from this ratio as a signal of N_2O production. Similarly, the $\delta^{15}\text{N}$ and $\delta^{18}\text{O}$ values at 135 m depth in the north basin, just below the oxic-anoxic interface, do not lie on the predicted O-to-N trend (Fig. 5.6a) and may hence be indicative for an in situ N_2O source. However, this is a tentative conclusion as it is based on a single measurement only.

Net N_2O consumption in the RTZ of the Lake Lugano north basin can further be elucidated by the SP-to- $\delta^{18}\text{O}$ or SP-to-bulk $\delta^{15}\text{N}$ trends, respectively. It has been shown that the SP and $\delta^{18}\text{O}$ - N_2O increase simultaneously when N_2O is reduced (Westley et al., 2006; Yamagishi et al., 2007), yet a positive correlation is also expected for N_2O production via nitrifier denitrification (Frame and Casciotti, 2010). Accepting a fixed ^{18}O to ^{15}N enrichment ratio during N_2O reduction, a positive correlation is also expected between the SP and the bulk $\delta^{15}\text{N}$. Indeed, the SP to ^{15}N enrichment ratio in the north basin (Fig. 5.6b) is quasi equal to the ^{18}O to ^{15}N enrichment ratio (Fig. 5.6a).

5.4.4 Summary and concluding remarks

In this study we have provided isotopic evidence for fundamentally different N_2O production and consumption dynamics in the two Lake Lugano basins. While the isotope signatures in the RTZ of the Lake Lugano south basin reflect a complex combination of N_2O production through NH_2OH oxidation, N_2O production through

incomplete denitrification, and N_2O reduction to N_2 - all occurring in close vicinity -, the interpretation of N and O isotope signatures in the Lake Lugano north basin is more straightforward. Here N_2O is consumed to completion within the RTZ and nitrification is thought to be of minor importance as NH_4^+ oxidation pathway (Wenk et al., 2013). Hence, the isotope and isotopomer profiles in the hypolimnion can be viewed as quasi-pure N_2O reduction signatures. In fact they are the first reports of their kind from a lacustrine environment where sulfur-driven denitrification is the dominant fixed N elimination process.

Our results likely represent a suitable testcase for the interpretation of N_2O isotope signatures in other freshwater and marine environments. For example, we suggest a robust O to N isotope enrichment ratio of ~ 2.5 for N_2O consumption by either lithotrophic or organotrophic denitrification, independent of the environment. Accordingly, we argue that any significant deviation from a fixed O-to-N (and a SP-to-N) isotope enrichment trend is due to N_2O production occurring simultaneously or in nearby waters. Modeling efforts will be needed to verify the sensitivity of the dual isotope approach toward N_2O production. Moreover, our data revealed differential N_2O dynamics in the two lake basins, which provide general insight into the controls on N_2O production vs. consumption. We have shown that the rather dynamic, and high-reactive environmental conditions such as found in the Lake Lugano south basin are more conducive to net N_2O production by denitrification than relatively stable conditions found in the Lake Lugano north basin. We speculate that a rapid increase in denitrification rates or physical disturbance of RTZs can cause a delayed or hindered transformation of N_2O to N_2 , fostering N_2O accumulation.

In both lake basins, surface water N_2O concentrations were comparatively low. This observation suggests that, independent of the geochemical conditions and the actual N_2O dynamics in the RTZ, most of the internally produced N_2O is eventually consumed before reaching the atmosphere. It has to be noted, however, that N_2O , which accumulates in deep waters is likely to escape to the atmosphere during (seasonal or sporadic) mixing events. Because such non steady-state water-atmosphere N_2O efflux is difficult to capture during regular sampling campaigns, it is even more important to better understand the driving mechanisms behind rapid N_2O accumulation in hypolimnetic waters.

5 - References

- R. B. Alexander, R. A. Smith, and G. E. Schwarz. Effect of stream channel size on the delivery of nitrogen to the Gulf of Mexico. *Nature*, 403:758–761, 2000.
- A. Barbieri and B. Polli. Description of Lake Lugano. *Aquatic Sciences*, 54:181–183, 1992.
- C. C. Barford, J. P. Montoya, M. A. Altabet, and R. Mitchell. Steady-state nitrogen isotope effects of N_2 and N_2O production in *Paracoccus denitrificans*. *Applied and Environmental Microbiology*, 65:989–994, 1999.
- B. Baumann, M. Snozzi, J. R. van der Meer, and A. J. B. Zehnder. Development of stable denitrifying cultures during repeated aerobic-anaerobic transient periods. *Water Research*, 31:1947–1954, 1997.
- R. S. Braman and S. A. Hendrix. Nanogram nitrite and nitrate determination in environmental and biological materials by vanadium(III) reduction with chemiluminescence detection. *Analytical Chemistry*, 61:2715–2718, 1989.
- T. Diem, S. Koch, S. Schwarzenbach, B. Wehrli, and C. J. Schubert. Greenhouse gas emissions (CO_2 , CH_4 , and N_2O) from several perialpine and alpine hydropower reservoirs by diffusion and loss in turbines. *Aquatic Sciences*, 74:619–635, 2012.
- P. Forster, V. Ramaswamy, P. Artaxo, T. Berntsen, R. Betts, D. W. Fahey, J. Haywood, J. Lean, D. C. Lowe, G. Myhre, J. Nganga, R. Prinn, G. Raga, M. Schulz, and R. Van Dorland. *Changes in atmospheric constituents and in radiative forcing*, pages 130–234. Cambridge University Press, Cambridge, UK and New York, NY, USA, 2007.
- C. H. Frame and K. L. Casciotti. Biogeochemical controls and isotopic signatures of nitrous oxide production by a marine ammonia-oxidizing bacterium. *Biogeosciences*, 7:2695–2709, 2010.

- C. V. Freymond, C. B. Wenk, C. H. Frame, and M. F. Lehmann. Year-round N_2O production by benthic NO_x reduction in a monomictic south-alpine lake. *Biogeosciences*, 10:8373–8383, 2013.
- C. Garside. A chemiluminescent technique for the determination of nanomolar concentrations of nitrate and nitrite in seawater. *Marine Chemistry*, 11:159–167, 1982.
- A. B. Hooper and K. R. Terry. Hydroxylamine oxidoreductase of *Nitrosomonas* production of nitric-oxide from hydroxylamine. *Biochimica Et Biophysica Acta*, 571:12–20, 1979.
- R. W. Howarth, G. Billen, D. Swaney, A. Townsend, N. Jaworski, K. Lajtha, J. A. Downing, R. Elmgren, N. Caraco, T. Jordan, F. Berendse, J. Freney, V. Kudeyarov, P. Murdoch, and Z. L. Zhu. Regional nitrogen budgets and riverine N and P fluxes for the drainages to the North Atlantic Ocean: Natural and human influences. *Biogeochemistry*, 35:75–139, 1996.
- F. Koroleff. *Determination of ammonia*. In: K. Grasshoff [ed.], *Methods of Seawater Analysis*, pages 126–133. Verlag Chemie, 1976.
- M. F. Lehmann, P. Reichert, S. M. Bernasconi, A. Barbieri, and J. A. McKenzie. Modelling nitrogen and oxygen isotope fractionation during denitrification in a lacustrine redox-transition zone. *Geochimica Et Cosmochimica Acta*, 67:2529–2542, 2003.
- M. F. Lehmann, S. M. Bernasconi, J. A. McKenzie, A. Barbieri, M. Simona, and M. Veronesi. Seasonal variation of the $\delta^{13}\text{C}$ and $\delta^{15}\text{N}$ of particulate and dissolved carbon and nitrogen in Lake Lugano: Constraints on biogeochemical cycling in a eutrophic lake. *Limnology and Oceanography*, 49:415–429, 2004.
- A. Liikanen and P. J. Martikainen. Effect of ammonium and oxygen on methane and nitrous oxide fluxes across sediment-water interface in a eutrophic lake. *Chemosphere*, 52:1287–93, 2003.
- A. Mariotti, J. C. Germon, P. Hubert, P. Kaiser, R. Letolle, A. Tardieux, and P. Tardieux. Experimental determination of nitrogen kinetic isotope fractionation: Some principles; Illustration for the denitrification and nitrification processes. *Plant and Soil*, 62:413–430, 1981.
- M. L. McCrackin and J. J. Elser. Atmospheric nitrogen deposition influences denitrification and nitrous oxide production in lakes. *Ecology*, 91:528–539, 2010.

- M. R. McIlvin and K. L. Casciotti. Fully automated system for stable isotopic analyses of dissolved nitrous oxide at natural abundance levels. *Limnology and Oceanography-Methods*, 8:54–66, 2010.
- M. Mengis, R. Gächter, and B. Wehrli. Nitrous oxide emissions to the atmosphere from an artificially oxygenated lake. *Limnology and Oceanography*, 41:548–553, 1996.
- A. Mosier, C. Kroeze, C. Nevison, O. Oenema, S. Seitzinger, and O. van Cleemput. Closing the global N₂O budget: Nitrous oxide emissions through the agricultural nitrogen cycle - OECD/IPCC/IEA phase II development of IPCC guidelines for national greenhouse gas inventory methodology. *Nutrient Cycling in Agroecosystems*, 52:225–248, 1998.
- N. E. Ostrom, A. Pitt, R. Sutka, P. H. Ostrom, A. S. Grandy, K. M. Huizinga, and G. P. Robertson. Isotopologue effects during N₂O reduction in soils and in pure cultures of denitrifiers. *Journal of Geophysical Research-Biogeosciences*, 112, 2007.
- S. Otte, N. G. Grobden, L. A. Robertson, M. S. M. Jetten, and J. G. Kuenen. Nitrous oxide production by *Alcaligenes faecalis* under transient and dynamic aerobic and anaerobic conditions. *Applied and Environmental Microbiology*, 62:2421–2426, 1996.
- B. N. Popp, M. B. Westley, S. Toyoda, T. Miwa, J. E. Dore, N. Yoshida, T. M. Rust, F. J. Sansone, M. E. Russ, N. E. Ostrom, and P. H. Ostrom. Nitrogen and oxygen isotopomeric constraints on the origins and sea-to-air flux of N₂O in the oligotrophic subtropical North Pacific gyre. *Global Biogeochemical Cycles*, 16, 2002.
- M. Poth and D. D. Focht. ¹⁵N kinetic analysis of N₂O production by *Nitrosomonas europaea*: An examination of nitrifier denitrification. *Applied and Environmental Microbiology*, 49:1134–1141, 1985.
- A. R. Ravishankara, J. S. Daniel, and R. W. Portmann. Nitrous oxide (N₂O): The dominant ozone-depleting substance emitted in the 21st century. *Science*, 326:123–125, 2009.
- Y. Sasaki, K. Koba, M. Yamamoto, A. Makabe, Y. Ueno, M. Nakagawa, S. Toyoda, N. Yoshida, and M. Yoh. Biogeochemistry of nitrous oxide in Lake Kizaki, Japan, elucidated by nitrous oxide isotopomer analysis. *Journal of Geophysical Research*, 116, 2011.
- D. M. Snider, S. L. Schiff, and J. Spoelstra. ¹⁵N/¹⁴N and ¹⁸O/¹⁶O stable isotope ratios of nitrous oxide produced during denitrification in temperate forest soils. *Geochimica Et Cosmochimica Acta*, 73:877–888, 2009.

- R. L. Sutka, N. E. Ostrom, P. H. Ostrom, H. Gandhi, and J. A. Breznak. Nitrogen isotopomer site preference of N_2O produced by *Nitrosomonas europaea* and *Methylococcus capsulatus* Bath. *Rapid Communications in Mass Spectrometry*, 17: 738–745, 2003.
- R. L. Sutka, N. E. Ostrom, P. H. Ostrom, H. Gandhi, and J. A. Breznak. Erratum: Nitrogen isotopomer site preference of N_2O produced by *Nitrosomonas europaea* and *Methylococcus capsulatus* Bath. *Rapid Communications in Mass Spectrometry*, 18:1411–1412, 2004.
- R. L. Sutka, N. E. Ostrom, P. H. Ostrom, J. A. Breznak, H. Gandhi, A. J. Pitt, and F. Li. Distinguishing nitrous oxide production from nitrification and denitrification on the basis of isotopomer abundances. *Applied and Environmental Microbiology*, 72:638–644, 2006.
- S. Toyoda and N. Yoshida. Determination of nitrogen isotopomers of nitrous oxide on a modified isotope ratio mass spectrometer. *Analytical Chemistry*, 71:4711–4718, 1999.
- S. Toyoda, H. Mutoke, H. Yamagishi, N. Yoshida, and Y. Tanji. Fractionation of N_2O isotopomers during production by denitrifier. *Soil Biology and Biochemistry*, 37:1535–1545, 2005.
- S. Toyoda, H. Iwai, K. Koba, and N. Yoshida. Isotopomeric analysis of N_2O dissolved in a river in the Tokyo metropolitan area. *Rapid Communications in Mass Spectrometry*, 23:809–821, 2009.
- R. F. Weiss and B. A. Price. Nitrous-oxide solubility in water and seawater. *Marine Chemistry*, 8:347–359, 1980.
- C. B. Wenk, J. Blees, J. Zopfi, M. Veronesi, A. Bourbonnais, C. J. Schubert, H. Niemann, and M. F. Lehmann. Anaerobic ammonium oxidation (anammox) bacteria and sulfide-dependent denitrifiers coexist in the water column of a meromictic south-alpine lake. *Limnology and Oceanography*, 58:1–12, 2013.
- M. B. Westley, H. Yamagishi, B. N. Popp, and N. Yoshida. Nitrous oxide cycling in the Black Sea inferred from stable isotope and isotopomer distributions. *Deep-Sea Research*, 53:1802–1816, 2006.
- P. Wunderlin, M. F. Lehmann, H. Siegrist, B. Tuzson, A. Joss, L. Emmenegger, and J. Mohn. Isotope signatures of N_2O in a mixed microbial population system: Constraints on N_2O producing pathways in wastewater treatment. *Environmental Science and Technology*, 47:1339–1348, 2013.

- H. Yamagishi, M. B. Westley, B. N. Popp, S. Toyoda, N. Yoshida, S. Watanabe, K. Koba, and Y. Yamanaka. Role of nitrification and denitrification on the nitrous oxide cycle in the eastern tropical North Pacific and Gulf of California. *Journal of Geophysical Research-Biogeosciences*, 112, 2007.
- N. Yoshida. ^{15}N -depleted N_2O as a product of nitrification. *Nature*, 335:528–529, 1988.
- N. Yoshida and S. Toyoda. Constraining the atmospheric N_2O budget from intramolecular site preference in N_2O isotopomers. *Nature*, 405:330–334, 2000.

CHAPTER 6

Conclusions and Outlook

6.1 Conclusions and implications

The main goal of this project was to investigate the pathways responsible for fixed N elimination in Lake Lugano and to interpret the N and O isotope signatures in the water column based on specific N cycling reactions. Our results demonstrate that:

- Anammox bacteria and sulfide-dependent denitrifiers can coexist in the same layer of a lacustrine water body.
- Organotrophic denitrification is a negligible nitrate-reducing pathway in the anoxic water column of the Lake Lugano north basin.
- Chemolithotrophic NO_3^- reduction in the Lake Lugano north basin was probably catalyzed by a nitrate reductase (Nap) that has been widely neglected, or considered irrelevant, in previous denitrification studies.
- The expression of biological N isotope fractionation in an environment can depend on various factors, such as physical conditions (e.g., stability of the water column, turbulent diffusion, dilution/open-system effects), biogeochemical conditions (e.g., cell specific N transformation rates, substrate availability), or organism-specific isotope fractionation at the enzyme-level.
- If the isotopic end-members are well constrained, a quantitative partitioning between pelagic and benthic nitrate reduction can be inferred from stable N isotope ratios of nitrate in the water column.
- A co-linearity between N and O isotope enrichment is expected during both organotrophic and sulfur-driven denitrification.
- The ^{18}O to ^{15}N enrichment ratio during microbial N_2O reduction is ~ 2.5 for both chemolithotrophic and organotrophic modes.
- The dynamic conditions in the Lake Lugano south basin are more conducive to net N_2O production and accumulation than the more stable conditions in the north basin.

The results presented in chapters 2 through 5 are significant on multiple levels. First, we demonstrate that, in contrast to previous data from marine environments, anammox bacteria and sulfide-dependent denitrifiers coexist in the same layer of a lacustrine water body. Together with the finding that organotrophic denitrification is negligible as a nitrate-reducing pathway in the Lake Lugano north basin, this study underscores the importance of chemolithotrophic fixed N elimination pathways in aquatic ecosystems.

Second, we demonstrate that the expression of the N (and O) isotope fractionation during NO_3^- reduction and NH_4^+ oxidation can be variable in nature and likely depends on the pathways of NO_3^- dissimilation (organotrophic vs. chemolithotrophic), the main catalyzing enzymes (Nar vs. Nap), the pathways of NH_4^+ oxidation (nitrification vs. anammox), and the controlling environmental conditions (e.g., substrate limitation, cell specific N transformation rates). Consequently, we recommend to refrain from a robust isotope enrichment factor for denitrification in N budget calculations and to include chemolithotrophic fixed N elimination pathways and their N and O isotope effects in local and global N isotope models.

Nevertheless, the interpretation of N isotope ratios of water column nitrate is an elegant method to quantitatively distinguish between pelagic and benthic denitrification, but only in a well constrained system, where sufficient knowledge about the mode and mechanism of ongoing N transformations is available and justifiable assumptions can be made for the isotopic end-members.

Finally, our results implicate that additional isotopic measurements such as O isotopes in NO_3^- , or the ^{15}N site preference in N_2O are powerful tools to identify and quantify microbial N transformation pathways occurring simultaneously or in close vicinity. For a successful interpretation of such data, however, a clear mechanistic understanding of the processes leading to certain characteristic isotopic patterns in the environment is needed.

6.2 Outlook

This study identified the dominant N transformation pathways in Lake Lugano and elucidated their respective community isotope effects. However, this thesis also opens a multitude of new questions, that point to new research directions:

Interplay between anammox bacteria and sulfide-dependent denitrifiers:

We have shown that the two chemolithotrophic processes co-occur in the same water layer, but we could only speculate about their potential interaction. Our suggestion that the bacteria live in an aggregate-like community, in which the denitrifiers create a sulfide-free microenvironment in the aggregate interior and provide NO_2^- for anammox needs experimental verification. This could be addressed by analysis of particles collected from the water column of the Lake Lugano north basin by e.g., fluorescence in situ hybridization and 16S rRNA gene analysis. Further evidence for the spacial distribution of different organisms and their interplay could be obtained by NanoSIMS.

N and O isotope fractionation by chemolithotrophic denitrifiers: In this thesis, we presented the first report of such from a natural ecosystem. However, N (and O) isotope fractionation experiments with pure or enrichment cultures of

chemolithotrophic denitrifiers are completely missing. To get a clear understanding about organism-specific (and enzyme-specific) isotope fractionation, culture experiments are inevitable. Sulfide-dependent denitrifiers could be enriched (or even isolated) from the water column of the Lake Lugano north basin. Such an enrichment culture would not only allow to conduct systematic N and O isotope fractionation experiments, it would also allow to investigate the phylogenetic affiliation of the sulfide-oxidizing microbes, their enzymatic machineries, and metabolic pathways.

Isotope fractionation factors for anammox and potential under-expression under natural conditions: If the anammox-specific fractionation factors were well constrained in enrichment cultures under optimal growth conditions, it is not clear as to how the isotopic signatures are expressed in the environment. Similar to the experiments by Kritee et al. (2012) with organotrophic denitrifiers, anammox-specific N isotope fractionation could be studied under conditions that are more relevant to natural ecosystems. In this thesis we speculate that the “efflux model”, which has been used to explain the under-expression of the Nar-specific isotope effect in the environment (Kritee et al., 2012), could also be applicable to anammox bacteria. I hypothesize, that the peculiar cell structure of anammox bacteria, with energy-dependent substrate uptake into the anammoxosome, makes the expression of N isotope fractionation in the medium sensitive to changes, such as substrate availability, cell specific N transformation rates, etc.

Nap-specific ^{18}O to ^{15}N enrichment ratio: To date, only one culture (*R. sphaeroides*) study has addressed the potential Nap-specific ^{18}O to ^{15}N enrichment ratio (Granger et al., 2008). Additional experiments with a variety of bacterial strains should be carried out to confirm the characteristic N and O isotope fractionation by this enzyme. *E. coli* mutants that only possess the Nap encoding genes (Potter et al., 1999) would make a suitable model organism to conduct such isotope fractionation experiments.

Microbial diversity in the Lake Lugano north basin: Microbial diversity and community structure studies are of particular interest when they can be linked to independent constraints on metabolic pathways, rates, and also isotopic signatures. The Lake Lugano north basin would provide an excellent natural, well characterized system for such a project. Particulate organic matter from the water column could be collected, DNA extracted, and analyzed by next generation sequencing. Spatial (and temporal) variability of the microbial population could be monitored and possibly correlated to changes in geochemical conditions.

6 - References

- J. Granger, D. M. Sigman, M. F. Lehmann, and P. D. Tortell. Nitrogen and oxygen isotope fractionation during dissimilatory nitrate reduction by denitrifying bacteria. *Limnology and Oceanography*, 53:2533–2545, 2008.
- K. Kritee, D. M. Sigman, J. Granger, B. B. Ward, A. Jayakumar, and C. Deutsch. Reduced isotope fractionation by denitrification under conditions relevant to the ocean. *Geochimica et Cosmochimica Acta*, 92:243–259, 2012.
- L. C. Potter, P. Millington, L. Griffiths, G. H. Thomas, and J. A. Cole. Competition between *Escherichia coli* strains expressing either a periplasmic or a membrane-bound nitrate reductase: Does Nap confer a selective advantage during nitrate-limited growth? *Biochemical Journal*, 344:77–84, 1999.

Acknowledgments

I am grateful to Moritz Lehmann for the opportunity to work on this very interesting and multidisciplinary project. His mentoring and continuous support throughout the last 4 years were great. I also enjoyed the pleasant and highly motivating work environment, as well as the opportunity to broaden my horizon in several conferences, courses, and collaborations.

I am equally grateful to Jakob Zopfi, who co-initiated this project and who is a fantastic microbiology teacher. I deeply appreciate the many creative suggestions and insightful discussions. I would like to thank both, Moritz and Jakob, for sharing their enthusiasm for stable isotope geochemistry, microbiology, and science in general. It was a true honor working with them.

I would also like to express my gratitude to Bernhard Wehrli and Julie Granger, who did not hesitate to be part of my PhD committee and to evaluate this thesis.

The most continuous and crucial collaboration for the success of this project was with Mauro Veronesi from the Scuola Universitaria Professionale della Svizzera Italiana (SUPSI). He, together with Marco Simona and Stefano Beatrizotti, not only generously agreed to all our requests for additional sampling campaigns, they also shared their data collection. Moreover, they always ensured a fantastic mood on the boat.

Equally responsible for the mood during sampling campaigns was Jan Blees, whom I would like to thank for elucidating the carbon-side of the story, for always openly sharing data, results, and new insights, and for many enjoyable coffee and lunch breaks.

Without the help of several people, a smooth start into my laboratory work would have been impossible. Mark Rollog managed the stable isotope lab and I greatly benefited from his broad experience in isotope ratio mass spectrometry. Marianne Caroni conducted most NH_4^+ concentration measurements presented in this thesis and Heinz Hürlimann run the ICP-OES samples.

During the last four years I appreciated the help and support of many co-workers and colleagues. I would like to thank Helge Niemann and Carsten Schubert for helpful inputs and suggestions in- and outside of meetings, Caitlin Frame for valuable comments on an earlier version of the N₂O isotopomer chapter, Sylvia Humbert for her help with anammox phylogenetic and qPCR analyses, Pilar Junier for letting me use the facilities in her microbiology lab, Gaute Lavik for hosting me in Bremen and for valuable advice regarding anoxic incubations, Bo Thamdrup for fruitful discussions during his visit in Basel, Annie Bourbonnais for sharing her experience with ammonium isotope measurements, Karen Casciotti and Keisuke Koba and their labs for the N₂O isotopomer analyses, Gijs Nobbe for technical support with N₂O concentration measurements, Wayne Gardner for hosting me in Texas, the introduction to the HPLC method and for analyzing my ¹⁵NH₄⁺ samples, Mark McCarthy for his help with setting up the sediment-core incubations, Todd Kana for tirelessly answering questions regarding the MIMS, Boswell Wing and Natella Mirzoyan for valuable comments on my work and for proof-reading the introduction chapter of this thesis, and Anja Gramlich for providing great help with L^AT_EX layouting. Chantal Freymond wrote her master thesis within the frame of this PhD project. It was a pleasure to work with her and I appreciated her motivation and trust in the success of our sediment-core incubations. The Swiss National Science Foundation is acknowledged for funding this PhD project (No. 129491 - Nitrogen elimination pathways and associated isotope effects in Swiss eutrophic Lake Lugano).

A lot of people contributed to a cheerful workaday life in the Bernoullianum offices and labs and I thank all of them for the fantastic 4 years.

I also wish to express my gratitude to Itay Halevy, who hosted me at the Weizmann Institute of Science in Rehovot, Israel, during the past few months. I greatly enjoy the lively discussions in group meetings and seminars and the inspiring work atmosphere.

Lastly, I am deeply grateful to my family and friends, in particular to my parents, Paul and Ursula, and my husband, Benjamin Towbin, for continuous support and patience. My little daughter Nora is certainly not responsible for good night rests, but for very effective after-work distractions.

Curriculum Vitae - Christine Wenk

Date of birth: 21 May 1982

Nationality: Swiss

Civil status: married, 1 daughter

Education

University of Basel, Basel, Switzerland, since Apr. 2009

PhD graduate student, Department of Environmental Sciences.

International Geobiology Course, California, USA, Jun. 2010 - Jul. 2010

ETH Zürich, Zürich, Switzerland, Oct. 2002 - Oct. 2008

Bachelor and Master studies in Environmental Sciences.

Gymnasium Kirschgarten, Basel, Switzerland, Aug. 1998 - Jun. 2001

University entrance diploma (mathematical major).

Work experience

Eawag, Dübendorf, Switzerland, Oct. 2008 - Dec. 2008

Assistant researcher in the Department of Water Resources and Drinking Water.

DEZA, Bern, Switzerland, Sep. 2007 - Feb. 2008

Internship in Disaster Risk Reduction, Middle East and North Africa.

Ciba Specialty Chemicals, Qingdao, China, Oct. 2005 - May 2006

Internship in wastewater treatment.

ETH Zürich, Zürich, Switzerland, Oct. 2004 - Jun. 2007

Teaching assistant for a basic course in systems analysis.

Gymnasium Kirschgarten, Basel, Switzerland, Nov. 2003 - Mar. 2004

Substitute teacher at a high school.

Instituto Antonio Provolo, Encarnación, Paraguay, Feb. 2002 - Aug. 2002

Volunteering teacher at a school for deaf children.